ABSTRACT

A versatile apparatus was constructed for the measurement of adsorption equilibria over the temperature interval 77.4°K to 273.2°K and at pressures from 1 mm Hg to 50 atm.

Pure component equilibrium data were obtained for a commercial activated carbon, Pittsburgh BPL, and the adsorbates N_2, H_2, CO, A and CH_4. Binary adsorption equilibria for three systems were measured at several temperatures and total pressures of 1, 7.85 and 28.5 atm. The mixtures investigated were, (1) N_2 - CO

(2) H_2 - CO

(3) H_2 - N_2

A novel correlation of pure component equilibrium data, based on Polanyi's potential method, was proposed and applied with success to measured and literature data on charcoal over a wide range of temperature and pressure. The method makes use of adsorbate molar volumes determined by an empirical extrapolation of saturated liquid volumes. It was found that high pressure adsorption data could be correlated satisfactorily if the quantity adsorbed was defined as the total amount of gas contained within the micropore volume.

A method for predicting binary equilibria from pure component data was also developed. Based on Basmadjian's "pressure ratio integral" (1), the proposed method was applied with good results to measured and literature data, including high pressure and high and variable relative volatility systems.

PREFACE

The experimental program on which this dissertation is based, was conducted in the Department of Chemical Engineering of the University of Ottawa, during the years 1960-64, and was financially supported by grants in aid of research from the National Research Council and the Ontario Research Foundation. In addition, the writer gratefully received studentships from the Consolidated Mining and Smelting Co. in 1960 and 1961.

The writer wishes to express his thanks to Dr. D. Basmadjian, who directed the work, for his guidance and extreme patience; to the various members of the staff for helpful discussion; to Messrs. Giacobbi and Gasperetti for aid in constructing the experimental equipment; and to Mr. Augustine Lee for invaluable assistance in performing many of the tedious calculations.

Also acknowledged, are the offset facilities made available by Dominion Tar and Chemical Co., Central Research Laboratories.

Finally the writer notes, with affection, the support given by his wife throughout the, sometimes trying, duration of this program.

Montreal
February 1965
W.H.C.

TABLE OF CONTENTS

LIST OF PLATES AND FIGURES

LIST OF TABLES

NOMENCLATURE

f_g	Fugacity of gas phase, atm
f_s	Fugacity of adsorbed phase, atm
f_{sat}	Fugacity of saturated liquid, atm
N	Moles gas adsorbed, moles/gm adsorbent
M	Molecular wt of adsorbate, gm/mole
P_c	Critical pressure, atm
P_g	Gas phase pressure, atm
P_s	Adsorbate saturation pressure, atm
P_{sat}	Vapor pressure saturated liquid, atm
P_1	Partial pressure component 1, atm
P_1°	Equilibrium pressure, pure component 1, atm
R	Gas constant, cal/mole
T	Temperature, °K
T_b	Normal boiling temperature, °K
T_c	Critical temperature, °K
V	Volume of gas adsorbed, cc STP/gm
V_A	Volume of adsorbate, cc/gm
V_c	Gas equivalent of empty cell, cc STP
V_{DS}	Dead space volume, cc STP
v_p	Pellet volume of sample, cc
v_{mac}	Total macropore volume of sample, cc

V_g	Molar volume of gas phase cc/mole
V_g°	Standard molar volume of gas phase cc STP/mole
V_L	Liquid molar volume, cc/mole
V_T	Total volume binary adsorption, cc STP/gm
V_{pore}	Gas equivalent of total pore volume, cc STP
V_p	Gas equivalent, pellet volume, cc STP
V_{mic}	Gas equivalent, micropore volume, cc STP
V_{mac}	Gas equivalent, macropore volume, cc STP
V_{solid}	Gas equivalent, adsorbent solid, cc STP
V_s	Molar volume of adsorbate, cc/mole
V_1	Volume of component 1 adsorbed, from binary, cc STP/gm
$V_{1\pi}^\circ$	Volume of pure component 1, cc STP/gm
W	Weight of adsorbent sample, gm
X	Mole fraction, adsorbed phase
Y	Mole fraction, gas phase
V_m, C	Constants BET equation
b	van der Waals' constant
α	Relative volatility or separation factor
ϵ	Polanyi potential (modified), cal/cc
π	Total pressure, atm
ϕ	Hiza's enhancement factor

ρ	Density, gm/cc
$\leq$	B.E.T. surface area, m^2/gm

Subscripts

1	More volatile component in binary mixture
SL or L	Saturated liquid
g	Gas phase
A	Adsorbed phase

INTRODUCTION

There has been renewed interest in the industrial use of gas-solid adsorption as a separation process, economically competitive with the more usual operations distillation and absorption. Until recently, adsorption was used chiefly to recover trace quantities from process streams at ambient temperature, and pressures up to a few atmospheres. Solvent recovery from air streams has been effected in this way (2, 3, 4).

Large scale gas processing in the cryogenic range (below 150°K) has provided new opportunities for the use of adsorption. For example, final purification of liquefaction grade hydrogen (5) and helium (6) is currently carried out using carbon and silica gel adsorbents at the temperature of liquid nitrogen.

The trend to high pressure operation in the chemical process industry has brought about a similar increase in the use of adsorbers operating at elevated pressures. Thus, carbon-dioxide has been removed from ethylene streams by adsorption at 2000 psi (7).

Adsorption separations involving higher than trace concentrations have been slow in developing because of technical difficulties with moving-bed adsorption, which provides the countercurrent operation suited to this type of problem. However, consideration is now being given to the use of fixed-bed units for high concentration applications (8). Two processes, U.O.P.'s "Molex" (9) and Texaco's

"Selective finishing" (10), have been proposed to upgrade gasoline by removing n-paraffin fractions occurring in feedstocks at concentrations as high as 26%. A number of feasible adsorption separations which are of industrial significance are given in Table 1.

Fixed-bed adsorbers can be operated in one of four main ways depending on the mode of regeneration. These are known as:

1) thermal swing cycles
2) inert purge-gas cycles
3) displacement stripping cycles
4) pressure swing cycles

Thermal swing cycles have been used most frequently. Desorption is achieved by raising the adsorber temperature, usually by introducing a hot gas stream to the saturated adsorber after the adsorption step of the cycle is completed.

High pressure operations favour pressure swing cycles with their low thermal load and rapid cycle time. Desorption is carried out by releasing the pressure in the adsorber after saturation. Vacuum pumping is often used to reduce the adsorber pressure still further.

The foregoing brief outline indicates the range of variables encountered in adsorption operations and the corresponding need for extensive equilibrium data for design purposes. Particularly lacking are high pressure data, and a valid correlation suitable for extrapolating experimental data.

TABLE 1

Adsorption Processes of Industrial Significance

PROCESS	OPERATING CONDITIONS	
	T°F	P psi
(1) Final scrubbing of liquefaction grade hydrogen (5)	-301	295
(2) Final stage helium purification (6)	-340	2750
(3) C_5^+ recovery from natural gas including dehumidification (11)	75	850
(4) Dehumidification of air (14-17)	75	350
(5) Carbon dioxide removal (400 ppm) from ethylene (7)	77	2000
(6) Hydrogen purification for ammonia synthesis, drying and hydrocarbon removal (12)	60	400
(7) Gas sweetening with sulphur recovery (13)	65	500

Some separation problems simply involve the removal of one adsorbable component from an inert gas stream. For many binary feeds, however, both components are adsorbed simultaneously and binary equilibrium data covering a wide range of temperature pressure and composition are therefore required. However, pure component equilibria are easier to measure, and a desirable approach would therefore be to correlate pure component isotherms over a wide range of temperature and pressure and utilize these pure component data to predict binary equilibria.

The research program on which this dissertation is based, was therefore divided into the following sections:

1) the design and construction of an apparatus, suitable for measuring pure component and binary equilibrium data over a wide range of experimental variables.

2) the measurement of several pure gas and binary adsorption isotherms on an activated carbon adsorbent, particularly at high pressures and above the critical temperature.

3) the correlation of measured and literature pure component data.

4) the prediction of binary equilibria from pure component data.

LITERATURE REVIEW

The pertinent literature was reviewed with particular attention to the following three topics:

1. methods for correlating pure component adsorption equilibria.
2. prediction of binary equilibrium data from pure component isotherms.
3. numerical data for pure component and binary adsorption equilibria on commercial adsorbents.

Selected references concerning these subjects will be discussed in the following section. General reviews on most aspects of adsorption have been given by Brunauer (18), de Boer (19) and Young and Crowell (20).

1. CORRELATION OF PURE COMPONENT EQUILIBRIUM DATA

(a) Isotherm equations

Many equations have been proposed to correlate isothermal p-v adsorption data. Some, such as the Freundlich (21) are empirical, while others are based on a particular adsorbed phase model, e.g. the Langmuir (22) and B.E.T. (23) equations. Other semi-empirical equations have been proposed by Sips (22*), Toth (23*), (36) and Redlich (24).

The constants in these equations depend on temperature as well as other parameters, some of which are difficult to evaluate (e.g. interaction energy). Hence, the temperature dependence of the isotherm equation is difficult to predict. These equations usually fit experimental data over a limited pressure interval only. In addition, those involving the relative pressure P/P_s° are not applicable at temperatures higher than critical.

(b) Potential theory

A different approach to the correlation of pure component equilibria was taken by Polanyi (25) and Berenyi (26) in their "Potential theory". The pure component correlation which will be proposed here is a modification of this potential method. Consequently, the development of the Polanyi potential theory and various past modifications will be discussed in some detail.

The total volume of the adsorbed phase was found by Polanyi (25) and Berenyi (26) to be a unique function of

the "adsorption potential" ϵ' which was defined as the work required to compress the adsorbate gas phase from the adsorption pressure to a pressure equal to the vapor pressure of the adsorbate bulk liquid phase. The adsorbed phase was assumed to be similar in behaviour to the bulk liquid. If the total volume of the adsorbed phase is expressed in terms of the product of the adsorbate density, and the number of moles adsorbed, one obtains the following expressions

$$V_A = \int_0^N \frac{M}{\rho_A} \, dN = \int_0^N V_s \, dN \qquad (1)$$

where V_A is the total volume of the adsorbate, and

$$\epsilon' = f(V_A) = \int_{P_g}^{P_{SAT}} V_g \, dP \qquad (2)$$

If one assumes that the gas phase behaves ideally, the potential may be written,

$$\epsilon' = f(V_A) = RT \ln \frac{P_s}{P_g} \qquad (3)$$

The potential was found to be temperature independent, and a characteristic curve, $\epsilon' = f(V_A)$, could be obtained by trial and error, which would correlate pure component adsorption data over a wide range of the variables.

Above the critical temperature the saturated vapor pressure ceases to have a realistic meaning, and Berenyi (26) proposed the following empirical expression for the adsorption potential:

$$\epsilon' = RT \ln \frac{0.14T}{P_g b} \quad , \quad T > T_c \qquad (4)$$

Various equations of state were used to allow for deviations from ideal gas behaviour in calculating the work integral. Lowry and Olmstead (27) improved Berenyi's (26) method for calculating characteristic curves but still required successive approximations to arrive at an adsorbate density distribution.

It is evident from the foregoing that the parameters of interest in the potential method which are not directly measurable are,

1) P_s - the saturation pressure, and

2) V_s - the adsorbed phase molar volume. To simplify the Polanyi-Berenyi method, subsequent workers made various assumptions in order to define P_s, particularly above the critical temperature. As a further simplification, the total volume of the adsorbed phase was expressed in terms of an average value for V_s, rather than as a density distribution. This approach was used by Dubinin (28) Lewis et al (29) and Maslan et al (30). Their modifications will be discussed in the following section.

Potential theory modifications

Dubinin (28) calculated the total volume of the adsorbed phase by assuming an adsorbate density, equal to the saturated liquid density, at adsorption temperatures up to the boiling point.

$$V_A = N.\frac{M}{\rho_{sL}} = N.V_{sL}\ ,\ T \leq T_b \qquad (5)$$

For temperatures between the boiling and critical points, the adsorbate density was given by a linear relation.

$$\rho_A = \rho_b + \left(\frac{T - T_b}{T_c - T_b}\right)\left(\frac{M}{b} - \rho_b\right) \qquad (6)$$

$$T_b \leq T \leq T_c$$

Above the critical temperature the adsorbate molar volume was assumed to be constant and equal to the van der Waals' co-volume b.

$$V_s = b\ ,\ T \geq T_c \qquad (7)$$

In addition, the potential ϵ' is treated empirically for the temperature region above the critical

$$\epsilon' = RT \ln\left[\left(\frac{T}{T_c}\right)^2 \quad \frac{P_c}{P_g}\right] \quad T \geq T_c \qquad (8)$$

This proposal for calculating the adsorption potential above the critical gives rise to negative values of ϵ' at high ad-

sorption pressures. For example, the "saturation pressure", $\left(\frac{T}{T_c}\right)^2 P_c$ calculated for nitrogen at -76°C is 81 atm, while Antropoff (31) has shown that saturation does not occur even at 400 atm, resulting in a large negative value for ϵ'.

Dubinin (28) also proposed that for equal volumes of the adsorbed phase, the potentials calculated for two different adsorbates should have a constant ratio, over the whole characteristic curve. This quantity was called the "affinity coefficient" and was found to be equal to the ratio of the liquid molar volumes of the two adsorbates.

$$\frac{\epsilon'_1}{V_{L_1}} = \frac{\epsilon'_2}{V_{L_2}} \quad \text{when } V_{A_1} = V_{A_2} \tag{9}$$

For simplicity the potential can now be defined as

$$\epsilon = \frac{\epsilon'}{V_s} = \frac{RT}{V_s} \ln \frac{P_s}{P_g} \tag{10}$$

Lewis et al (29) also arrived at the above simplified definition for ϵ, and in addition introduced fugacities to account for real gas behaviour, thus

$$\epsilon = \frac{RT}{V_s} \ln \frac{f_s}{f_g} \tag{11}$$

The adsorbed phase molar volume V_s was however assumed to be equal to the saturated liquid volume at a pressure equal

to the adsorption pressure p_g. The adsorbed phase volume change with temperature was completely neglected. At temperatures greater than the critical, Lewis et al (29) obtained f_s by extrapolating the saturated vapor pressure curve using the Cox-Antoine relation (32).

The method of these authors has proved most popular and has been used by Kaser et al (33), Szepesy et al (34), Grent, Manes and Smith (35) and others. It should be noted that the vapor pressure extrapolation is open to question, and that the procedure for calculating V_s is not applicable at adsorption pressures above the critical.

Maslan et al (30) calculated f_s above the critical temperature, by extrapolating the vapor pressure curve in a manner similar to that used by Lewis et al (29). However, values for the adsorbate molar volume, V_s, were obtained using the extrapolated vapor pressure data and assigning compressed gas properties to the adsorbed phase. For this reason the method is not applicable much below the critical temperature, i.e. in the region where the adsorbate assumes liquid-like properties.

Toth (36) has proposed a correlation, based in part on potential theory, utilizing a pure component parameter $\left[\frac{A_d}{A_a}\right]$ related to the intercepts of slopes to the isotherm curve. This method is limited to type I isotherms, but does give excellent results when applied to hydrocarbon

data measured by Szepesy and Illes (37,38). Toth's equation predicts a constant limiting monolayer coverage independent of temperature, a condition which cannot be expected to hold over a wide temperature range.

It is seen from the above that the successful application of the potential method requires the proper evaluation of adsorbate fugacity f_s and molar volume V_s.

An improved correlation resulting from this work has been given by Cook and Basmadjian (39) and will be described in detail in following sections.

2. PREDICTION OF BINARY EQUILIBRIUM DATA

Several methods for predicting binary data from pure component isotherms are given in the literature. Most are of limited use but form the basis for further work and will be briefly discussed.

A number of pure component isotherm equations have been extended to include binary mixtures. A binary Langmuir equation has been given by Markham and Benton (40); a binary Freundlich equation by Glueckauf (41) and a binary B.E.T. equation by Hill (42). These expressions apply to binary systems in which the individual pure component isotherms are fitted by the same pure component form of isotherm equation.

Young and Crowell (20) have given several systems which do obey some particular equation. These equations,

however, often do not fit experimental data over the full range of variables, and were not applicable to the data measured by the writer.

Lederman (43) has used both Langmuir and Freundlich equations to correlate binary high pressure data for the system nitrogen-methane-Linde molecular sieve type 5A. The binary constants used, however, were not the same as those obtained from pure component data, and had to be determined experimentally.

Szepesy (44) and Toth (45) have attempted to predict binary equilibria for the more usual case in which the two pure component isotherms do not follow the same equation.

Szepesy's method (44), applicable to systems having a variable relative volatility, α, involves the use of the Markham-Benton (40) equation with "constants" dependent on coverage. In addition, Szepesy assumed that the binary data obey the volume fraction relation given by Lewis et al (46),

$$\frac{V_1}{V_{1\pi}^{\circ}} + \frac{V_2}{V_{2\pi}^{\circ}} = 1 \qquad (12)$$

which is applicable to a number of hydrocarbon systems ($\pm 6\%$) with the exception of CH_4 - C_2H_4 on silica gel. The data of Kaser et al (33) show that this expression does not hold for the system carbon dioxide - propane - vycor glass, and the N_2 - H_2, CO - H_2 data measured by the writer are similarly inapplicable.

Toth (45) has recently proposed a method for predicting binary equilibrium data from individual pure component isotherms which gives excellent results when used on the data of Szepesy and Illes (47) measured at a total pressure of 1 atm. This method utilizes a linear approximation for the $\left[\frac{A_d}{A_a}\right]$ vs. P_g relation, where $\left[\frac{A_d}{A_a}\right]$ is the pure component parameter mentioned previously. A binary parameter $\left[\frac{A_d}{A_a}\right]_{ad}$ is determined using an empirical additivity rule and the total and partial volumes calculated by a somewhat lengthy procedure.

The linear approximation for $\left[\frac{A_d}{A_a}\right]$ vs. P_g is valid over a limited pressure range ($\sim$50 - 1000 mm Hg), and does not apply to higher pressure regions.

A different semi-empirical approach was used by Lewis et al (46) based on a theoretical relation given by Broughton (48).

Broughton derived an equation, similar to the Duhem-Margules relation, which is of value in checking the consistency of adsorption equilibrium measurements of binary gas mixtures.

$$\int_0^{V_{1\pi}^\circ} \ln\left(\frac{P_1}{P_1^\circ}\right)_V \, dV = \int_0^{V_{2\pi}^\circ} \ln\left(\frac{P_2}{P_2^\circ}\right)_V \, dV \qquad (13)$$

Lewis et al (46) combined Broughton's equation with their experimentally observed volume fraction relation (equation 12), to obtain an expression for the relative volatility in terms of pure component isotherm data. This expression is valid only for systems having α constant over the whole range of binary composition, and must be solved by trial and error.

Basmadjian (1) modified the Lewis-Broughton equation and showed that for constant α systems, where

$$\alpha < 4 \quad \text{and} \quad \frac{V^{\circ}_{2\pi}}{V^{\circ}_{1\pi}} < 1.5$$

the relative volatility could be expressed by the simple relation

$$\log \alpha = \frac{1}{V^{\circ}_{1\pi}} \int_{\circ}^{V^{\circ}_1} \log \left(\frac{P^{\circ}_1}{P^{\circ}_2}\right)_V dV \qquad (14)$$

When $\left(\frac{P^{\circ}_1}{P^{\circ}_2}\right)_V$ is constant this expression reduces to

$$\alpha = \left(\frac{P^{\circ}_1}{P^{\circ}_2}\right)_{V^{\circ}_{1\pi}} \qquad (15)$$

which is analogous to Raoult's law for vapor-liquid equilibria.

Yet another approach, based on the potential theory, was used by Lewis et al (46) Maslan et al (30), and Kapfer et al (50). Lewis and Maslan used trial and error methods which gave fair results when used at low total pressure. Lewis et al (46) have stated that uncertainty exists in choosing the proper molar volume for the adsorbed phase and Maslan's method

is not applicable below the critical temperature. Kapfer et al (50) assume no binary interference, that is, each gas is adsorbed from the mixture as if the other binary component were not present, which of course holds only at low coverage.

An improved semi-empirical method has been given by Cook and Basmadjian (51) and will be described in detail in a subsequent section.

THEORETICAL CONSIDERATIONS

In the following section, details are given of two novel methods resulting from this work, which permit pure component and binary equilibria to be correlated over a wide range of variables.

1. PROPOSED METHOD FOR THE CORRELATION OF PURE COMPONENT EQUILIBRIA

It is apparent from the literature survey that the success of a potential correlation will to a large degree depend on the proper choice of values for V_s and f_s. Quantitative expressions for these variables are difficult to arrive at, but the qualitative behaviour of the adsorbate may reasonably be assumed to approach that of a liquid near the boiling point of the sorbate and a compressed gas at more elevated temperatures. It was therefore felt that the proper approach should consist in establishing an appropriate molar volume-temperature relation which would reflect this transition in adsorbate properties, followed by the computation of the fugacity f_s based on the sorbed phase molar volume and compressibility. Below the normal boiling point of the gas, the sorbed phase may be considered as a slightly compressed liquid and its molar volume approximated by that of the saturated liquid. This is in agreement with previous correlation methods as well as the underlying concepts of the BET Theory.

Above the boiling point, the adsorbate, although still in a quasi-liquid state, will be subject to increasing compression and its molar volume will as a result be less than that of the corresponding saturated liquid. Dubinin's method (28) for representing this variation in density has already been mentioned. In the present correlation, the adsorbate molar volume is expressed empirically by a linear extrapolation of the log V_L vs. log T plot. This choice was based in part on the near-linearity of the plot below the normal boiling point and also on its superiority over alternative extrapolation methods which frequently led to negative values of the adsorption potential or else yielded abnormally high adsorbate pressures. The exact position of the V_s - T line was not critical.

It should be noted that no allowance was made in this procedure for any variation of properties throughout the adsorbate. This is equivalent to assuming that the variation of interaction forces along the solid surface or perpendicular to it has no effect on adsorbed phase density or fugacity. The influence of surface heterogeneity is known to be most prominent at low coverages and a complete evaluation of its magnitude would have to be based on data extending to pressures below those considered here (< 1 mm.Hg.). It is therefore conceivable that the present correlation will prove inadequate at very low values of P_g. The effects in

the direction perpendicular to the solid surface, on the other hand, should become apparent under conditions favouring multilayer formation, i.e. well within the pressure and temperature range considered in this work. The correlations obtained appear to show no trend which would indicate such an effect. Although this does not exclude its existence, it is worth noting that there is a precedent for assuming constant adsorbate densities in the derivation of the BET equation.

The calculation of N, the moles of gas adsorbed per unit weight adsorbent, requires some additional discussion. Normally, this quantity is derived by subtracting the moles of non-sorbed gas taken up by the so-called dead space from the moles of gas admitted during adsorption measurements at the same temperature and pressure. The dead space V_{DS} has been variously defined as (52):

$$V_{DS} = V_c \tag{16}$$

$$V_{DS} = V_c - V_{solid} \tag{17}$$

$$V_{DS} = V_c - V_{solid} - V_{pore} \tag{18}$$

Equation (17) is the definition commonly used in the course of the usual helium dead space determination and yields the amount adsorbed <u>in excess</u> of non-sorbed gas occupying the same volume. In the low pressure region, all

three definitions lead to almost identical isotherms. At elevated pressures, on the other hand, the negative terms assume increasing importance in relation to the amount adsorbed and it becomes necessary to choose an appropriate value of the dead space. It can be shown that equation (16) and (17) yield isotherms which go through a maximum and then tend to negative values of N and zero respectively, while equation (18) gives the absolute adsorption uptake which increases monotonously with pressure. The latter equation is the proper expression to use in any application of the Polanyi theory, since the potential forces are visualized as acting on the <u>total</u> amount of gas present within the effective adsorption space. The use of either equation (16) or (17) was in fact found to result in poor correlation of the high pressure data.

In order to bring equation (18) more closely in line with potential theory concepts, V_{pore} is replaced by the micropore volume which may be considered as a reasonable approximation of the effective adsorption space. Thus,

$$V_{DS} = V_c - V_{solid} - V_{mic} \qquad (19)$$

For the systems under consideration here, the error caused by neglecting the gas phase in the micropores or the adsorbate in the macropores does not materially affect the calculated results.

Since values for the last two terms will often vary depending on the displacement liquid used in the measurements, it is preferable to compute their sum by subtracting the macropore volume from the total particle volume. The latter is obtained in the usual manner from the geometry and weight or by mercury displacement measurements. The macropore volume is measured by mercury injection, and comprises all pores down to a radius of 100-500 angstrom. The demarkation between the two pore classes is normally taken at the minimum of the differential pore size distribution plot.

The dead space considerations outlined above assume their full importance in the correlation of high pressure data measured by Antropoff (31) and in this work. Appropriate values of particle and macropore volume are given in Table 8. No such data is given in the work of Antropoff, but he has reported values for the solid specific volume of his adsorbent (0.474 to 0.617 cc/gm) and a micropore volume of 0.15 cc/gm evaluated indirectly from adsorption isotherms. The latter is almost certainly too low and was replaced by a value of 0.5 cc/gm in agreement with results obtained in this work for various carbons and with literature values. The specific volume of the solid was taken as 0.505 cc/gm, as recommended by Antropoff, and the dead space computed from equation (19).

Summarizing briefly, the procedure for deriving the correlation is as follows: Values of the saturated liquid molar volume are plotted against temperature on logarithmic co-ordinates (Fig. 1). At a point corresponding to the normal boiling point of the gas (or the triple point in the case of CO_2), a tangent is drawn to the curve. The resulting values of V_s are combined with PVT data reported in the literature (53-55) to arrive at the adsorbate pressure P_s for a given temperature. Fugacities are then computed using the usual relations:

for liquid adsorbate $$\ln \frac{f_s}{f_{sat.}} = \frac{1}{RT} \int_{P_{sat.}}^{P_s} V_L \, dP \qquad (20)$$

for gaseous adsorbate $$\ln \frac{f_s}{P_s} = \frac{1}{RT} \int_{o}^{P_s} \left(V_g - \frac{RT}{P} \right) dP \qquad (21)$$

To calculate N, one subtracts the amount of gas contained in the dead space defined by equation (19) from the total gas admitted to the adsorption cell and divides the resulting expression by the sample weight and standard molar volume

$$N = \left(V_{admitted} - V_c + V_p - V_{mac} \right) / W V_g^{\circ} \qquad (22)$$

The resulting values are plotted on co-ordinates of $\frac{RT}{V_s} \ln \frac{f_s}{f_g}$ vs. $\log NV_s$.

A comparison of the proposed method with that of Lewis and Maslan for the system CH_4 - carbon is shown in Fig. 2.

FIG 1

SATURATED LIQUID MOLAR VOLUME EXTRAPOLATION

FOR

ADSORBATE VOLUME DETERMINATION

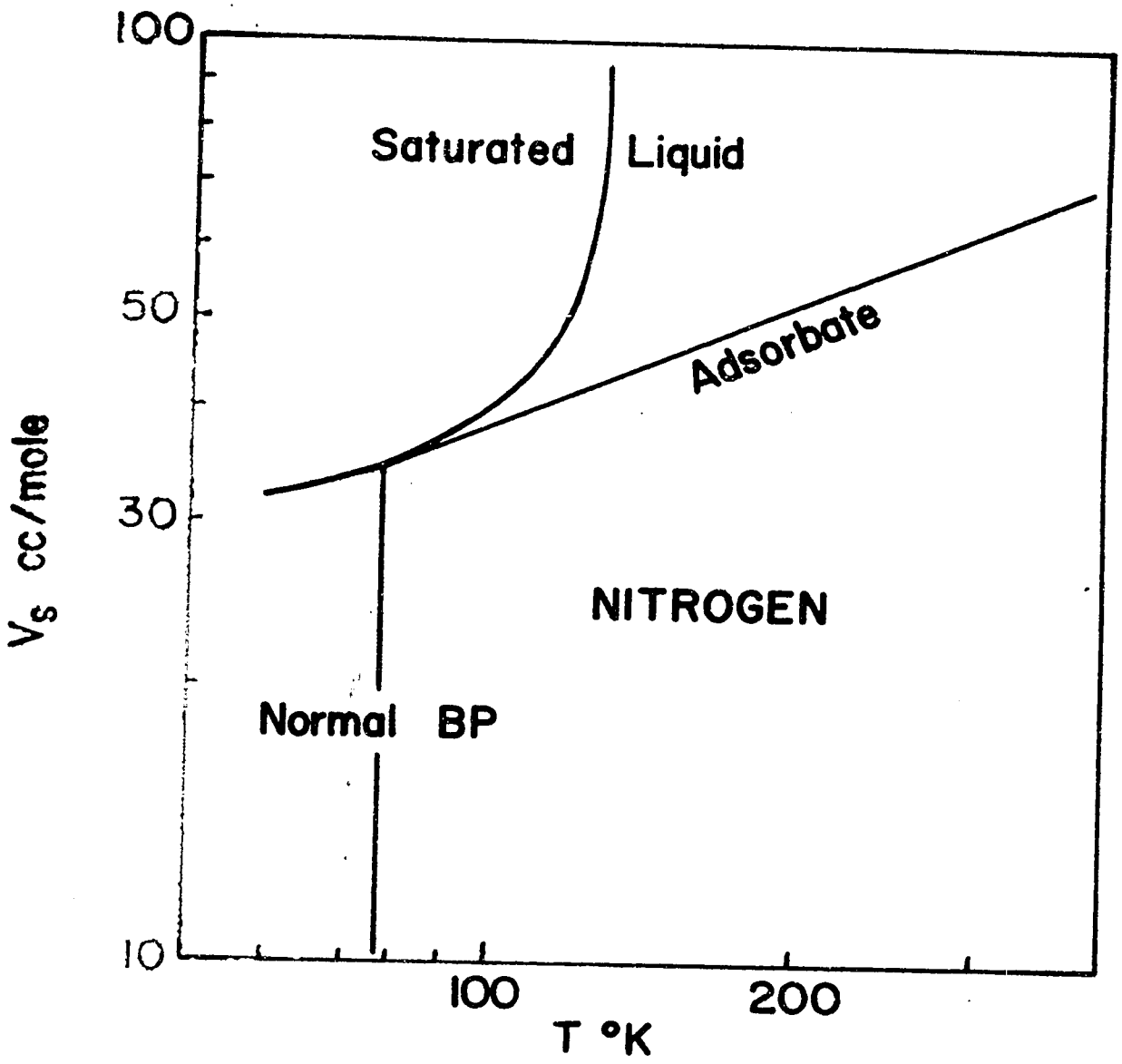
100
50
30
10
Saturated
Liquid
Adsorbate
NITROGEN
Normal BP
V_s cc/mole
100
200
T °K

FIG 2

COMPARISON OF POTENTIAL METHODS FOR ADSORPTION

OF

METHANE ON PITTSBURGH ACTIVATED CARBON

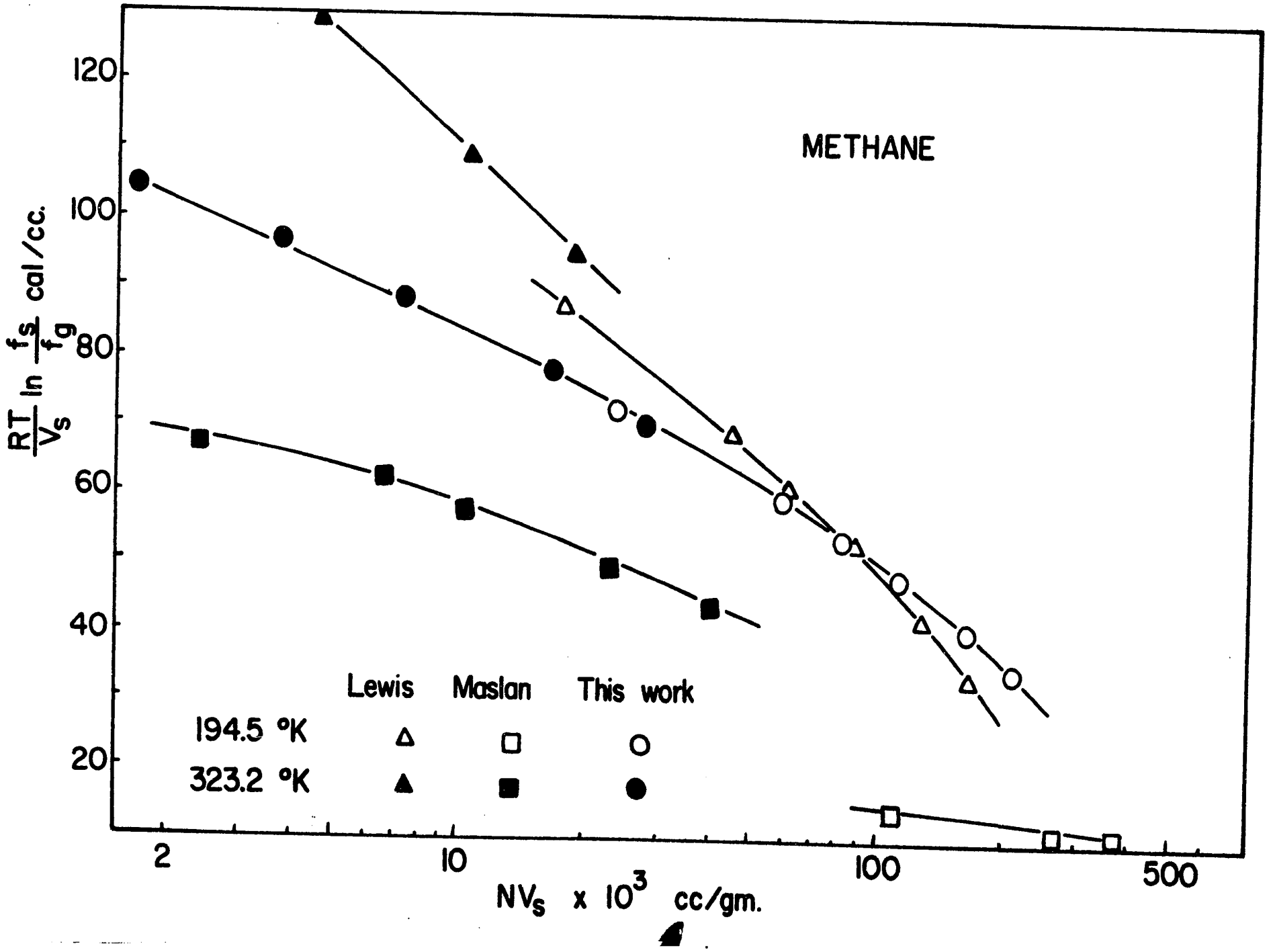
METHANE
$\frac{RT}{V_s} \ln \frac{f_s}{f_g}$ cal/cc.
120
100
80
60
40
20
2
10
100
500
$NV_s \times 10^3$ cc/gm.
Lewis
Maslan
This work
194.5 °K
323.2 °K

2. PROPOSED METHOD FOR THE PREDICTION OF BINARY EQUILIBRIA FROM PURE COMPONENT ISOTHERMS

Available methods for predicting binary equilibria (44,45,46,49) are, as indicated in the literature review, somewhat limited in their applicability. It is the purpose of the proposed method, to predict complete binary data ($V_1 = f_1(P_1)$ and $V_2 = f_2(P_2)$)at a given temperature and total pressure, solely from pure component isotherm data which extend over a sufficiently large pressure interval.

Binary systems investigated in this work have both constant and variable relative volatilities (α). Some of the binary equilibria were measured at high pressures and it was found that the pure component isotherms did not obey the same equation over a sufficiently wide range, or failed to satisfy other criteria, such as the Lewis relation (equation 12), to permit the use of previous binary correlation methods.

For a binary gas mixture in which component 2 is the more strongly adsorbed, the relative volatility α, may be defined as follows

$$\alpha_{V_T} \equiv \left(\frac{P_1}{X_1}\right)_{V_T} \cdot \left(\frac{X_2}{P_2}\right)_{V_T} \qquad (23)$$

If the relation between α_{V_T} and X_1 is considered, then

as $X_1 \rightarrow 1$; $\alpha_{V_T} \rightarrow \alpha_{V^\circ_{1\pi}}$

where $\alpha_{V^\circ_{1\pi}}$ is a "limiting" relative volatility.

Similarly $\alpha_{V_T} \rightarrow \alpha_{V^\circ_{2\pi}}$ when $X_2 \rightarrow 1$

Equation (23) has an indeterminate value for $X_1 = 1$ or $X_2 = 1$, and these limiting relative volatilities must therefore be found by some other method.

It will be assumed here that Basmadjian's (1) "pressure ratio integral" may be applied to determine the desired values for $\alpha_{V^\circ_{1\pi}}$ and $\alpha_{V^\circ_{2\pi}}$. Thus

$$\log \alpha_{V^\circ_{1\pi}} = \frac{1}{V^\circ_{1\pi}} \int_0^{V^\circ_{1\pi}} \log \left(\frac{P^\circ_1}{P^\circ_2}\right)_{V^\circ} dV^\circ \qquad (24)$$

$$\text{and } \log \alpha_{V^\circ_{2\pi}} = \frac{1}{V^\circ_{2\pi}} \int_0^{V^\circ_{2\pi}} \log \left(\frac{P^\circ_1}{P^\circ_2}\right)_{V^\circ} dV^\circ \qquad (25)$$

Using these limiting α's, end-point $\left(P/X\right)$ values for the binary $\left(P/X\right)$ vs. V_{total} curve may be obtained as follows,

$$\left(\frac{P_2}{X_2}\right)_{V^\circ_{1\pi}} = \left(\frac{P_1}{X_1}\right)_{V^\circ_{1\pi}} \cdot \frac{1}{\alpha\, v^\circ_{1\,\pi}} = \frac{\pi}{\alpha\, v^\circ_{1\,\pi}} \quad (26)$$

$$\left(\frac{P_1}{X_1}\right)_{V^\circ_{2\pi}} = \left(\frac{P_2}{X_2}\right)_{V^\circ_{2\pi}} \cdot \alpha\, v^\circ_{2\,\pi} = \pi \cdot \alpha\, v^\circ_{2\,\pi} \quad (27)$$

Referring to Fig. 3 these binary end-points are located at D and C respectively.

The binary V_T vs. P/X curves AC and BD in Fig. 3 are constructed to have the same curvature as the respective pure component curves (1) and (2) over the volume interval $V^\circ_{1\,\pi} - V^\circ_{2\,\pi}$. Pure component data can usually be plotted in linear form over this interval by an appropriate choice of co-ordinate scales. The binary curves may then be considered linear on the same scale.

Using the binary curves, the fraction X_2 may be calculated and hence also the partial isotherms $V_1 = f_1(P_1)$ and $V_2 = f_2(P_2)$ for a given total pressure π . The appropriate equation for X_2 is easily derived from the following expressions

$$P_1 + P_2 = \pi \quad (28)$$

$$X_1 + X_2 = 1$$

and is given by

$$X_2 = \frac{\left(\frac{P_1}{X_1}\right)_{V_T} - \pi}{\left(\frac{P_1}{X_1}\right)_{V_T} - \left(\frac{P_2}{X_2}\right)_{V_T}} \quad (29)$$

FIG 3

TYPICAL CONSTRUCTION DIAGRAM FOR BINARY PREDICTION

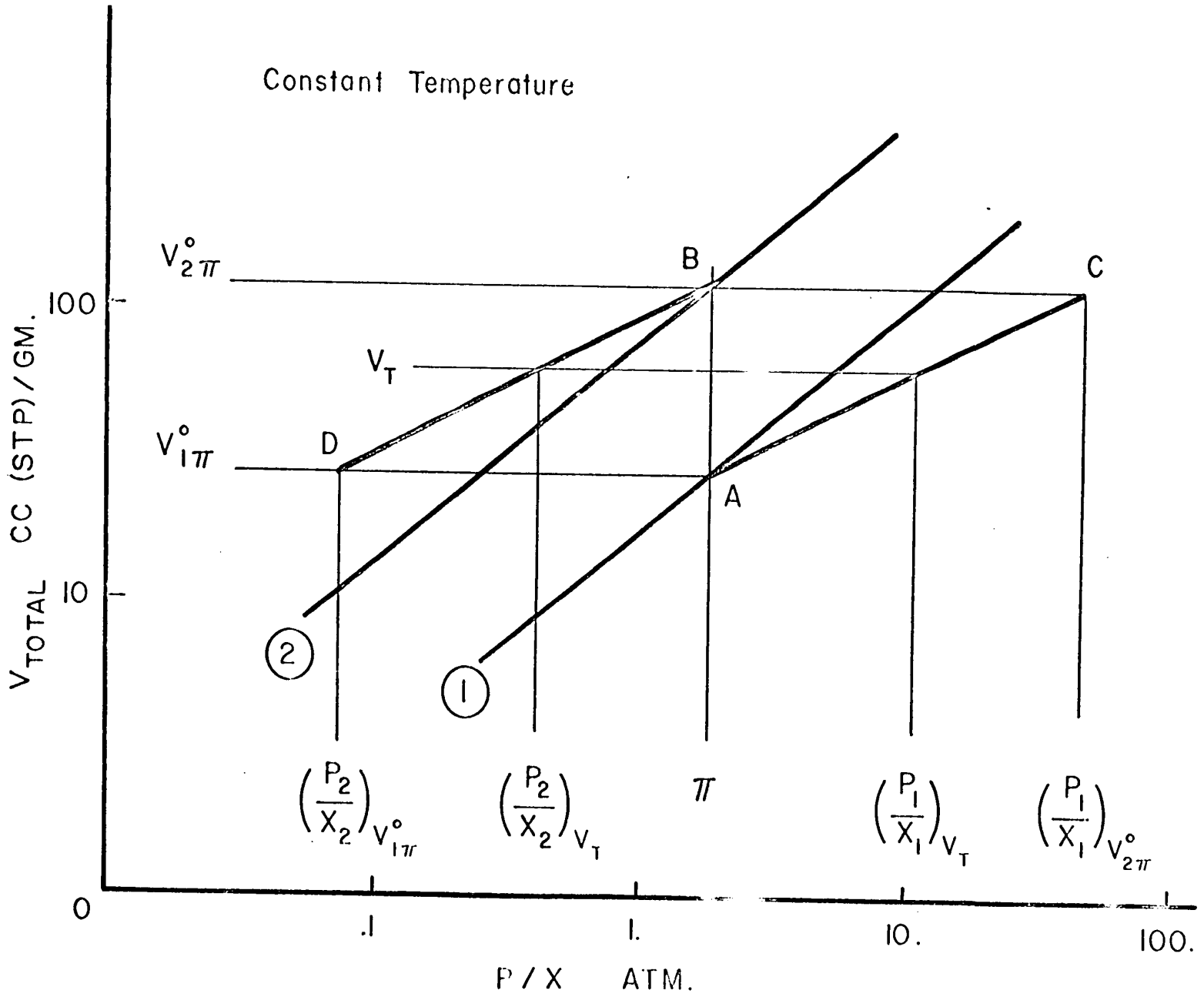
Constant Temperature
$V^{\circ}_{2\pi}$
V_T
$V^{\circ}_{1\pi}$
B
C
D
A
100
10
0
V_{TOTAL} CC (STP) / GM.
2
1
$\left(\frac{P_2}{X_2}\right)_{V^{\circ}_{1\pi}}$
$\left(\frac{P_2}{X_2}\right)_{V_T}$
π
$\left(\frac{P_1}{X_1}\right)_{V_T}$
$\left(\frac{P_1}{X_1}\right)_{V^{\circ}_{2\pi}}$
.1
1.
10.
100.
P / X ATM.

The integrations indicated in equations (24) and (25) require pressure ratio data to low coverage. This data may be difficult to measure, particularly when one component is near its normal boiling point. Typical pressure ratio curves are shown in Fig. 4. Extension to zero coverage was accomplished by linear extrapolation, a procedure verified by calculation of the individual pressure values using the previously proposed potential method. Good agreement with experimental results was obtained using this linear extrapolation.

FIG 4

PRESSURE RATIO PLOTS

DATA:

- N_2 - H_2 - Pittsburgh BPL carbon, this work
  T = 77.4°K, π = 760 mm Hg

o CO_2 - C_2H_4 - Nuxit Al carbon, data of Szepesy (47)
  T = 293°K, π = 760 mm Hg

△ A-N_2 - Silica Gel, data of Damköhler (63)
  T = 89.5°K π = 250 mm Hg

▲ Potential theory extrapolation

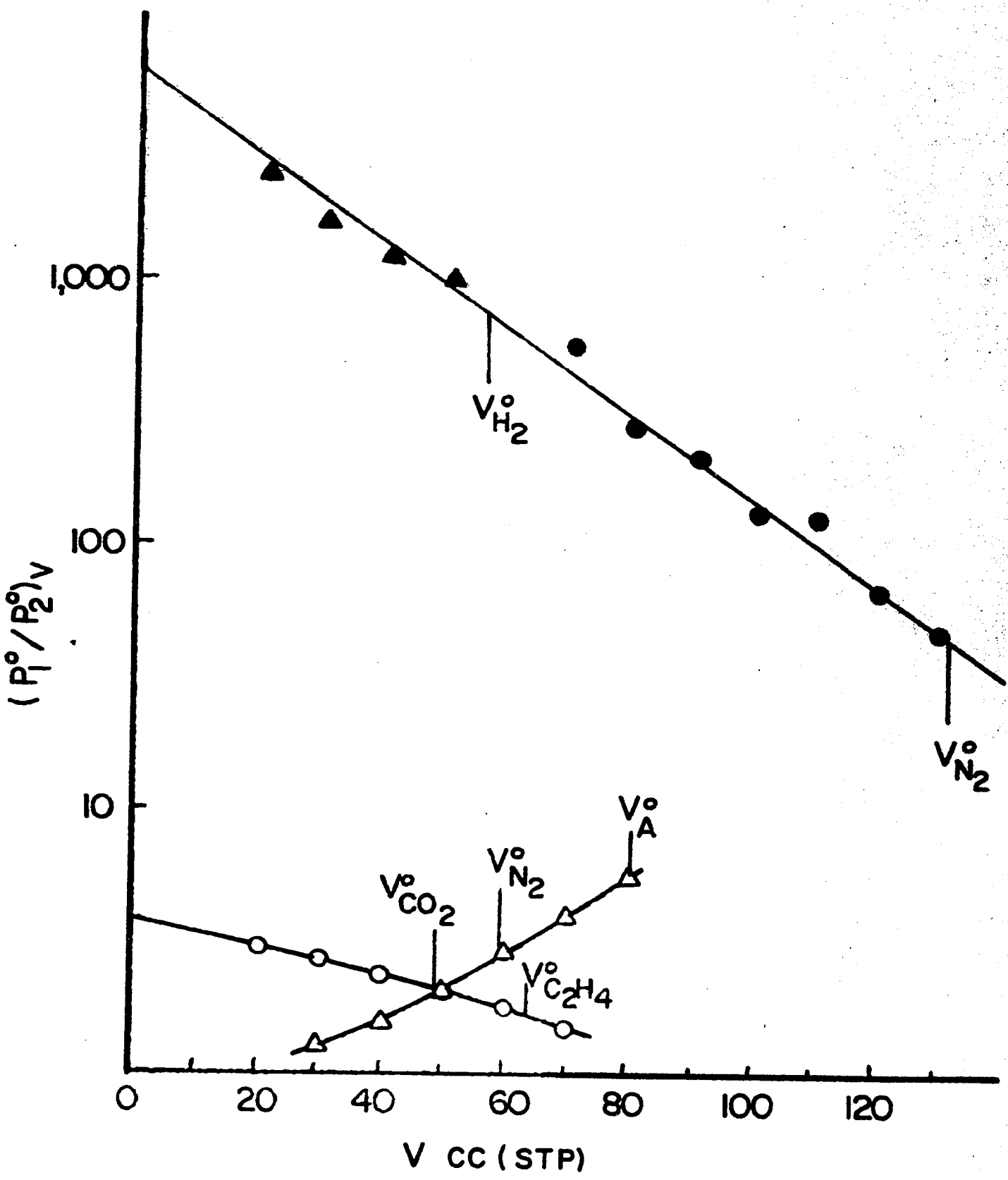
1,000
100
10
$(P_1^\circ/P_2^\circ)_V$
$V^\circ_{H_2}$
$V^\circ_{N_2}$
V°_A
$V^\circ_{N_2}$
$V^\circ_{CO_2}$
$V^\circ_{C_2H_4}$
0
20
40
60
80
100
120
V CC (STP)

EXPERIMENTAL EQUIPMENT & PROCEDURE

A description of the experimental equipment and procedures will be given, dividing each topic into high and low pressure sections (above and below 1 atm.).

General views of the experimental set-up are shown in plates 1, 2 and 3 and tabulated experimental data for pure component and binary systems are given in Appendix 1.

Tabulated information covering apparatus, adsorbents and adsorbates is given in Appendix 3, and various calibrations are described in Appendix 4.

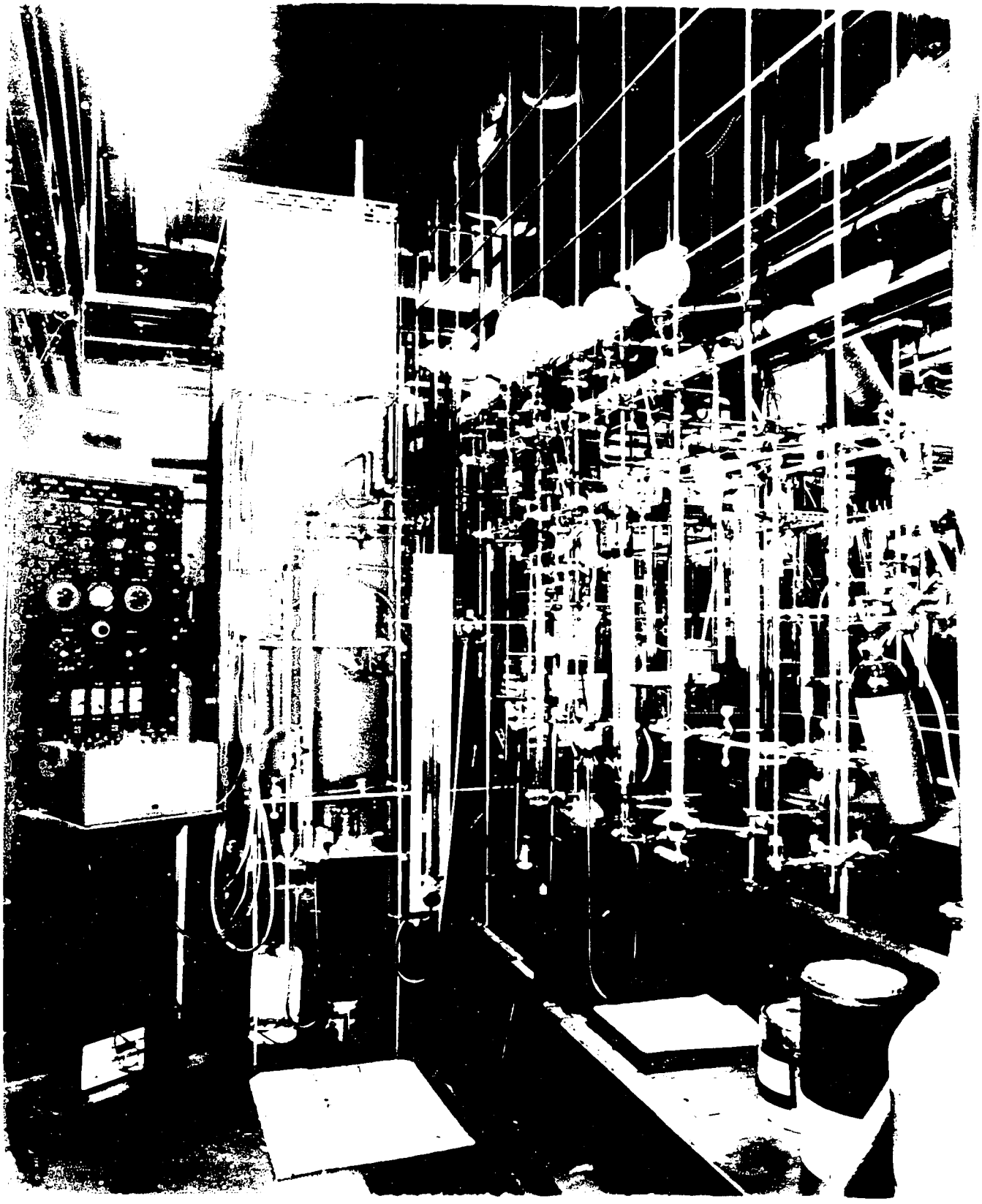

PLATE 2

VIEW OF HIGH PRESSURE SYSTEM

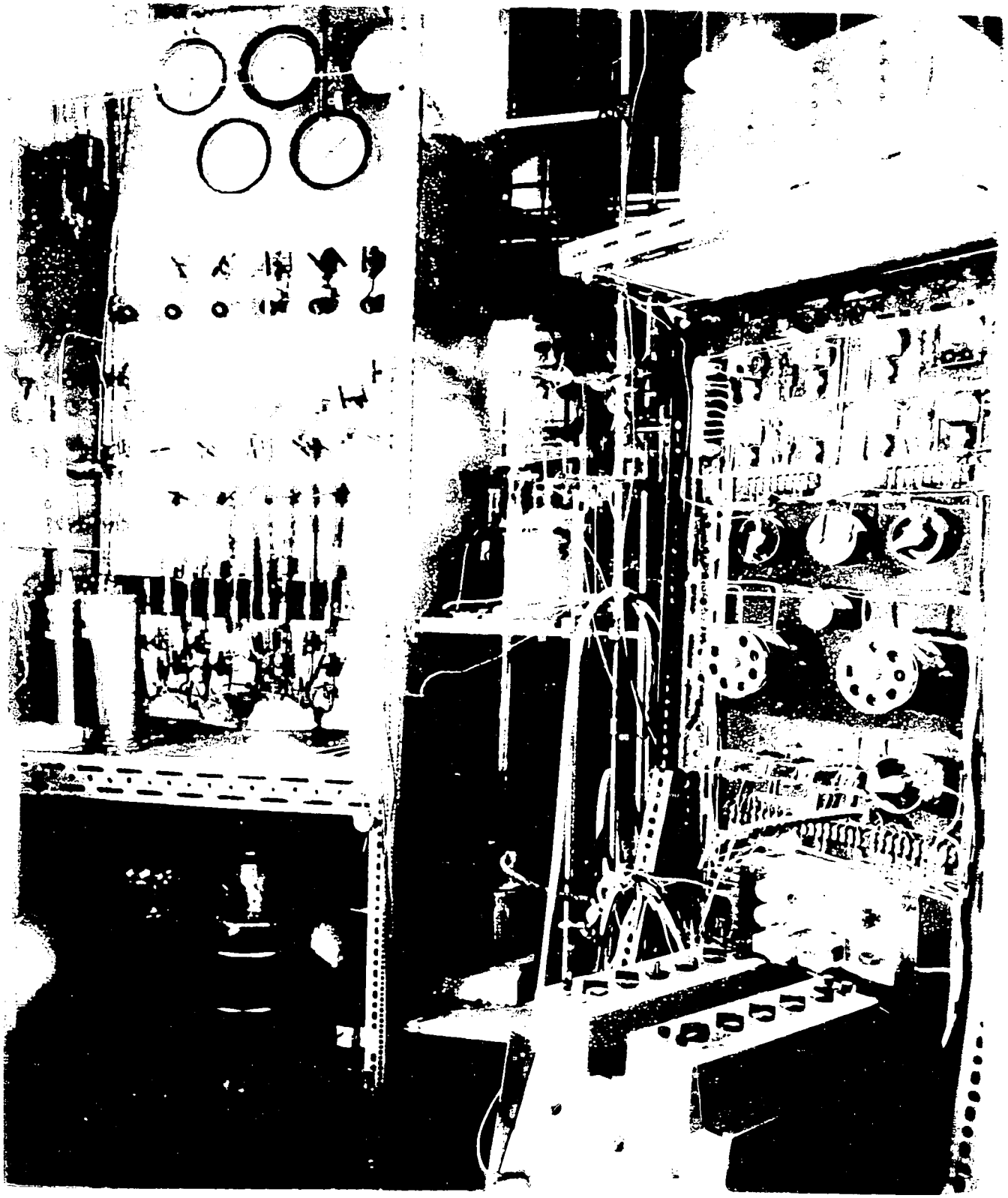

PLATE 3

VIEW OF LOW PRESSURE SYSTEM

INCLUDING BINARY MIX TANKS

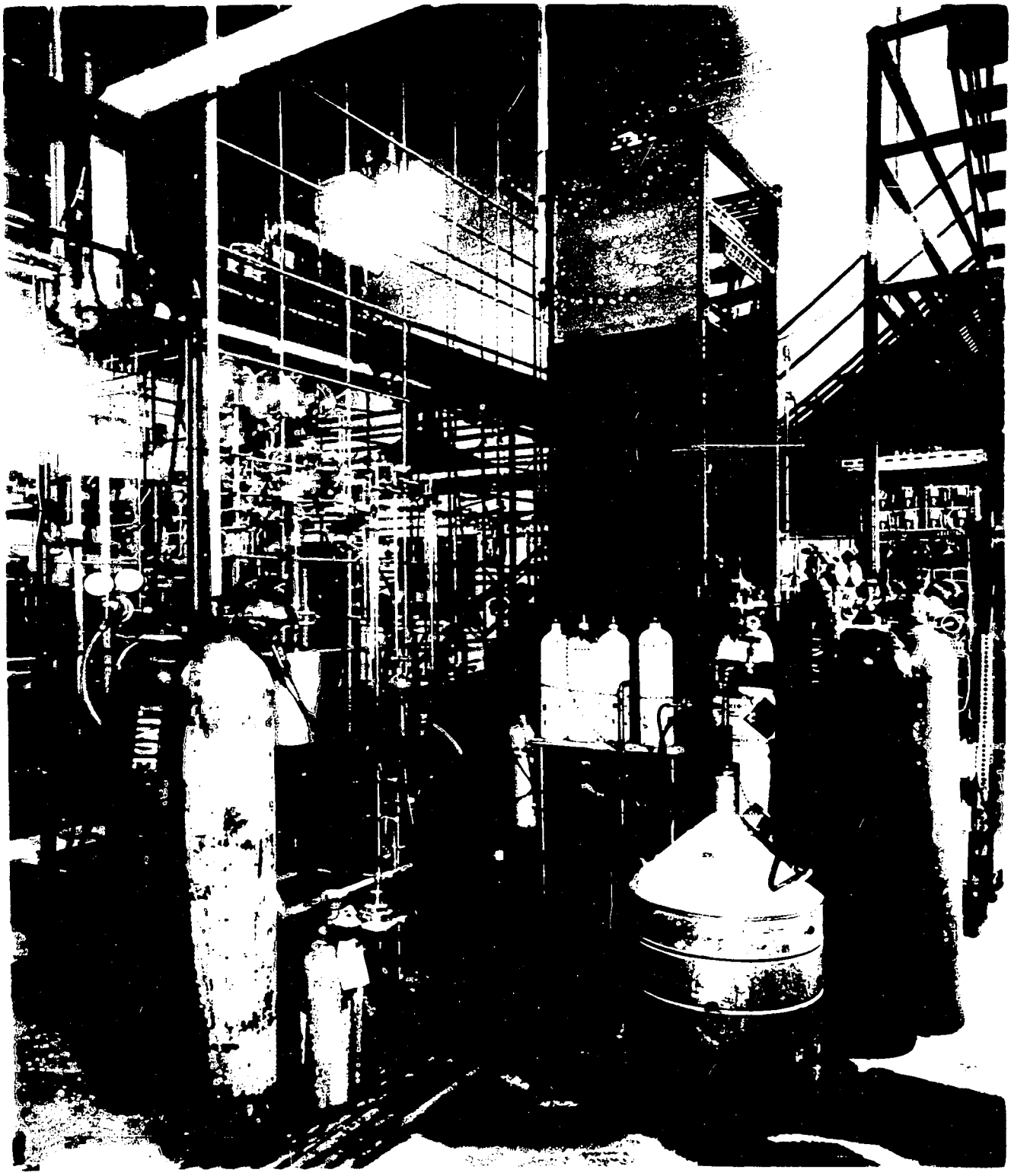
LINDE

1. HIGH PRESSURE APPARATUS

A volumetric apparatus was designed to provide flexibility of operation over wide ranges of temperature and pressure.

The design limits 77.4°K and 100 atm., required that care be taken in choosing materials of construction. To provide an additional margin of safety, the high pressure section was mounted in a heavy gauge steel enclosure, and gas volumes were kept to a minimum. No welded sections were used in the low temperature portion of the circulating loops.

A schematic diagram of the apparatus is shown in Fig. 5. The sorption system was constructed of 1/8"-316 SS tubing and Bench-scale (Autoclave) valves and fittings. Four circulating loops were carefully constructed to have equal volumes. Each loop consisted of the following:

1. a sample cell (5cc Micro-reactor) containing an aluminum sample holder, carefully machined to keep dead space to a minimum.
2. a single acting magnetically operated piston pump, constructed from a section of 3/8" steel tubing and two ball check valves.
3. gas sample volume, isolating valves, inlet and sampling valves, and necessary circulating lines.

The four cells were inserted (snug fit) into holes bored in an aluminum block which served as a heat sink. The temperature of the block was measured with a calibrated copper-constantan thermocouple located in a small diameter hole, drilled in the block.

The block and cells were thermostated in a simple cryostat shown schematically in Fig. 6. A brass sleeve cylinder wound with heating tape provided an easily demountable temperature controlled environment around the aluminum block. Powdered aluminum filled the space between the 1/8" tubing and the sleeve. Three thermistors acted as sensing elements for an on-off controller (Thermistemp) which operated the a.c. heater through an auto-transformer (Fig 7). The control sensitivity was improved by positioning the thermistors between the heating tape and the outer wall of the sleeve, and by having the 2 position on-off control act through a dummy resistor in series with the heater for half the cycle.

The thermistors had different individual resistance-temperature characteristics, and a wide range of temperatures could be covered by using the appropriate thermistor.

1. 77°K - 120°K (Keystone J-49)
2. 120°K - 150°K (Veco LOX)
3. 150°K - 210°K (Veco 21A5)

The 1/8" SS tubes and necessary electrical leads, were wax sealed into a rubber stopper which closed an outer glass vacuum jacket. The pressure in the jacket could be

FIG. 5

HIGH PRESSURE SYSTEM - SCHEMATIC DIAGRAM

1	Supply cylinders	13	Oil reservoir
2	Binary mix tanks	14	Oil filled gauge bank
3	Sample holders, 5cc "Micro" reactor	15	Autovac sensor
4	Simple cryostat	16	Calibrated bulbs
5	Magnetic single acting circulating pump	17	Constant volume mercury manometer
6,7	Sample isolating valves	18	Thermal conductivity analyzer
8	3-way sample valve	19	Toepler type sampler
9	Inlet valve	20	Pressure regulator
10,11	Manifold valves	21	To auxiliary equipment
12	Mercury seal	22	High vacuum manifold

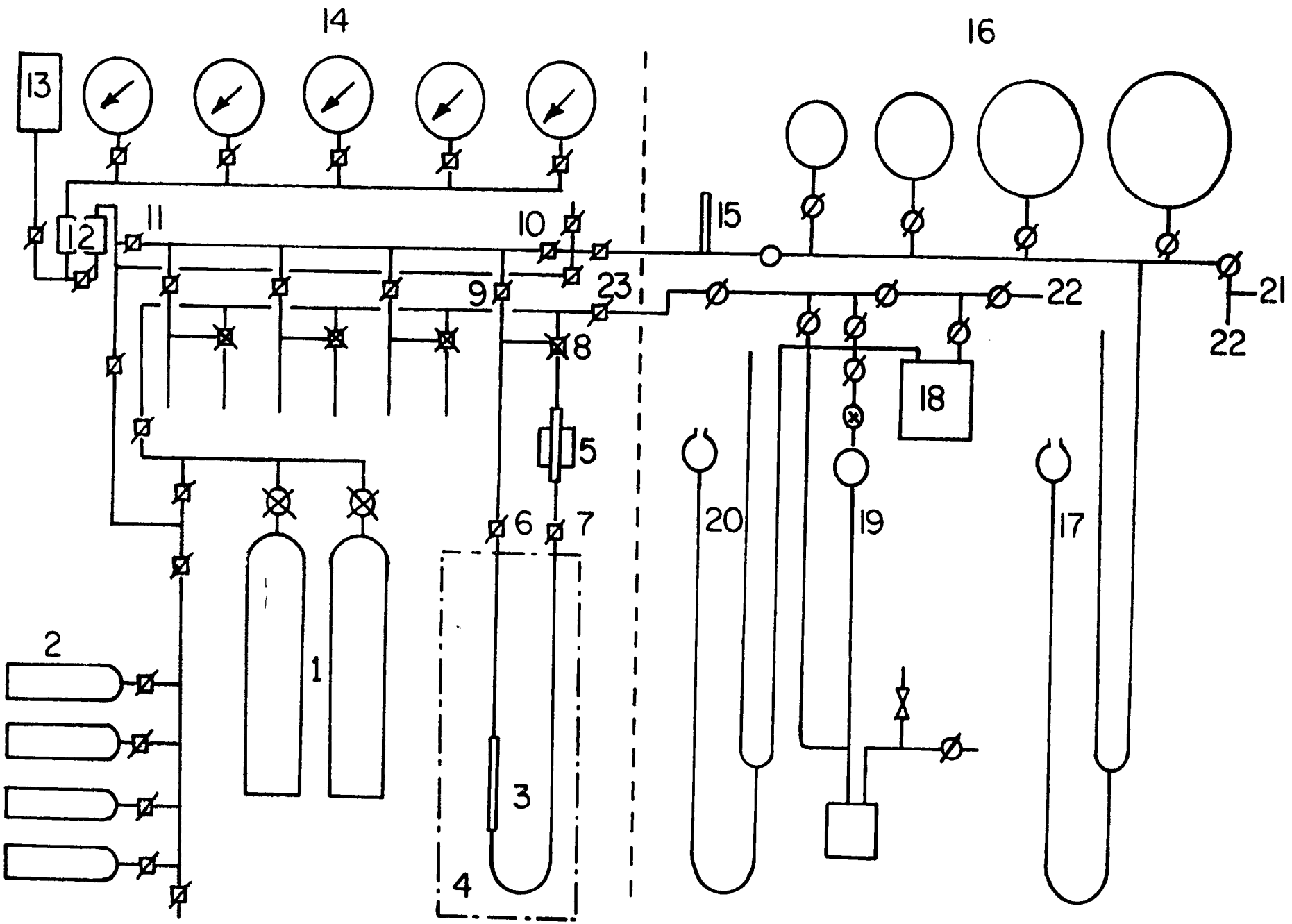
14
16
13
12
11
10
15
9
23
22
21
22
8
18
5
6
7
20
19
17
2
1
3
4

controlled by a Cartesian manostat in a vacuum line. Helium could be admitted into the jacket to increase the cooling rate at low temperatures.

Liquid nitrogen, used as a cooling medium, was contained in an outer Dewar constructed of rolled, welded 316 SS sheet. The vacuum space of the Dewar was filled with a 60% Santocel - 40% aluminum powder mixture (68) and evacuated to about 10^{-2} mm Hg. The liquid nitrogen level was maintained manually, utilizing a thermistor-activated pilot light as a level indicator.

Pressures above one atm. were measured on an oil filled bank of gauges (U.S. Gauge) separated from the gas system by a mercury seal. Pressures below one atm. were measured on a constant volume U-tube mercury manometer with mirror scale. Four gas measuring bulbs, calibrated by gas expansion and a low pressure sensing element (Autovac) were connected to the manometer manifold.

Auxiliary storage bulbs, molecular sieve gas purification cells and a gas burette were also provided. A mercury diffusion pump and a 2-stage mechanical backing pump (Duo-seal) were used for evacuating the system.

Gases were admitted to the system from supply cylinders, coupled directly to the metal system or through the low pressure manifold. Five small cylinders were provided for making up the binary gas mixtures.

FIG. 6

SIMPLE CRYOSTAT - SCHEMATIC DIAGRAM

1. Sample space ⌒ 1cc
2. Aluminum sample holder
3. 5cc "Micro" reactor
4. Aluminum block thermostat
5. Aluminum powder
6. Transite disc
7. Copper jacket
8. Heating tape
9. 1/8" 316 SS high pressure tubing
10. Cu-Const. thermocouple
11. Thermistors
12. Glass vacuum jacket
13. Liquid nitrogen level detector
14. Rubber stopper
15. Vacuum line to manostat
16. Electrical leads - wax seal

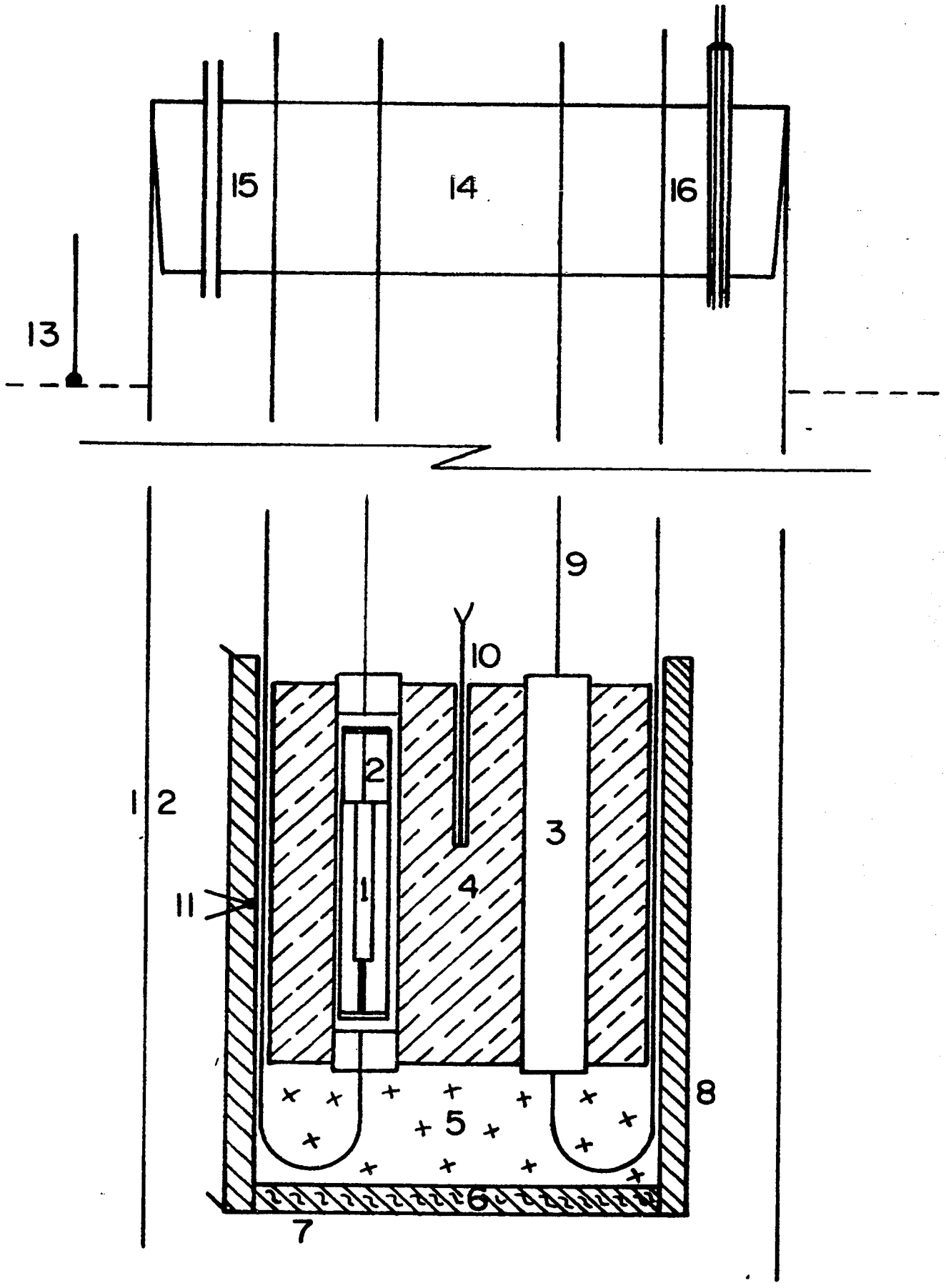
15
14
16
13
9
10
2
1
3
4
11
12
5
8
6
7

FIG. 7

CRYOSTAT TEMPERATURE CONTROL

1. Heating tape
2. Copper jacket
3. Thermistor Keystone J-49
4. Thermistor Veco LOX
5. Thermistor Veco 21A5
6. Rotary switch
7. Powerstat
8. Dummy resistor
9. Thermistemp controller RB 63

FIG. 8

THERMAL CONDUCTIVITY CELL CIRCUIT TEMPERATURE CONTROL

1. Thermistors Veco A-33. Standard Side
2. Thermistors Veco A-33. Sample Side
3. Tinsley potentiometer
4. Helipot 1000 ohm
5. Resistance - current control

6, 8, 9, 10 - Voltage adjust.

7. 12V storage battery
11. Heating tape
12. Aluminum block thermostat
13. Thermistor probe
14. Powerstat
15. Fisher temperature control

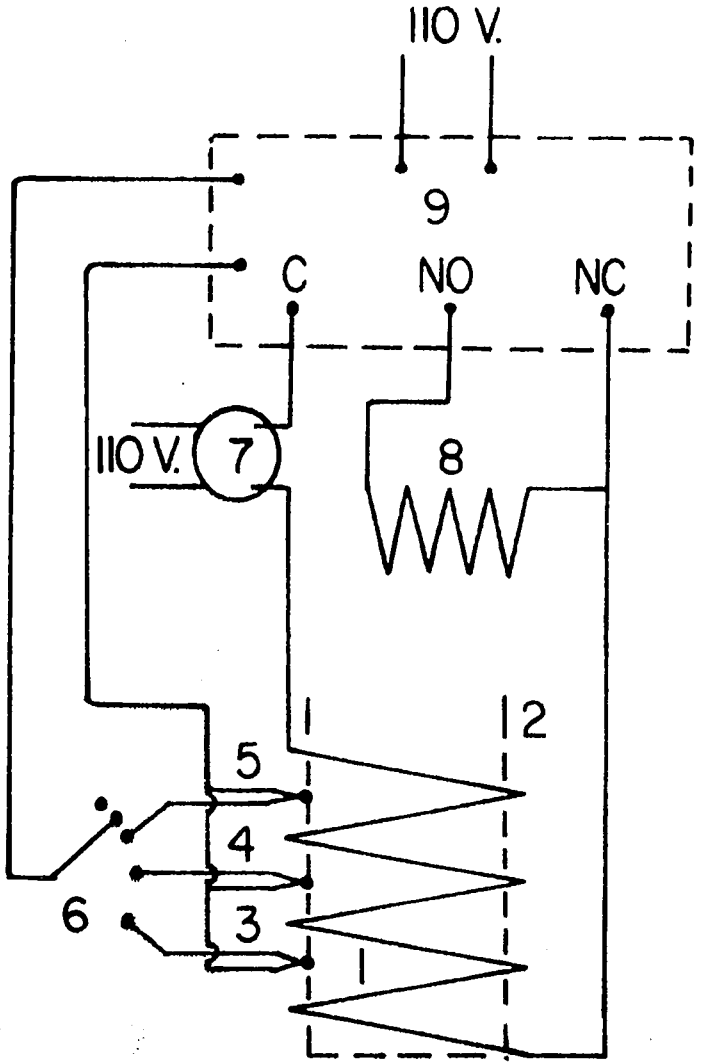
110 V.
9
C
NO
NC
110 V.
7
8
2
5
4
6
3
1

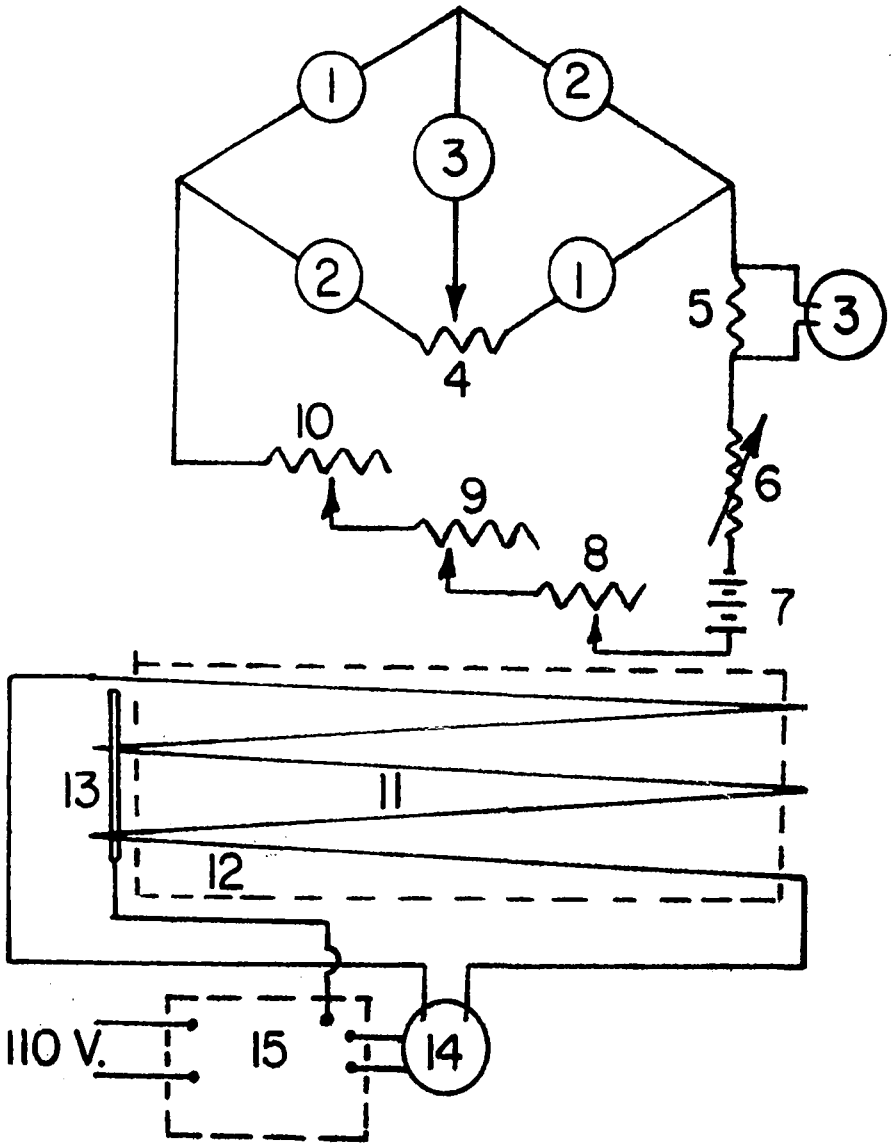
1
2
3
2
1
4
5
3
10
9
8
6
7
13
11
12
110 V.
15
14

2. LOW PRESSURE APPARATUS

A simple auxiliary volumetric glass apparatus, shown in Fig. 9, was constructed to measure adsorption isotherms at easily obtained temperatures (i.e. 77.4°K, 194.5°K, 273.2°K). Nitrogen isotherms measured on this equipment at the temperature of liquid nitrogen were used to estimate surface areas (B.E.T.).

A demountable sample bulb, tilt type McLeod Gauge (Edwards) and constant volume U-tube mercury manometer, with levelling bulb made up the sorption system. Gas volumes were measured in an air thermostated gas burette, and reduced to standard conditions.

Gases were admitted directly from cylinders through a molecular sieve drying column or from storage bulbs filled previously. A mechanical vacuum pump (Duo-seal) was connected to the manifold. Pressures above 1 mm Hg were measured on the manometer.

FIG. 9

SIMPLE VOLUMETRIC ADSORPTION SYSTEM

SCHEMATIC DIAGRAM

1. Gas inlet from supply tanks. Through dryer

2, 4, 6, 10 Isolation stop-cocks

3. Storage bulbs, 2 litre

5. Air thermostated gas burette 50cc

7. Constant volume mercury manometer with vacuum levelling bulb

8. Tilt-type McLeod gauge

9. Sample bulb in constant temperature bath

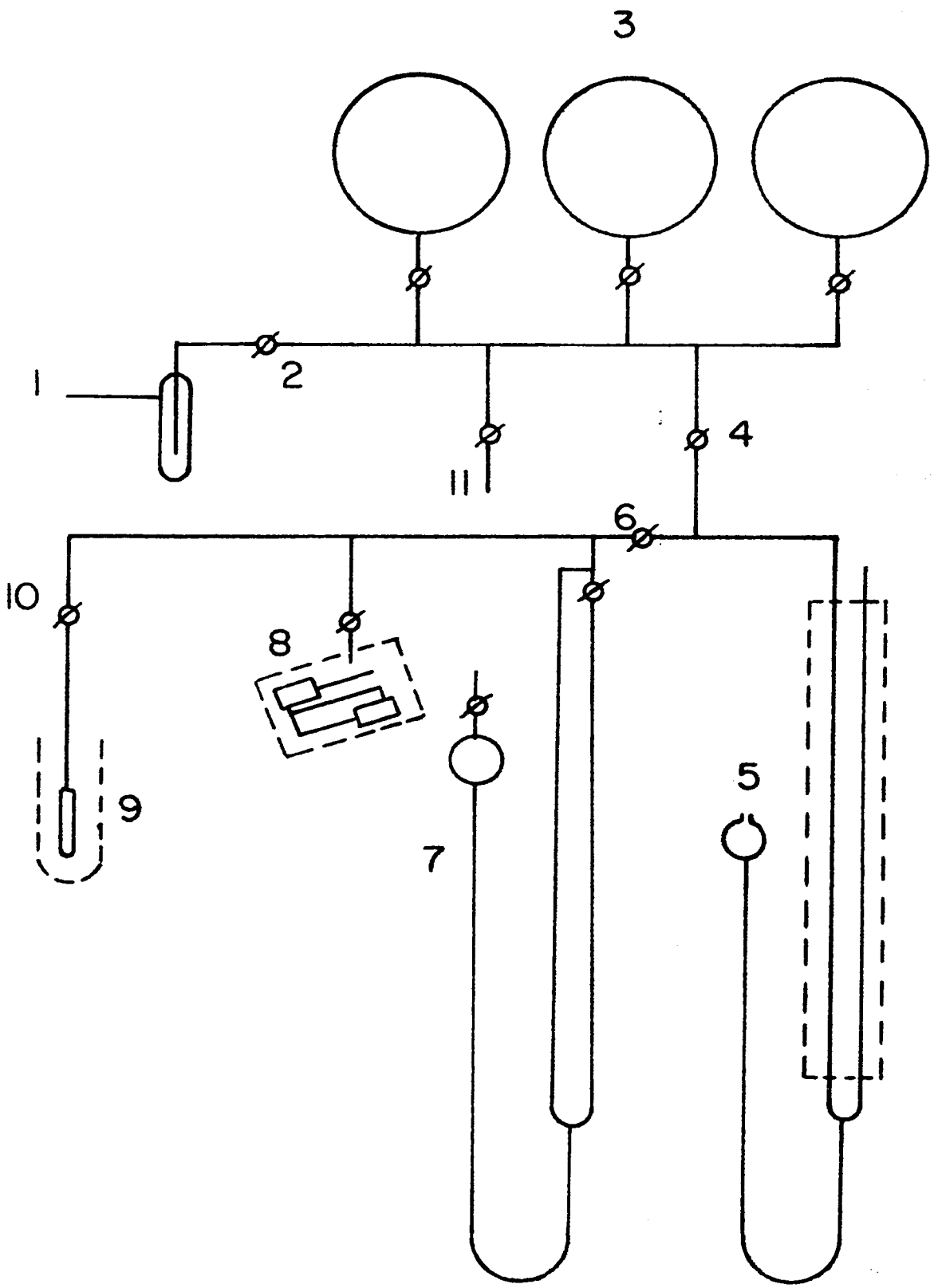
3
1
2
11
4
6
10
8
9
7
5

3. ANALYSER

Binary gas mixtures were analysed in a four element thermal conductivity cell (Fig. 8), a modification of a type used by Basmadjian (49). Four matched 2000Ω thermistors (Veco A-33) were soldered into brass capsules which were connected to the sample system, two capsules for the "standard"side and two for the "sample" side. The capsules were fitted into a large aluminum block for thermostating. A thermistor controlled (Fisher) a.c. heater and a tygon coil for thermostated cooling water were wound round the aluminum block, to provide temperature control and maximum bridge sensitivity. A Toepler type sampling device and mercury U-tube manometer were also provided. A calibrated copper-constantan thermocouple was used in conjunction with a potentiometer (Tinsley) to measure the block temperature.

The potentiometer was also used to measure the bridge imbalance for the Wheatstone bridge circuit formed by the four thermistors and the voltage drop across a standard resistor. A constant current was supplied by a 12V storage battery through several variable resistors, a milliammeter and a standard resistor.

4. ADSORBENT SAMPLE TREATMENT

Pre-activated samples of adsorbent were weighed in the aluminum sample holders of the 4-cell unit. The holders were inserted into the cells, and the samples re-activated at 350°C and 10^{-3} mm Hg for 24 hrs. Between isotherm determinations, the adsorbent samples were out-gassed at 130°C and 10^{-3} mm Hg for 12-16 hrs. When using the simple glass system, it was possible to weigh the activated samples in the evacuated sample bulb, otherwise the procedure was the same as that used for the high pressure system.

5. ADSORPTION MEASUREMENTS - LOW PRESSURE

Referring to Fig. 5, measured volumes of pure gas from a calibrated bulb 16, were admitted through valves 10 into the evacuated sorption system and allowed to contact the adsorbent thermostated in 3. Equilibrium pressures were measured on the constant volume mercury manometer 17. A series of pressure-volume measurements were made in a stepwise manner, and the pressures recorded when they did not change over a period of 10 or 15 minutes. The time required to reach equilibrium varied from a few minutes to an hour or more.

A similar set of measurements was also made, using a cell containing no adsorbent, to provide dead space data.

Binary gas mixtures were made up in mix tanks 2, and allowed to stand a minimum of 24 hrs. before being used. This was found sufficient to achieve complete mixing. Binary measurements at a total pressure of one atm. were carried out, by admitting a previously analysed gas mixture from a mix tank into a calibrated bulb 16, and then admitting a measured volume into the evacuated system through valves 10, until the total pressure over the adsorbent was raised to 1 atm. Inlet valve 9 was closed, and the gas mixture circulated over the adsorbent. The magnetic pump 5 was operated by energizing a solenoid periodically using a synchronous pulse timer. Pumping speeds of about 15 cc/min. were used in all experiments. The total pressure was checked intermittently, and additional quantities of the feed mixture admitted to maintain the desired total pressure. It was found in preliminary experiments that a circulation time of three or four hours was more than sufficient for equilibrium to be obtained.

For analysis, the sample isolating valves 6 and 7 were closed and a gas phase sample withdrawn through 8 into the previously evacuated sample line and analyser 18. Sufficient sample was taken by the Toepler device 19, to raise the sample gas pressure in the analyser to 1 atm.

6. ADSORPTION MEASUREMENTS - HIGH PRESSURE

The volume of pure gas adosrbed at pressures above one atmosphere was measured in two steps

1. Volume adsorbed - zero to 1 atm.
2. Volume desorbed - from the adsorption pressure to 1 atm.

To eliminate any possibility of bulk condensation, high pressure measurements were made only very near or above the critical temperature.

The adsorption step was identical to that described previously for low pressures. Reference is again made to Fig. 6. Pure gas from the supply cylinders 1 was admitted through 11 to contact the adsorbate 3. The pressure was raised to the desired adsorption pressure, measured on gauges 14, and the system allowed to reach a constant pressure. Valve 11 was closed and the gas desorbed through 10 and allowed to expand into the measuring bulb 16 until a steady pressure of 760 mm Hg over the adsorbent was obtained.

Binary measurements were made by admitting gas mixtures from the mix tanks 2 through valve 11 into the adsorption system until the desired total pressure was reached. With valve 9 closed, the gas mixture was circulated, keeping the total pressure constant by admitting additional gas from the mix tank. The gas phase was again circulated to constant composition, sampled and analysed.

The system was then desorbed through valves 9 and 10 with 11 closed until, with circulation, a new steady gas pressure equal to 760 mm Hg was obtained in the circulating loop. The desorbed volume was determined in the measuring bulb 16. Residual gas in the loop was sampled and analysed and its volume obtained from previous adsorption measurements at 1 atm.

7. GAS ANALYSIS

The thermal conductivity analyser was first calibrated with known binary mixtures, made up in the calibrated bulbs 16. Measurements were made by balancing the bridge circuit with a pure gas in both sections, then measuring the bridge imbalance when pure gas was replaced with a binary mixture in the sample side of the bridge. The bridge current was kept constant at a value giving maximum bridge imbalance for the two pure binary components.

Unknown mixtures were analysed in the same manner, the composition being determined from the calibration data.

A slight change in calibration due to ortho-para conversion was observed for hydrogen in contact with charcoal adsorbent at 77.4°K and 100°K, and a shift factor was introduced to allow for this effect. Similar results have been reported by Basmadjian (49).

Gas phase compositions for inlet and equilibrated samples, obtained by this method of analysis, were combined

with inlet and gas phase volumes to calculate adsorbed phase equilibrium compositions and volumes.

DISCUSSION OF RESULTS

The following section is devoted to a discussion of the results of this work and is divided into three parts:

A. Measurement errors and calculation of equilibrium data.

B. Correlation of pure component data.

C. Prediction of binary equilibria.

A. Measurement Errors & Calculation of Equilibrium Data

1. Isotherms were obtained by measuring the following variables,

a) total volume of gas in the adsorbent filled cell

b) total volume of gas in the empty cell

c) temperature of the cryostat

d) equilibrium adsorbate gas pressure

e) gas composition (for binary mixtures)

Maximum errors in the prime measuring variables (temperature, pressure, composition) are given in Table 2.

TABLE 2

Measurement Errors

1.		Temperature control		
	a)	Cryostat	77°K	$< \pm$ 0.1°C
			210°K	$< \pm$ 0.5°C
	b)	Conductivity cell		$< \pm$ 0.1°C
2.		Pressure measurement		
	a)	Hg manometer		$\pm$ 0.25 mm Hg
	b)	Press. gauge		$\pm$ 1/4% full scale
		(e.g. 0-600 gauge	$\equiv$	$\pm$ 1.5 psi)
3.		Gas composition	$<$	$\pm$ 0.002 mole fraction

Gas volumes were measured, as noted previously, in bulbs calibrated at room temperature by gas expansion from a burette. The calibration was assumed to be linear, and was adjusted for ambient temperature fluctuations in increments of 0.5°C. Because all volumes were measured at room temperature and pressures below 1 atm, ideal gas behaviour was assumed and a single calibration, made with nitrogen, used for all the pure gases and also for the binary mixtures.

The total volume of gas in the adsorbent-filled cell was measured as described previously in two steps, by adsorption up to 1 atm and desorption down to 1 atm from higher adsorption pressures. The amount adsorbed was calculated according to equation (22). The gas equivalent for the pellet-macropore term was calculated by multiplying the pellet and macropore volumes (determined by mercury displacement and penetration, respectively, (Table A3-3) by the appropriate value of the Amagat density $\frac{V_g^\circ}{V_g}$ taken from the literature (53-55). Thus,

$$V_p - V_{mac} = (v_p - v_{mac}) \frac{V_g^\circ}{V_g} \qquad (30)$$

A sample of the calculations necessary to obtain the volume adsorbed is given in Table 3 and an estimate of the maximum variation in the volume adsorbed due to temperature and pressure measurement errors in Table 4.

Assuming that all the gases measured behave in about the same way, the maximum error involved in calculating the total volume of gas adsorbed is shown to be ± 1% due to errors in volume measurement plus an additional ± 0.5cc/gm due to temperature and pressure errors.

2. Low pressure measurements (1 to 10 mmHg) were checked for thermal transpiration corrections using the method of Laing (56). This semi-empirical method relates the measured pressure to the true adsorption pressure, and takes into account the ambient and adsorption temperatures, the diameter of the interconnecting tubing, and the nature of the adsorbate gas. In all cases, pressure corrections could be neglected. For example, the correction for a nitrogen pressure measurement of 7.6 mm Hg at 300°K when the adsorption temperature was 77.4°K, amounted to less than 10^{-3} mm Hg for 1/16" ID connecting tubing.

TABLE 3

SAMPLE CALCULATION - VOLUME ADSORBED

System: H_2 - Pittsburgh BPL Carbon

Temp.	77.4°K	Sample weight	0.3241 gm
Press.	28.5 atm	Macropore volume	0.30 cc/gm
Amagat $\frac{V_g^\circ}{V_g}$	103	Pellet volume	1.22 cc/gm

Sample correction $(v_p - v_{mac})$ = 0.30 cc

	ADSORBENT CELL	EMPTY CELL
Volume in (0 to 1 atm)	51.2	10.2
Volume out (28.5 to 1 atm)	315.8	299.4
Total gas in cell	367.0	309.6
$(v_p - v_{mac})\ \frac{V_g^\circ}{V_g}$		30.5
Dead space	279.1	279.1
Volume adsorbed	87.9 cc STP	
	≡ 271.0 cc STP/gm	

TABLE 4

MEASUREMENT ERROR - GAS VOLUME MEASUREMENT

System: H_2 - Pittsburgh BPL Carbon

T = 77.4°K P = 28.5 atm

Sample weight = 0.4360 gm

1. Pressures (mm Hg) in 200 cc Collector bulb

(max. error ± 0.25 mm Hg)

Desorption (28.5-1 atm)		Adsorption (0 - 1 atm)	
ADSORBENT CELL	EMPTY CELL	ADSORBENT CELL	EMPTY CELL
+ 724.0 ± 0.25	+ 723.2 ± 0.25	+ 287.8 ± 0.25	+ 249.5 ± 0.25
- 64.1 ± 0.25	- 71.9 ± 0.25	- 97.5 ± 0.25	- 212.0 ± 0.25
+ 704.2 ± 0.25	+ 644.5 ± 0.25		
- 191.0 ± 0.25	- 187.5 ± 0.25		
1173.1 ± 1.0	1108.3 ± 1.0	190.3 ± 0.5	37.5 ± 0.5

2. Calculation of Sorbed Volumes

	Desorption		Adsorption	
	Adsorbent Cell	Empty Cell	Adsorbent Cell	Empty Cell
Ambient Temp. (°C)	25	24	25	23.5
Bulb constant (cc STP/mm Hg)	.26924	.27013	.26924	.27059
Bulb Pressure (mm Hg)	1173	1108	190.3	37.5
Volume measured (cc STP)	315.8 ± 0.27	299.4 ± 0.27	51.2 ± 0.14	10.2 ± 0.14

3. Summary of Adsorbed Volumes (cc STP)

	ADSORBENT CELL	EMPTY CELL
Volume measured (adsorption)	51.2 ± 0.14	10.2 ± 0.14
Volume measured (desorption)	315.8 ± 0.27	299.4 ± 0.27
Total volumes	367.0 ± 0.41	309.6 ± 0.41
Pellet and pore (assume error small)		- 30.5
Dead space	- 279.1 ± 0.41	279.1 ± 0.41
Volume adsorbed	87.9 ± 0 8	
	≡ 271 0 ± 2.7 cc STP/gm	

TABLE 5

MEASUREMENT ERROR - TEMPERATURE AND PRESSURE

System: N_2 - Pittsburgh BPL Carbon

1.	P atm	T °K	V cc STP/gm	ΔP	ΔT	ΔV	Max. Error
(a)	1	77.4	300.0				
	1	100.0	212.0	-	22.6	88.0	± 0.1 °K
(b)	28.5	210.0	120.0				
	28.5	297.0	66.0	-	87.0	54.0	± 0.5 °K
(c)	0.790	77.4	283.3				
	0.906	77.4	294.5	90	-	11.2	± 0.25 mm Hg
(d)	24.2	210.0	113.2				
	31.1	210.0	118.1	6.9	-	4.9	± 0.1 atm

2. Volume error (cc STP/gm)

(a) $\pm 0.1 \times \frac{88}{22.6} = \pm 0.4$

(b) $\pm 0.5 \times \frac{54}{87} = \pm 0.3$

(c) $\pm 0.25 \times \frac{11.2}{90} = \pm 0.03$

(d) $\pm 0.1 \times \frac{4.9}{6.9} = \pm 0.07$

∴ Maximum error in volume measurement due to errors in pressure measurement and temperature fluctuation ≐ 0.5 cc STP/gm

3. The total volume of gas adsorbed from binary mixtures was calculated in a similar manner to that used for pure components. The amount of gas desorbed, from the total pressure π to 1 atm was readily measured. However, due to the large variation with concentration of the amount adsorbed for some systems (N_2-H_2; H_2-CO) it was necessary to calculate the total volume of gas remaining in the adsorption cell at 1 atm (after desorption) using the gas phase composition of the residual.

The dead space volume, measured in the empty cell, was also adjusted for any slight change due to gas phase composition.

Solid and micropore volume corrections were made, using an assumed linear relation between the pure component Amagat densities and the composition of the gas phase

$$\left(\frac{V_g^\circ}{V_g}\right)_{mix} = Y_1\left(\frac{V_g^\circ}{V_g}\right)_1 + Y_2\left(\frac{V_g^\circ}{V_g}\right)_2 \qquad (31)$$

Solid and micropore volume corrections calculated using Kay's pseudo-critical method (69) were not significantly different from those calculated by equation (31).

Sample calculations for a typical set of binary data are given in Table 6.

TABLE 6

BINARY DATA SAMPLE CALCULATION

System: N_2 - CO - Pittsburgh BPL Carbon

210°K 28.5 atm

1. Solid sample wt. 0.4360 gm

2. Gas analysis

	% CO
Inlet gas	43.11
Equilibrium gas phase	41.53
Residual gas phase	49.00

3. Gas volumes measured

	cc STP	
	SAMPLE CELL	EMPTY CELL
Gas admitted (0 - 1 atm)	27.5	12.4
Analysis sample volume	225.2	225.2
Gas vented (28.5 - 1 atm)	159.7	135.7
	412.4	373.3
Pore and solid correction		15.6
Dead space	357.7	357.7

Total volume adsorbed 54.7 cc STP

4. Carbon monoxide balance

	cc STP
Inlet gas .4311 × 412.4	177.78
Equilibrium gas .4153 × 357.7	148.55
Carbon monoxide sorbed	29.23
Nitrogen sorbed	25.47

5. Summary

P_{N_2} - 16.7 atm V_{N_2} - 58.4 cc STP/gm

P_{CO} - 11.8 atm V_{CO} - 67.0 cc STP/gm

An error analysis, for the sample binary calculations shown in Table 6, has been made using a "range" method (57) and the results are given in Table 7. This method combines limit values for the variables so as to obtain the maximum and minimum possible values for the calculated data. A maximum error of $\pm$ 7.5% is thus obtained for carbon monoxide adsorption in the N_2-CO binary at 210°K and π = 28.5 atm. The error may be as high as $\pm$ 10% using this method, for systems having large amounts adsorbed.

TABLE 7

ERROR PROPAGATION IN BINARY CALCULATIONS

System: N_2 - CO - Pittsburgh BPL

T = 210°K π = 28.5 atm

Adsorbent sample wt. 0.4360 gm

1. Measured data

Total gas mixture into cell	412.4 cc STP
Gas phase volume	357.7 cc STP
Inlet gas composition	43.11% CO
Equilibrium gas comp.	41.53% CO
Maximum volume error	± 0.75 cc STP
Maximum analysis error	± 0.002 mole fraction

2.

CO balance (cc STP)	Max.	Measured	Min.
Total gas in	413.15	412.4	211.65
Gas phase	356.95	357.7	358.45
Total Adsorbed	56.2	54.7	53.2
CO in	178.94	177.78	176.64
CO gas phase	147.53	148.55	149.58
CO adsorbed	31.41	29.23	27.06
N_2 adsorbed	24.79	25.47	26.14

3. Summary

	Volume adsorbed (cc STP/gm)		
	Max.	Measured	Min.
CO	72.04	67.04	62.06
N_2	56.86	58.42	59.95
Total	128.90	125.46	122.01

B. POTENTIAL CORRELATION FOR PURE COMPONENT ISOTHERMS ON CARBON ADSORBENTS

The modified potential theory correlation proposed in the theoretical discussion, was applied to data measured in this work as well as literature data. Table 8 summarizes some of the values calculated in the course of deriving a typical characteristic curve. The final result is plotted in Fig. 10 and additional potential diagrams are given in Appendix 2.

The data, with the exception of hydrogen, correlated within $\pm$ 10% over most of the temperature and pressure range covered with occasional errors of 30% at low coverage ($<$ 10 cc STP/gm). Hydrogen data measured by the writer and Van Dingenen (70) showed some deviation with temperature, but still correlated within $\pm$ 20% over the temperature interval considered.

TABLE 8

SAMPLE CALCULATION

Adsorbate - Nitrogen

Adsorbent-Pittsburgh BPL 6 x 16 Activated Carbon

T = 210°K

V_s = 53.6 cc/mole

P_s = 423 atm

f_s = 368 atm

Pellet volume: 1.22 cc/gm

Macropore Volume: 0.30 cc/gm

Micropore Volume: 0.44 cc/gm

Average Micropore Radius: 10 angstrom

P atm	f_g atm	Volume Adsorbed cc STP/gm	$NV_s \times 10^3$ cc/gm	$\frac{RT}{V_s} \ln f_s/f_g$ cal/cc
.1		6.7	16.0	63.9
.5		21.9	52.4	51.4
1.0		33.0	79.0	46.0
4.4	4.38	64.0	153.1	34.5
7.8	7.68	79.5	190.5	30.1
28.2	27.0	116.0	278.0	20.3
52.0	43.3	133.0	318.0	15.8
			450 limiting value	

FIG. 10

POTENTIAL DIAGRAM

DATA: THIS WORK

SYSTEM: N_2 - PITTSBURGH BPL CARBON

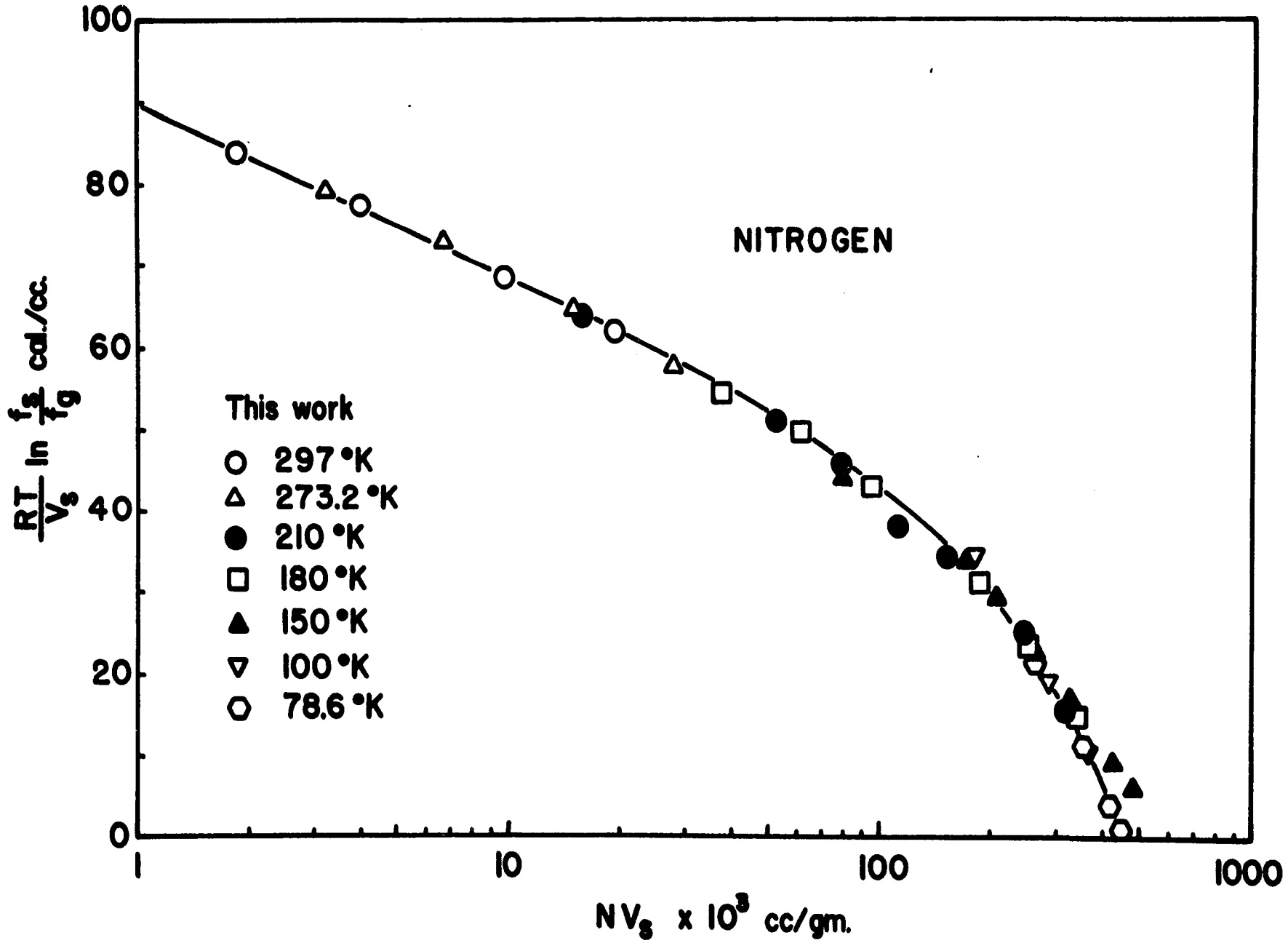
NITROGEN
This work
297 °K
273.2 °K
210 °K
180 °K
150 °K
100 °K
78.6 °K
$\frac{RT}{V_s} \ln \frac{f_s}{f_g}$ cal./cc.
$NV_s \times 10^3$ cc/gm.
0
20
40
60
80
100
1
10
100
1000

To test the accuracy of the present correlation, isotherms for the system N_2 - Pittsburgh BPL activated carbon were calculated from a single characteristic curve (Fig. 10) and compared with measured values in Fig. 11. The inclusion of the V_s term in both ordinate and abscissa does not distort the correlation, and in fact even rather large variations in the potential curve do not alter the isotherms to any great extent. A comparison of the proposed method with those of Lewis et al (29) and Maslan et al (30) for the system methane - activated carbon is shown graphically in Fig. 2. The methods of Lewis and Maslan do not give single characteristic curves for this system.

The potential curves obtained using the present method (Appendix 2) all have a characteristic parabolic shape at higher coverage, and intersect the abscissa at a point corresponding to the limiting uptake of the micropore volume as noted previously by Dubinin (28). However, unlike the correlation proposed by Lewis and co-workers (29) the present method does not yield single characteristic curves for saturated and unsaturated hydrocarbons. This disadvantage is partially offset by the fact that a plot ϵ^2 vs. log NV_s gives a straight line for higher coverage ($NV_s > 20\text{-}30 \times 10^{-3}$) which can be located in principle by a single adsorption measurement and a knowledge of the adsorbent micropore volume. The data of Ray and Box (58) are shown in linear form in Fig. 12.

FIG. 11

COMPARISON OF ISOTHERMS CALCULATED

FROM

POTENTIAL PLOT WITH EXPERIMENTAL DATA

DATA: THIS WORK

SYSTEM: N_2 - PITTSBURGH BPL CARBON

— PREDICTED

• EXPERIMENTAL

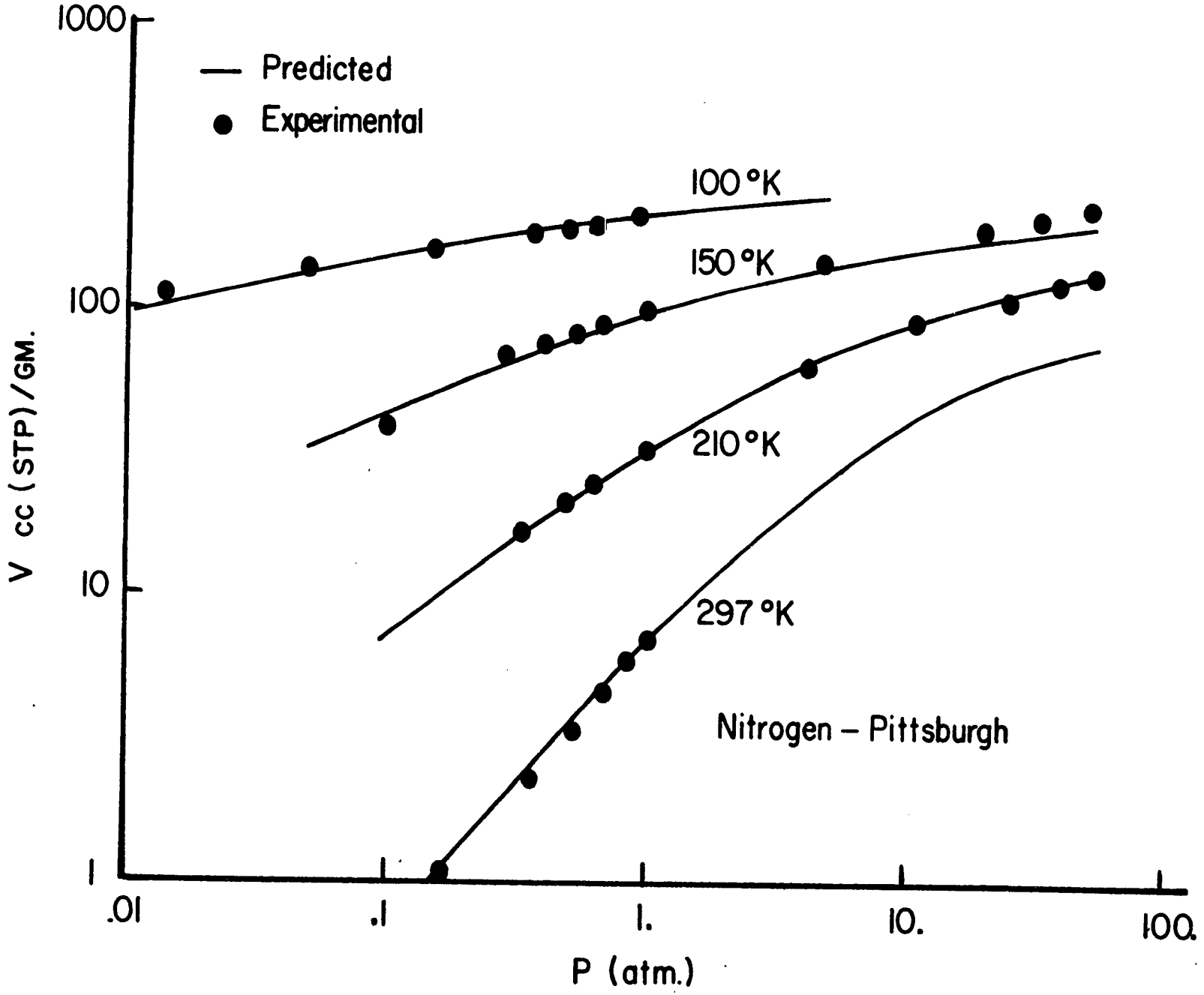
1000
100
10
1
V cc (STP)/GM.
Predicted
Experimental
100 °K
150 °K
210 °K
297 °K
Nitrogen – Pittsburgh
.01
.1
1.
10.
100.
P (atm.)

FIG. 12

LINEAR FORM OF POTENTIAL CURVES

DATA: RAY AND BOX (58)

SYSTEM: N_2

CH_4

C_2H_4

- COLUMBIA L CARBON

C_2H_6

C_3H_8

C_4H_{10}

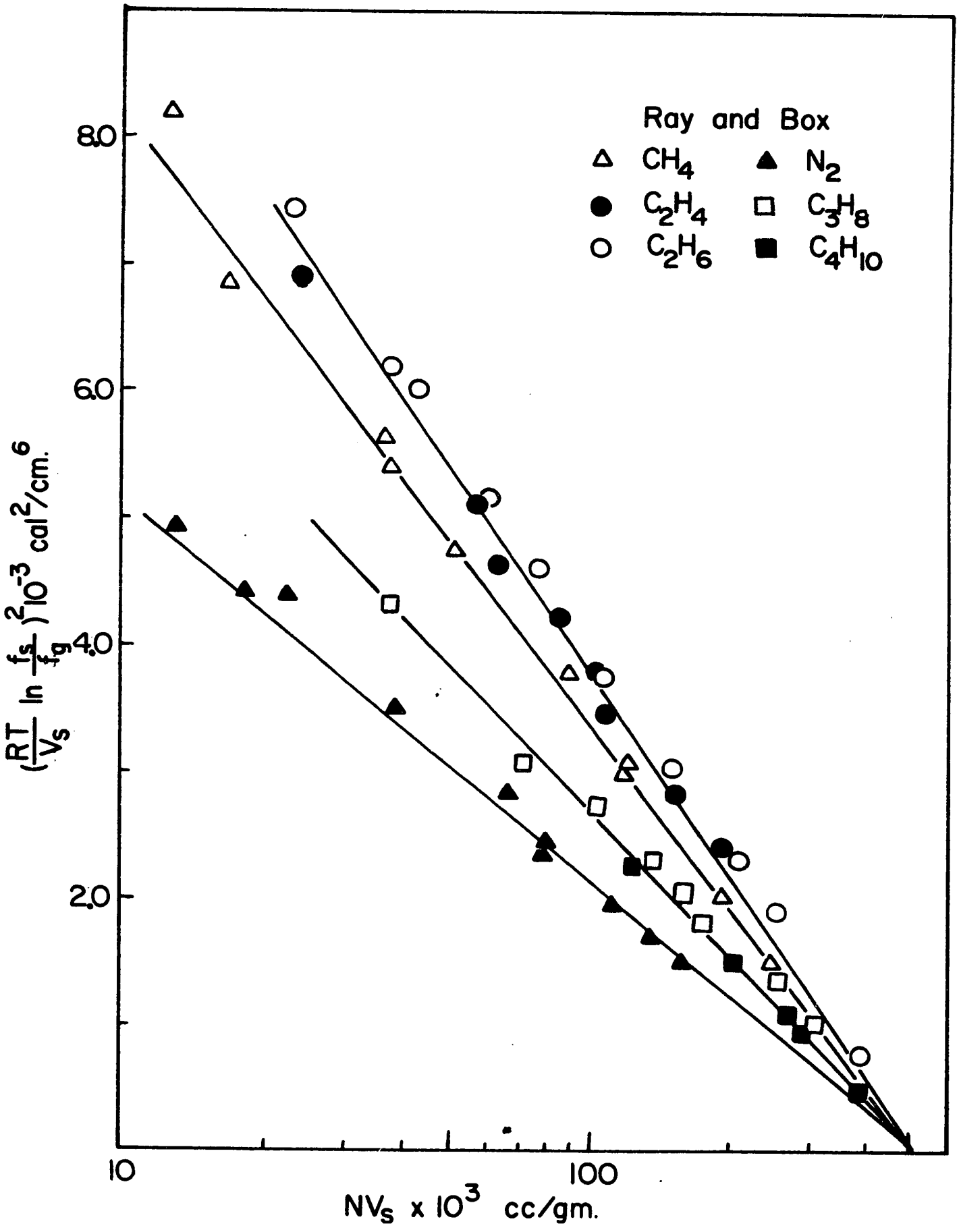
Ray and Box
△ CH4
▲ N2
● C2H4
□ C3H8
○ C2H6
■ C4H10
8.0
6.0
4.0
2.0
10
100
(RT/Vs ln fs/fg)2 10-3 cal2/cm.6
NVs x 10^3 cc/gm.

The choice of published material was limited to data measured over a reasonably wide pressure and temperature range. The amount of reported numerical results is surprisingly small and for adsorbents other than charcoal almost non-existent. A summary of the correlated data is presented in Table 9. It comprises a good deal of the pertinent work published since 1900, with the notable exception of certain measurements made by Homfray (59) and Titoff (60). Most of their data correlated well, but some, particularly that for carbon dioxide (Titoff) and methane (Homfray) showed deviations from the correlation curve of up to 50%. In both cases there are certain ambiguities in the reported values (59, 60) which may account in part for the poor results obtained. Since similar data from other sources were correlated satisfactorily the measurements in question were for the time being omitted from further consideration.

It is of some interest to consider the possibility of extending the method to other adsorbents. Literature data covering a sufficiently wide range of the variables are scarce, but the correlation for the system ethylene-silicagel (61) shown in Fig. A2-6 indicates that the present method is in principle applicable to solids other than activated carbon.

TABLE 9

SUMMARY OF CORRELATED DATA

Gas	T_c(°C)	P_c(atm)	Temperature Range (°C)	Pressure Range	Source
N_2	-147.0	33.5	-76° to 20°	1 to 400 atm*	Antropoff (31)
A	-122.4	48.0	-76° to 20°	1 to 400 atm*	
N_2	-147.0	33.5		200 mm Hg to 15 atm	
CO	-140.2	34.5		200 mm Hg to 15 atm	
CO_2	31.1	72.9		127 mm Hg to 1 atm	
CH_4	- 82.1	45.8	37° to 204°	194 mm Hg to 15 atm	Ray and Box (58)
C_2H_6	32.4	48.5		50 mm Hg to 15 atm	
C_2H_4	9.5	50.0		93 mm Hg to 15 atm	
C_3H_8	97.0	42.1		17 mm Hg to 1 atm	
C_4H_{10}	152.0	37.5		40 mm Hg to 1 atm	
CO_2	31.1	72.9		53 mm Hg to 7 atm	
CH_4	- 82.1	45.8		200 mm Hg to 7 atm	
C_2H_6	32.4	48.5	20° to 90°	19 mm Hg to 7 atm	Szepesy and Illes (37,38)
C_2H_4	9.5	50.0		9 mm Hg to 7 atm	
C_3H_8	97.0	42.1		1 mm Hg to 1 atm	
C_4H_{10}	152.0	37.5		3 mm Hg to 1 atm	

cont'd . . . . .

Table 9 cont'd

Gas	T_c (°C)	P_c (atm)	Temperature Range (°C)	Pressure Range	Source
CO_2	31.1	72.9	0° to 132°	20 mm Hg to 1 atm	
A	- 122.4	48.0	-78° to 100°	5 mm Hg to 1 atm	Homfray (59)
N_2	- 147.0	33.5	-79° to 151°	5 mm Hg to 1 atm	Titoff (60)
CH_4	- 82.1	45.8	-80° to 50°	1 mm Hg to 1 atm	
CO	- 140.2	34.5	-196° to 100°	1 mm Hg to 30 atm	This work
N_2	- 147.0	33.5	-196° to 25°	1 mm Hg to 50 atm	
A	- 122.4	48.0	-196° to 25°	1 mm Hg to 30 atm	
C_2H_4 (silicagel)	9.5	50.0	0° to 40°	2 mm Hg to 1 atm	Lewis et al (61)

* 0°C isotherm extends below 1 atm (~ 1 mm Hg)

C. PROPOSED METHOD FOR PREDICTING BINARY EQUILIBRIA

1. The binary systems tested are summarized in Table 10, and include those measured by the writer as well as literature data. For the most part predicted adsorption volumes were within ± 2.5% of the experimentally determined values.

The 210°K - N_2-CO data, and some of the high relative volatility systems measured during this work were not as good, but this has been attributed to the experimental method used.

A typical set of calculations, necessary to predict a complete set of binary data using the proposed method is given in Table 11 and experimental binary data measured by the writer are tabulated in Appendix 1 along with values predicted by this method.

TABLE 10

Summary of Tested Binary Data

Gases	Adsorbent	Π(atm)	T°K	α	Ref.
N_2-CO	Carbon	1-28.5	130-210	1.5-2.7	This work
H_2-CO	Carbon	1-28.5	150-210	3.8-880	
H_2-N_2	Carbon	1-28.5	77-100	150-4000	
C_2H_4-CO_2	Carbon	1	293	2.6-3.2	Szepesy(47)
C_2H_6-CH_4	Carbon	1	293	14.4-22.7	
C_2H_6-C_3-H_8	Carbon	1	293	4.7-8.1	
C_2H_6-C_2H_4	Carbon	1	293	1.5-1.6	
N_2-A	Silica gel	0.329	89.5		Damköhler (63)
H_2-D_2	5A Sieve	0.988	90		Basmadjian (49)

Note: Subsequently, additional systems were tested (51) with good agreement

TABLE 11

Sample Calculations for Binary Prediction

System: N_2 - CO - Pittsburgh Carbon

T = 210°K π = 28.5 atm

V_T	$(P/X)_{N_2}$	$(P/X)_{CO}$	X_{CO}	P_{CO}	V_{CO}	P_{N_2}	V_{N_2}
51	29.1	18.2	.055	1.0	2.8	27.5	48.2
52	31.4	19.8	.250	4.95	13.0	23.55	39.0
53	34.0	21.4	.4365	9.34	23.1	19.16	29.9
54	37.0	23.1	.6115	14.12	33.0	14.38	21.0
55	40.0	25.1	.772	19.37	42.4	9.13	12.6
56	43.2	27.1	.975	26.43	54.6	2.07	1.4

2.

For discussion purposes, binary systems may be conveniently classified according to the relative volatilities exhibited.

a) Systems with low relative volatility ($\alpha < 5$)

Previous methods (44,45,46) in general give satisfactory results especially if α is constant. The present method gives equally good agreement with experimental results, and offers the added advantage of simplicity. A comparison of predicted and measured data for the system N_2-CO-carbon is shown in Fig. 13 and 14.

b) Systems with intermediate relative volatility ($5 < \alpha < 25$)

Adsorption systems falling in this category often exhibit a variation of α with concentration. The previous methods of Lewis (46) and Szepesy (44) are less suitable for these systems although the method of Toth (45) has been successfully applied to some of Szepesy's data.

The present method has also been applied successfully to the data of Szepesy (47) and graphical comparisons are shown in Fig. 15 and 16. Data predicted by the present method for the systems CO_2-C_2H_4 and C_2H_4-C_2H_6 are compared with values predicted by Toth (64) and measured by Szepesy (47), in Tables 12 and 13. It may be seen that the present method gives good results, and is much easier to use than the involved and lengthy method of Toth.

COMPARISON OF MEASURED AND PREDICTED BINARY EQUILIBRIA

System: N_2-CO - Pittsburgh BPL Carbon

Data: This work

Fig. 13

T = 210°K

π = 1 atm

Fig. 14

T = 210°K

π = 28.5 atm

— Predicted Values

o Experimental, CO

• Experimental, N_2

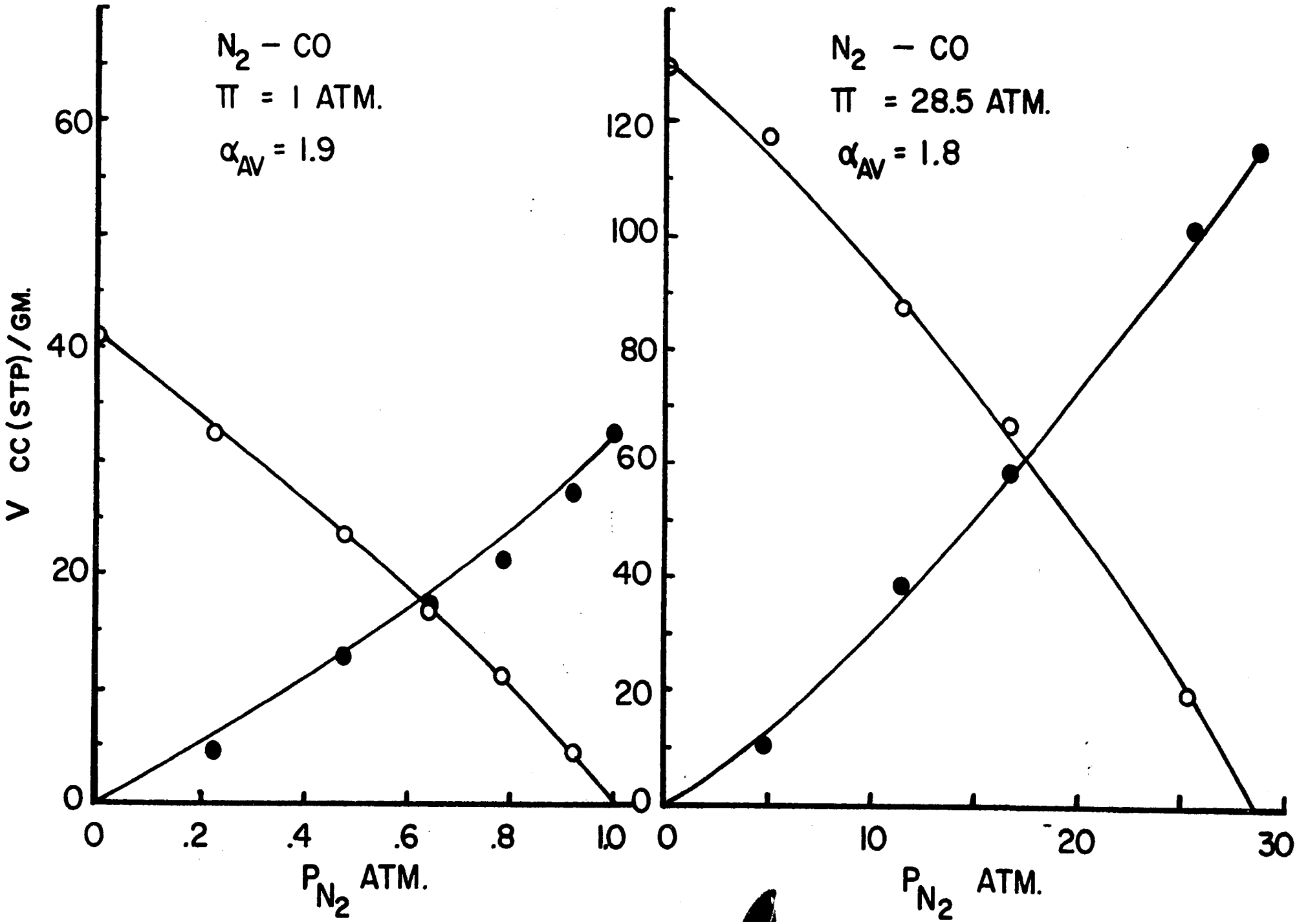
N2 – CO
π = 1 ATM.
αAV = 1.9
V cc (STP)/GM.
PN2 ATM.
N2 – CO
π = 28.5 ATM.
αAV = 1.8
PN2 ATM.

COMPARISON OF MEASURED AND PREDICTED BINARY EQUILIBRIA

Fig. 15
Data: Szepesy (47)

System: CH_4 - C_2H_6 - Nuxit AL Charcoal

T = 20°C

π = 1 atm

— Predicted Values

o Experimental, C_2H_6

● Experimental, CH_4

Fig. 16
Data: Szepesy (47)

System: C_2H_4 - C_2H_6 - Nuxit AL Charcoal

T = 20°C

π = 1 atm

— Predicted Values

o Experimental, C_2H_6

● Experimental, C_2H_4

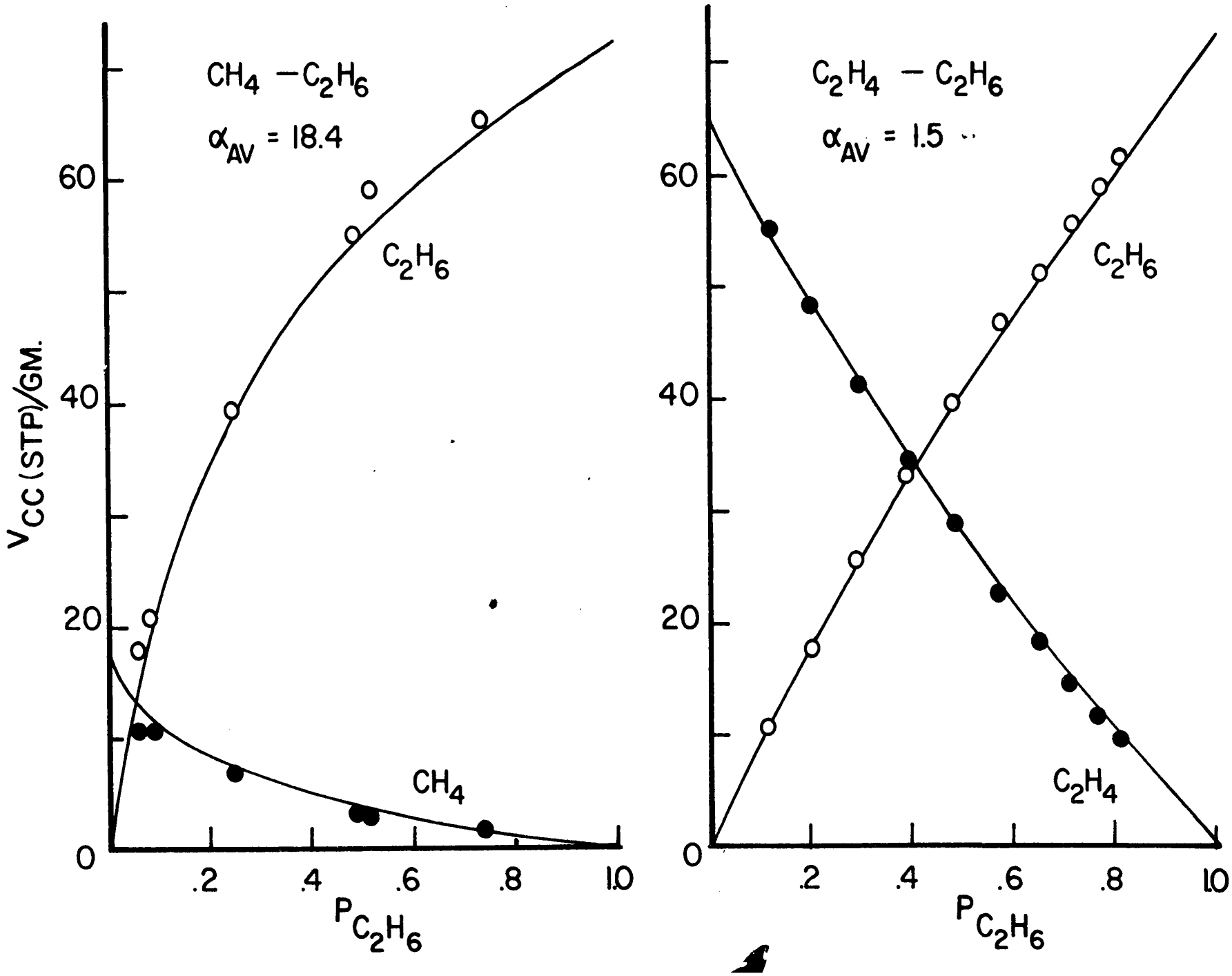
$CH_4 - C_2H_6$
α_{AV} = 18.4
C_2H_6
CH_4
V_{CC} (STP)/GM.
0
20
40
60
.2
.4
.6
.8
1.0
$P_{C_2H_6}$
$C_2H_4 - C_2H_6$
α_{AV} = 1.5
C_2H_6
C_2H_4
0
20
40
60
.2
.4
.6
.8
1.0
$P_{C_2H_6}$

TABLE 12

Comparison of Measured and Predicted Binary Equilibria

System: CO_2 - C_2H_4 - Charcoal, Data of Szepesy (47)

T = 20°C π = 760 mm Hg

P_{CO_2} mm Hg	V cc STP/gm		
	Measured	Predicted	
	Szepesy (47)	Toth (64)	Proposed Method
196.8	7.5	6.4	7.5
271.2	10.7	9.4	10.7
369.3	15.4	14.0	15.5
462.7	21.4	19.4	21.0
593.4	28.8	29.2	30.4
696.0	37.4	39.9	40.2
$P_{C_2H_4}$			
166.4	24.0	24.8	23.1
297.1	35.1	37.5	35.8
390.5	43.7	44.7	43.1
488.6	50.2	51.2	49.6
563.0	55.2	54.6	54.2
759.8	64.6	64.0	64.7

TABLE 13

Comparison of Measured and Predicted Binary Equilibria
System: Ethylene - Ethane - Charcoal, Data of Szepesy (47)

T = 20°C π = 760 mm Hg

$P_{C_2H_4}$ mm Hg	V cc STP/gm		
	Measured Szepesy (47)	Predicted Toth (64)	Proposed Method
100	6.6	6.5	6.6
200	13.3	13.4	14.0
300	20.6	21.0	21.6
400	28.6	29.1	29.8
500	37.6	37.8	38.6
600	47.3	47.4	47.8
$P_{C_2H_6}$			
100	12.0	12.3	11.7
200	23.4	23.6	22.7
300	33.3	33.9	32.9
400	43.0	43.3	42.3
500	52.0	52.2	51.4
600	61.0	60.4	60.2

c) Systems with high relative volatility ($\alpha \geq 25$)

Binary gas mixtures whose components have widely differing boiling points, will generally have high relative volatilities. Adsorption data for these systems are often estimated by assuming that each component follows its pure component behavior. The uptake of each may then be obtained from a knowledge of binary partial pressures and the appropriate pure component isotherms.

At low partial pressures of the heavy component for low total pressures ($\sim$1 atm) these assumptions are valid, but as π becomes larger, the increased adsorption of the light component interferes with the uptake of the heavier gas.

The separation factors or relative volatilities (α) of such systems may vary 1 to 2 orders of magnitude over the full binary concentration range and under these conditions the methods of Lewis (29) and Szepesy (44) are no longer applicable. The method of Toth (64) although not tested directly, was thought not to apply because of its limited pressure range.

Hiza and Kidnay (62,65) have investigated the industrially important system N_2-H_2, adsorbed on charcoal and silica gel, and have presented an empirical "enhancement factor" (ϕ) which may be used to calculate the equilibrium

nitrogen loading of adsorbers, used to purify liquifaction grade hydrogen, operating at liquid nitrogen temperature and at total pressures up to 100 atm.

$$\phi = \left(\frac{y_{N_2} \Pi}{P^\circ_{N_2}} \right)_V = \left(\frac{P_{N_2}}{P^\circ_{N_2}} \right)_V$$

In order to apply the method proposed by the writer to systems such as N_2-H_2, it was necessary to extend the pressure ratio plot linearly, as may be seen in Fig. 17, and to calculate artificial values for the heavy component uptake, above its dew point (in this case, nitrogen). Nitrogen data estimated for Pittsburgh BPL carbon are compared with the data of Hiza (62) in Table 14, and although the adsorbents were different, the agreement is quite good. It may be seen that nitrogen adsorption does not follow pure component behavior and in fact tends to decrease rather than increase at high total pressures. Errors as high as 50% could thus arise by ignoring this effect in estimating the nitrogen uptake directly from pure component data.

It is possible that a rigorous treatment would require the use of fugacity in the proposed method. However, in all cases reported here the substitution of fugacity for pressure would not make a significant change in the results obtained.

FIG. 17

PRESSURE RATIO PLOT

EXTRAPOLATION FOR HIGH PRESSURES

SYSTEM: H_2 - N_2

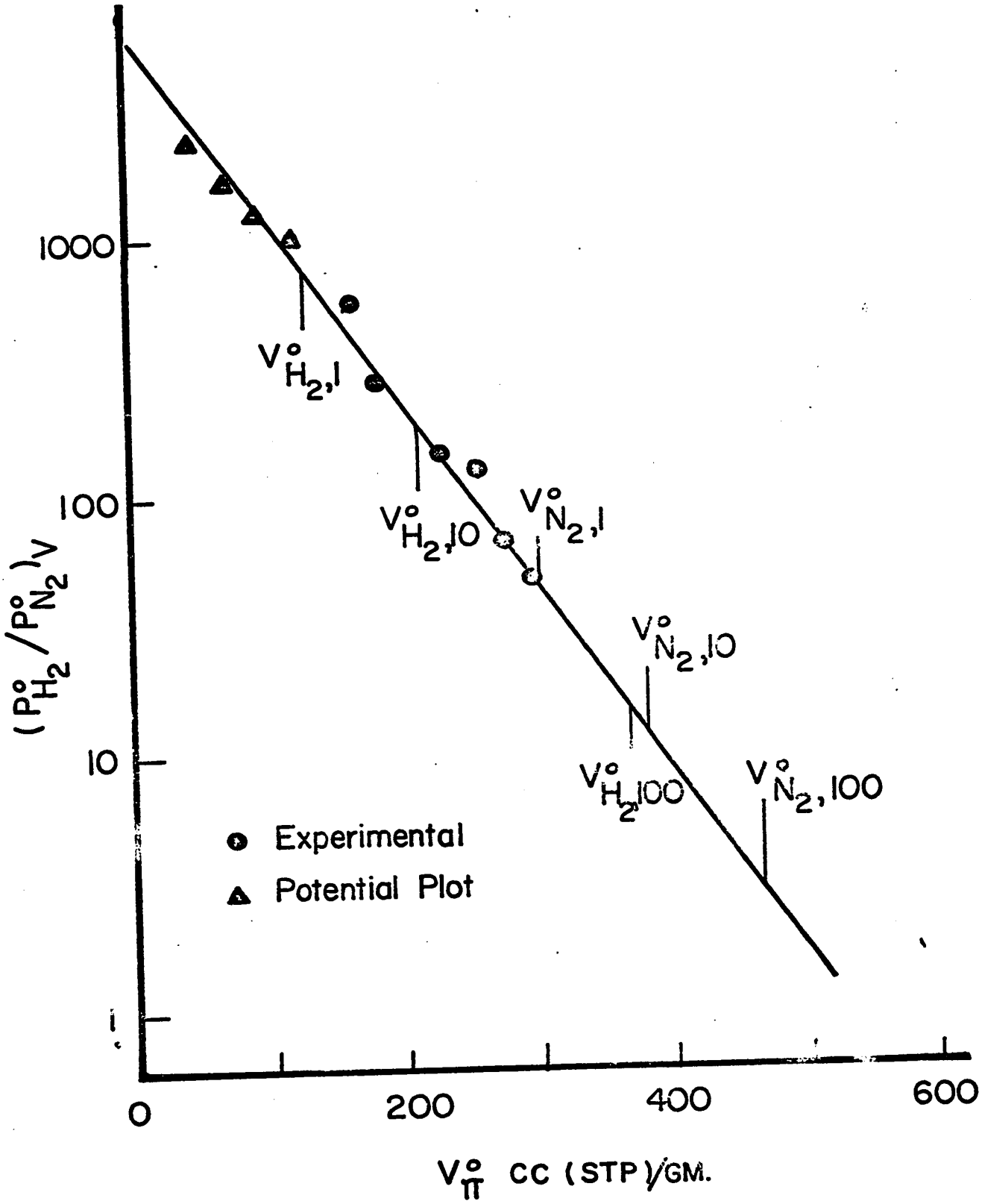
1000
100
10
1
$(P^{\circ}_{H_2}/P^{\circ}_{N_2})_V$
$V^{\circ}_{H_2,1}$
$V^{\circ}_{H_2,10}$
$V^{\circ}_{N_2,1}$
$V^{\circ}_{N_2,10}$
$V^{\circ}_{H_2,100}$
$V^{\circ}_{N_2,100}$
Experimental
Potential Plot
0
200
400
600
V°_{II} CC (STP)/GM.

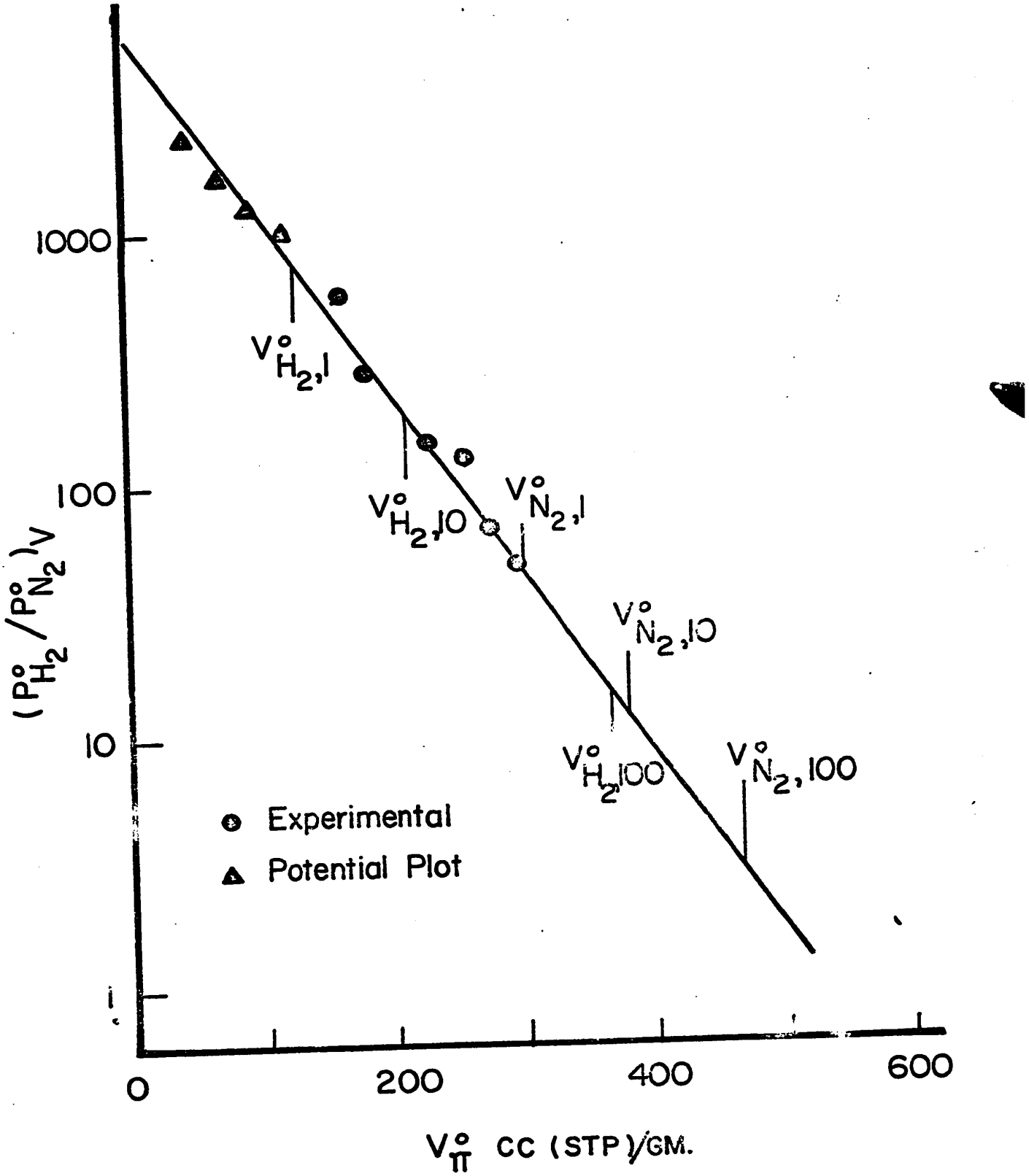
1000
100
10
1
$(P^\circ_{H_2}/P^\circ_{N_2})_V$
$V^\circ_{H_2,1}$
$V^\circ_{H_2,10}$
$V^\circ_{N_2,1}$
$V^\circ_{N_2,10}$
$V^\circ_{H_2,100}$
$V^\circ_{N_2,100}$
Experimental
Potential Plot
0
200
400
600
V°_{II} CC (STP)/GM.

TABLE 14

Binary Prediction N_2 - H_2

Comparison (a) Present method
(b) Hiza's Enhancement Factor (62)
(c) Experimental values
(d) Pure component isotherm

System: N_2-H_2 - Barnebey-Cheney Charcoal

T = 76°K N_2 impurity: 915 ppm

π atm	Volume Sorbed cc STP/gm			
	(a) Present Method	(b) ϕ	(c) Experi-mental	(d) Pure Component
15	163.0	169.0	176.7	202.0
28	164.0	169.5	175.4	212.5
35	164.0	168.0	175.4	216.0
100	150.5	142.0	-	231.5

3. Azeotropes

The proposed method for predicting binary equilibria from pure component isotherms should also be applicable to systems which exhibit "azeotropic" behaviour. When applied to Damköhler's data for A-N_2 at 89.5°K (63) the partial volume prediction was within experimental error, however the low coverage pressure ratio data was in doubt and no azeotrope could be predicted with certainty.

At present it does not seem possible to predict quantitatively the partial isotherms in the azeotropic region, since the precise shape of the binary (P/X) curve is not known. However, a qualitative description of this region is still useful, since it involves a "pinch" and should be avoided in adsorber design.

CONCLUSIONS AND RECOMMENDATIONS

1. Experimental

The adsorption apparatus used in this work was satisfactory for measuring pure component adsorption data over a wide temperature interval and at pressures up to 50 atm. High pressure adsorption measurements would be more convenient if a quantitative gas compressor were used instead of a desorption procedure.

The error propagated in calculating adsorbed phase compositions for binary equilibria could be reduced, by desorbing the adsorbate at a high temperature, and measuring the composition of the desorbed gas. To be practical, this method would require a cryostat which could be heated and cooled rapidly.

The circulating type of apparatus used in this work is best suited to regions where both components in a binary mixture appear at fairly high concentrations in the gas and adsorbed phases. Small errors in measurement have an exaggerated effect on low concentration regions and a flow system similar to that used by Hiza (62) is recommended where one component appears in trace quantities. It should also be noted that condensation problems occur if an attempt is made to measure binary systems at pressures higher than the bulk saturation pressure of one of the components, with the present apparatus.

2. Correlation of pure component isotherms

The proposed method, for correlating pure component equilibrium data, based on Polanyi's potential theory has been successfully applied to measured and literature data.

Briefly the method may be summarized as follows:

1) Saturated liquid molar volume data are plotted, log V_L vs. log T, and the tangent to the curve at the boiling point drawn.

2) Using this empirical curve, the adsorbate molar volume (V_s) at the temperature of adsorption is determined, and the corresponding pressure (P_s) and fugacity (f_s) are calculated from P-V-T data.

3) The adsorption potential is calculated for each experimental equilibrium pressure P_g (using fugacity (f_g) if required)

$$\epsilon = \frac{RT}{V_s} \ln \frac{f_s}{f_g}$$

4) The amount of gas adsorbed N, is calculated as the total adsorbate within the micropore volume.

5) The characteristic curve is plotted

$$\frac{RT}{V_s} \ln \frac{f_s}{f_g} \quad \underline{VS} \quad \log NV_s$$

Dubinin and co-workers (28) have suggested that solid adsorbents with small micropores will give rise to parabolic potential curves, while those solids with larger micropores will have linear curves. This work indicates that even for fine pore solids there may be a linear portion of the curve at low coverage ($NV_s < 20 \times 10^{-3}$).

For many systems, a limited amount of high coverage experimental data at a single temperature, should permit one to calculate adsorption isotherms at any desired temperature by utilizing the linear form of the potential plot (Fig. 12). In addition, extrapolation of the linear portion of this curve to intersect the abscissa will give a good approximation of the adsorbent micropore volume.

As indicated previously, this method of correlation seems applicable to adsorption on silica gel adsorbents. However, data for several gases adsorbed on Linde molecular sieves measured by the writer, and taken from the literature (66) did not correlate as well over the full range of temperature. Because of the peculiar cage-like structure of the sieves the proposed correlation may not be applicable. Further work on sieve type adsorbents is required.

3. Prediction of binary equilibria

The method proposed to predict complete binary data ($V_1 = f_1(P_1)$ and $V_2 = f_2(P_2)$) has been applied with success to measured and literature data. Based on Basmadjian's "pressure ratio integral" the present empirical method (51) is accurate and easy to use. It should be particularly useful for high pressure cryogenic applications (67), where the relative volatility changes widely with varying gas phase composition.

The method may be summarized as follows,

1) Pure component pressure ratio data are plotted $\log \frac{P_1^\circ}{P_2^\circ}$ vs. V and extrapolated linearly if necessary.

2) Limiting relative volatilities are calculated using Basmadjian's (1) "pressure ratio integral". For example,

$$\log \alpha_{V_{1\pi}^\circ} = \frac{1}{V_{1\pi}^\circ} \int_0^{V_{1\pi}^\circ} \log \left(\frac{P_1^\circ}{P_2^\circ}\right)_V \, dV$$

3) End-point (P/X) values are calculated from the limiting α's, for example,

$$(P_2/X_2)_{V_{1\pi}^\circ} = \frac{\pi}{\alpha_{V_{1\pi}^\circ}}$$

4) (P/X) vs. V_T curves are constructed to have the same curvature as the pure component data over the interval $V_{1\pi}^\circ$ to $V_{2\pi}^\circ$. This is done by choosing an appropriate

set of co-ordinate scales (semi-log or log-log) which result in linear pure component isotherms over the volume interval of interest.

5) Complete partial isotherms are calculated utilizing the equation

$$x_2 = \frac{(P_1/X_1)_{V_T} - \pi}{(P_1/X_1)_{V_T} - (P_2/X_2)_{V_T}}$$

The proposed method, should be useful to predict the regions in which azeotropes might be found, but is not presently capable of giving a quantitative description of the partial isotherms.

This method is not applicable to systems which exhibit a maximum in the total volume vs. composition curve.

BIBLIOGRAPHY

(1) Basmadjian, D.
Can. J. Chem. 38 149 (1960)

(2) Mantell, C.L.
Adsorption, p224
McGraw-Hill New York 2nd Ed. (1951)

(3) Browning, F.M.
Chem. Eng. 59 158 (1952)

(4) Shreve, R.N.
The Chem. Proc. Ind. p164
McGraw-Hill New York 2nd Ed. (1956)

(5) Baker, C.R.; Paul, R.S.
Chem. Eng. Prog. 59 61 (1963)

(6) Deaton, W.M.; Haynes, R.D.
Pet. Ref. 40 205 (1961)

(7) Anon.
Pet. Ref. 36 136 (1957)

(8) Barry, H.M.
Chem. Eng. 67 105 (1960)

(9) Carson, D.B.; Broughton, D.B.
Pet. Ref. 38 130 (1959)

(10) Franz, W.F.; Christensen, E.R.; May, J.E.; Hess, H.V.
Pet. Ref. 38 125 (1959)

(11) Russell, G.F.
Pet. Ref. 40 103 (1961)

(12) Cochran, G.S.
Chem. Eng. 66 129 (1959)

(13) Haines, W.H.; Van Weilingen, G.A.; Palmer, G.H.
Pet. Ref. 40 123 (1961)

(14) N.R.C. - Air Establishment, Ottawa
Private Communication

(15) Carter, J.W.
Brit. Chem. Eng. 5 472 (1960)

(16) Ibid 5 552 (1960)

(17) Ibid 5 625 (1960)

(18) Brunauer, S.
The Adsorption of Gases and Vapours
Princeton University Press (1945)

(19) de Boer, J.H.
The Dynamical Character of Adsorption
Oxford Press (1953)

(20) Young, D.M.; Crowell, A.D.
Physical Adsorption of Gases
Butterworths (1962)

(21) Freundlich, H.
Colloid and Capillary Chemistry
Methune and Co. (1926)

(22) Langmuir, I.
J. Am. Chem. Soc. 40 1361 (1918)

(23) Brunauer, S.; Emmett, P.H.; Teller, E.
J. Am. Chem. Soc. 60 309 (1938)

(22)* Sips, N.N.
J. Chem. Phys. 16 490 (1948)

(23)* Toth, J.
Mag.Kem. Foly. 66 213, 398, 431 (1960)

(24) Redlich, O.; Peterson, D.L.
J. Chem. & Eng. Data 7 570 (1962)

(25) Polanyi, M.
Verhandl deut. physik Ges. 16 1012 (1914)

(26) Berenyi, L.
Z. physik Chem. 94 628 (1920)

(27) Lowry, H.H.; Olmstead, P.S.
J. Phys. Chem. 31 1601 (1927)

(28) Dubinin, M.M.
Chem. Rev. 60 235 (1960)

(29) Lewis, W.K.; Gilliland, E.R.; Chertow, B.; Cadogan, W.P.
Ind. Eng. Chem. 42 1326 (1950)

(30) Maslan, F.D.; Altman, M.; Aberth, E.R.
J. Phys. Chem. 57 106 (1953)

(31) Antropoff, A.
Kolloid Z 129 1 (1952)

(32) Cadogan, W.P.
Private Communication

(33) Kaser, J.D.; Rutz, L.O.; Kammermeyer, K.
J. Chem. Eng. Data 7 211 (1962)

(34) Szepesy, L.; Illés, V.; Benedek, P.
Acta Chim. Hung. 35 433 (1963)

(35) Grant, R.J.; Manes, M.; Smith, S.B.
AIChE. J. 8 403 (1962)

(36) Toth, J.
Acta Chim. Hung. 30 415 (1962)

(37) Szepesy, L.; Illés, V.
Acta Chim. Hung. 35 37 (1963)

(38) Ibid 35 53 (1963)

(39) Cook, W.H.; Basmadjian, D.
Can. J. Chem. Eng. 42 146 (1964)

(40) Markham, E.C.; Benton, A.F.
J. Am. Chem. Soc. 53 497 (1931)

(41) Glueckauf, E.
J. Chem. Soc. 1321 (1947)

(42) Hill, T.L.
J. Chem. Phys. 14 46, 268 (1946)

(43) Lederman, P.B.
PhD Thesis (1961) University of Michigan
Adsorption of N_2-CH_4 on Linde Molecular Sieves

(44) Szepesy, L.
Mag. Kem. Foly. 66 20 (1960)

(45) Toth, J.
Acta Chim. Hung. 38 233 (1963), 39 331 (1963)

(46) Lewis, W.K.; Gilliland, E.R.; Chertow, B.; Cadogan, W.P.
Ind. Eng. Chem. 42 1319 (1950)

(47) Szepesy, L.; Illés, V.
Acta Chim. Hung. 35 245 (1963)

(48) Broughton, D.B.
Ind. Eng. Chem. 40 1506 (1948)

(49) Basmadjian, D.
Can. J. Chem. 38 141 (1960)

(50) Kapfer, W.H.
AIChE.J. 2 456 (1956)

(51) Cook, W.H.; Basmadjian, D.
Can. J. Chem. Eng. - to be published (1965)

(52) Coolidge, A.S.; Fornwalt, J.
J. Am. Chem. Soc. 56 555 (1934)

(53) Din, F.
Thermodynamic Functions of Gases, Vol. 1, 2, 3
Butterworths (1962)

(54) Reamer, H.H.; Olds, R.H.; Sage, B.H.; Lacey, W.N.
Ind. Eng. Chem. 36 956 (1944)

(55) Lange, N.A.
Handbook of Chemistry 9th Ed.
Handbook Publishers Inc. (1956)

(56) Laing, S.C.
J. Phys. Chem. 57 910 (1953)

(57) De Farges, J.W.
Chem. Eng. 71 157 (1964)

(58) Ray, G.C.; Box, E.O.
Ind. Eng. Chem. 42 1315 (1950)

(59) Homfray, I.
Z. physik Chem. 74 129 (1910)

(60) Titoff, A.
Z. physik Chem. 74 641 (1910)

(61) Lewis, W.K.; Gilliland, E.R.; Chertow, B.; Bareis, D.
J. Am. Chem. Soc. 72 1160 (1950)

(62) Hiza, M.J.; Kidnay, A.J.
Adv. Cryog. Eng. 8 174
Plenum Press (1963)

(63) Damköhler, G.
Z. physik Chem. B23 69 (1933)

(64) Toth, J.
Mag. Kem. Foly. 68 346 (1962)

(65) Hiza, M.J.
Chem. Eng. Prog. 56 68 (1960)

(66) Linde Technical Bulletins

(67) Basmadjian, D.; Cook, W.H.
Adv. Cryog. Eng. - to be published
Plenum Press (1965)

(68) Power, W.H.
Adv. Cryog Eng. 6
Plenum Press (1961)

(69) Reid, R.C.; Sherwood, T.K.
Properties of Gases and Liquids
McGraw-Hill (1958)

(70) van Dingenen, W.; van Itterbeek, A.
Physica 6 49 (1939)

Appendix 1

TABLE A1-1

System: Nitrogen - Pittsburgh BPL Carbon
Subatmospheric Pressure

77.4°K

P mm Hg	V cc STP/gm
15.2	194.3
49.0	223.6
124.5	248.9
233.5	261.6
342.0	268.8
475.0	275.9
598.0	283.3
688.0	294.5

78.6°K

P	V
1.0	139.0
2.7	156.8
6.5	170.2
11.4	183.0
35.6	208.9
78.6	230.8
233.5	257.0
343.8	265.7
433.8	271.6
724.7	287.0

100°K

P	V
1.0	67.7
4.0	93.2
10.8	114.7
37.5	138.2
114.9	160.0
270.5	179.8
367.2	187.7
472.8	195.4
686.2	207.3

130°K

P	V
12.4	41.6
55.2	72.1
118.2	90.7
257.4	110.8
418.2	123.6
547.2	130.8
780.2	139.6

150°K

P	V
75.0	38.4
211.0	69.1
309.0	76.8
403.5	81.9
505.8	90.6
772.1	102.7

TABLE A1-1 (Cont'd)

180°K

P	V
134.0	25.1
249.0	34.4
343.8	40.3
482.0	47.6
660.5	54.0
816.1	60.5

194.5°K

P	V
3.8	1.0
9.3	2.3
22.9	4.8
57.8	9.5
146.1	17.4
249.0	23.9
352.1	29.1
497.1	35.2
628.6	39.0
713.1	43.0
758.2	44.5

210°K

P	V
247.3	16.9
361.7	21.2
477.7	24.2
735.4	32.1

273.2°K

P	V
7.4	0.16
20.6	0.35
35.2	0.56
74.2	1.22
239.9	3.37
340.4	4.60
428.2	5.70
527.6	6.90
624.0	8.00
753.1	9.40

297°K

P	V
46.7	0.4
120.0	1.0
270.2	2.3
398.5	3.4
516.8	4.5
630.0	5.8
755.8	6.9

TABLE A1-2

System: Nitrogen - Pittsburgh BPL Carbon
Superatmospheric Pressure

150°K		180°K		210°K	
P atm	V cc STP/gm	P	V	P	V
4.84	145.5	4.15	96.0	4.18	63.7
11.74	175.5	10.57	129.6	10.72	92.8
19.12	193.5	17.40	146.0	17.35	106.6
25.60	204.0	24.50	152.4	24.20	113.2
32.10	212.7	31.30	156.0	31.10	118.1
39.20	222.0			38.10	123.4
45.80	230.0			44.90	127.8
51.60	235.0			51.80	133.0

TABLE A1-3

System: Carbon Monoxide - Pittsburgh BPL Carbon
Subatmospheric Pressure

77.4°K		85°K		100°K	
P mm Hg	V cc STP/gm	P	V	P	V
2.4	182.0	1.2	133.0	1.5	103.7
5.2	197.7	14.6	178.8	16.3	141.5
13.8	211.6	41.2	201.4	70.3	166.5
23.6	225.8	175.2	241.0	136.5	182.1
33.0	240.7	345.3	255.2	248.0	195.9
75.0	253.1	441.0	259.4	355.8	205.1
162.0	263.5	689.2	269.3	472.5	214.6
244.0	277.7	862.7	276.6	623.8	221.7
351.0	284.0	950.4	280.8	868.8	231.0
403.0	291.9				

130°K		150°K		180°K	
1.9	29.8	2.5	14.5	22.3	13.5
16.1	63.3	9.1	25.5	53.2	21.0
49.9	88.2	20.2	35.3	110.4	30.5
124.9	110.9	60.1	53.8	235.1	41.9
213.0	122.9	164.1	76.9	304.4	46.6
402.9	137.1	251.9	90.6	380.3	50.8
496.8	141.8	349.1	94.9	463.4	55.5
631.9	147.9	467.1	102.4	586.4	61.2
824.9	154.5	567.1	107.2	785.6	68.6
		740.2	113.9		
		845.7	116.9		

TABLE A1-3 (cont'd)

194.7°K		273.2°K		296.9°K	
P mm Hg	V cc STP/gm	P	V	P	V
4.6	2.2	25.6	0.5	35.7	0.4
11.5	5.3	49.9	1.0	102.5	1.3
32.3	10.1	94.4	1.9	227.5	2.7
73.5	17.1	168.6	3.3	387.7	4.5
146.3	24.8	239.6	4.4	493.7	5.8
311.3	36.8	396.6	7.1	602.2	7.0
472.3	44.0	505.9	8.6	758.5	9.1
613.5	49.6	625.3	10.2		
758.5	54.3	764.6	11.8		

373.7°K	
52.2	0.2
117.5	0.4
228.5	0.8
422.3	1.5
611.8	2.0
762.0	2.6

TABLE A1-4

System: Carbon Monoxide - Pittsburgh BPL Carbon
Superatmospheric Pressure

130°K		150°K		180°K	
P atm	V cc STP/gm	P	V	P	V
3.63	186.5	1.00	115.0	3.34	103.5
6.63	204.7	5.03	116.0	5.81	120.7
11.80	218.7	7.85	163.7	12.29	140.5
18.37	223.3	9.46	173.5	19.70	153.0
25.50	224.5	28.50	190.6	26.26	160.8
				32.70	165.0

TABLE A1-5

System: Argon - Pittsburgh BPL Carbon
Subatmospheric Pressure

77.4°K		100°K		130°K	
P mm Hg	V cc STP/gm	P	V	P	V
3.0	206.3	3.5	94.8	7.0	32.1
8.5	235.0	23.0	154.9	25.8	56.9
18.0	264.0	75.5	189.8	49.5	75.3
38.5	292.5	181.0	220.6	76.5	89.2
74.5	307.1	273.2	237.6	107.2	101.3
114.5	317.7	371.4	251.2	208.8	124.5
172.5	331.3	476.7	261.6	292.7	135.8
		610.8	271.6	390.2	145.3
		797.2	280.7	495.2	153.5
				601.8	159.5
				743.0	166.6
150°K		180°K			
10.5	14.7	112.2	20.1		
27.7	25.2	203.0	28.8		
89.9	47.0	286.8	35.1		
209.9	70.7	431.9	44.9		
298.5	81.9	494.0	48.2		
362.0	87.8	634.0	55.1		
511.0	99.1	781.9	61.1		
632.0	105.9				
748.0	112.6				

TABLE A1-5 (cont'd)

194.6°K		273.2°K		297°K	
P	V	P	V	P	V
5.2	1.0	25.0	0.3	27.0	0.2
11.5	2.2	64.0	0.8	96.8	0.8
39.3	6.0	108.9	1.3	213.6	1.6
85.7	10.9	161.4	1.9	364.6	2.7
161.5	16.9	274.0	3.2	527.3	3.8
326.1	26.6	375.7	4.2	756.6	5.4
448.5	32.3	471.9	5.3		
589.5	38.1	593.2	6.5		
759.8	43.7	753.0	7.9		

TABLE A1-6

System: Argon - Pittsburgh BPL Carbon
Superatmospheric Pressure

130°K		150°K		180°K	
P atm	V cc STP/gm	P	V	P	V
3.20	215.0	2.31	144.0	3.79	108.0
4.77	229.0	5.03	217.0	6.08	128.5
7.69	248.0	8.20	194.0	12.00	162.5
11.74	260.0	14.35	173.5	19.30	190.0
16.05	269.0	20.60	228.0	25.60	206.0
				32.30	217.0
				39.10	222.0
				45.80	228.0

TABLE A1-7

System: Hydrogen - Pittsburgh BPL Carbon
Subatmospheric Pressure

77.4°K		85°K		100°K	
P mm Hg	V cc STP/gm	P	V	P	V
54.9	50.2	25.4	23.3	200.2	33.5
166.0	78.8	67.0	38.4	366.0	46.2
264.0	92.4	103.5	47.5	443.0	51.3
405.1	106.4	167.5	59.3	592.2	59.3
545.0	116.6	259.6	74.0	787.4	68.2
754.0	127.7	368.0	84.9		
		429.5	88.7		
		526.6	93.9		
		684.5	103.5		
		774.5	107.8		
150°K		180°K			
472.2	9.7	190.9	2.0		
604.2	11.9	246.0	2.9		
821.2	15.3	674.8	7.3		
		790.5	9.0		
		431.5	4.9		

TABLE A1-8

System: Hydrogen - Pittsburgh BPL Carbon
Superatmospheric Pressure

77.4°K		100°K		85°K	
P atm	V cc STP/gm	P	V	P	V
4.40	178.2	3.74	112.0	3.37	149.0
7.82	204.2	9.45	150.2	5.30	170.5
14.70	231.6	16.45	174.7	11.43	203.6
28.50	262.5	23.10	191.7	17.75	222.5
49.80	311.6	30.20	207.2	24.20	235.5
		37.40	220.3	30.55	244.2
		44.90	232.5	37.00	250.0
		51.90	243.5	44.20	256.2
				51.00	262.0
150°K		180°K		210°K	
4.28	40.0	4.08	23.3	1.00	2.1
8.57	61.6	8.64	39.3	7.85	17.0
14.55	82.4	15.73	60.8	28.50	42.0
21.70	101.8	23.00	81.0		
28.70	119.0	29.55	99.3		
		37.85	119.7		
		44.10	133.3		
		51.20	147.5		

TABLE A1-9

System: Methane - Pittsburgh BPL Carbon
Subatmospheric Pressure

194.5°K		273.2°K		323.2°K	
P mm Hg	V cc STP/gm	P	V	P	V
1.0	2.4	12.0	0.9	29.3	0.6
4.7	6.7	89.2	5.5	92.0	1.7
9.3	12.8	183.7	9.5	174.2	3.1
22.6	21.3	274.2	12.7	287.5	4.9
39.3	27.8	392.4	16.3	441.5	6.9
69.3	37.3	512.0	19.4	609.0	9.3
135.3	51.6	755.3	25.0	760.5	10.8
244.3	66.0				
357.3	76.2				
487.8	85.5				
624.8	92.3				
765.4	98.3				

TABLE A1-10

System: Nitrogen - Carbon Monoxide - Pittsburgh BPL Carbon

P_{N_2} atm	V_{N_2} cc STP/gm measured	V_{N_2} cc STP/gm calc.	P_{CO} atm	V_{CO} cc STP/gm measured	V_{CO} cc STP/gm calc.
130°K	π = 1 atm				
.8325	94.3	94.0	.1675	43.3	44.7
.735	75.4	76.1	.265	64.0	64.4
.560	51.8	50.5	.430	90.8	91.7
.285	20.6	21.1	.715	125.2	126.1
.2875	18.8	21.3	.7125	126.1	125.9
130°K	π = 7.85 atm				
6.10	124.5	121.6	1.75	71.3	73.4
5.12	92.4	92.0	2.73	103.9	103.7
3.73	62.4	60.8	4.12	137.8	137.8
1.63	23.8	22.9	6.22	178.2	177.3
1.63	22.9	22.9	6.22	181.9	177.3
210°K	π = 1 atm				
.9211	27.3	28.9	.0789	4.6	4.6
.7828	21.3	23.6	.2172	11.2	11.0
.6467	17.4	19.0	.3533	17.0	16.7
.4738	12.6	13.5	.5262	23.6	23.8
.2252	4.6	6.2	.7748	32.5	33.0

TABLE A1-10 (cont'd)

P_{N_2} atm	V_{N_2} cc STP/gm measured	V_{N_2} cc STP/gm calc.	P_{CO} atm	V_{CO} cc STP/gm measured	V_{CO} cc STP/gm calc.
210°K Π = 7.85 atm					
6.98	70.4	65.4	0.87	14.4	14.4
4.73	42.0	41.7	3.12	46.1	43.3
3.28	26.4	22.0	4.57	64.4	60.1
1.46	8.5	107.0	6.39	86.4	79.1
210°K Π = 28.5 atm					
25.36	101.1	98.7	3.14	19.7	20.9
16.66	58.5	56.9	11.84	67.0	64.9
11.31	39.0	36.7	17.19	87.8	88.3
4.79	10.3	13.8	23.71	117.7	114.7
180°K Π = 1 atm					
.800	404.0	41.3	.200	19.5	19.0
.670	32.8	32.5	.330	30.0	28.9
3475	13.8	15.1	.6525	50.7	50.5
.2375	9.2	9.4	7625	58.3	56.9
180°K Π = 7.85 atm					
5.96	73.8	76.8	1.89	47.0	41.5
4.83	57.6	58.4	3.02	64.9	63.3
2.34	21.3*	25.0	5.51	102.3	99.9
1.52	14.2*	15.6	6.33	111.9	110.5
180°K Π = 28.5 atm					
20.90	95.6	96.3	7.60	59.4	60.5
16.86	74.3	73.4	11.64	86.9	87.2
7.84	24.8	31.2	20.66	138.7	137.6
5.20	12.8	20.4	23.30	152.0	145.6

* From Smoothed Data

TABLE A1-11

System: Hydrogen - Nitrogen - Pittsburgh BPL Carbon

77.4°K π = 1 atm

P_{N_2} atm	V_{N_2} cc STP/gm measured	V_{N_2} cc STP/gm calc.	P_{H_2} atm	V_{H_2} cc STP/gm measured	V_{H_2} cc STP/gm calc.
8.393×10^{-4}	122.2	105.5	.9991607	37.8	45.9
1.722×10^{-3}	147.9	128.1	.998278	23.8	32.1
.02153	181.6	195.2	.97847	13.7	6.9
.1348	226.3	243.1	.8652	6.9	1.6

100°K π = 1 atm

.00623	83.5	83.0	.99377	17.6	18.3
.01979	109.8	109.2	.98021	13.1	10.8
.0983	143.8	146.8	.9017	9.9	3.9
.3056	171.8	176.1	.6944	7.1	1.3

TABLE A1-12

System: Hydrogen - Carbon Monoxide - Pittsburgh BPL Carbon

100°K π = 1 atm

P_{CO} atm	V_{CO} cc STP/gm measured	V_{CO} cc STP/gm calc.	P_{H_2} atm	V_{H_2} cc STP/gm measured	V_{H_2} cc STP/gm calc.
.00503	122.9	98.6	.99497	9.6	15.8
.1316	174.5	174.3	.8648	3.7	2.1
150°K π = 1 atm					
.000446	4.4	3.0	.000554	11.7	13.1
.00445	15.4	13.8	.99555	9.6	9.9
.0212	30.5	29.8	.9788	3.9	5.3
.1377	65.1	63.7	.8623	3.2	3.2
.5637	99.3	99.7	.4363	2.3	0.9
150°K π = 28.5 atm					
.806	77.5	88.5	27.70	53.2	41.3
10.89	173.1	168.6	17.60	1.4	4.8
19.65	184.8	181.9	8.85	1.8	1.6
23.49	189.4	185.8	5.01	0.9	0.4
210°K π = 1 atm					
.0398	2.3	4.6	.9612	3.2	1.9
.0830	8.9	9.2	.9170	2.1	1.8
.3078	15.1	21.8	.6922	6.0	1.1
.4800	26.1	28.2	.5200	1.8	0.7
.7700*	33.9	36.0	.2300	0.7	0.2
210°K π = 28.5 atm					
2.21	53.7	50.4	26.29	24.1	22.9
12.27	105.0	102.0	16.23	10.3	6.4
24.74	133.7	125.2	3.76	1.4	1.1

* From Smoothed Data

Appendix 2

FIG A2-1

POTENTIAL DIAGRAM

DATA: THIS WORK

SYSTEM: CARBON MONOXIDE - PITTSBURGH BPL CARBON

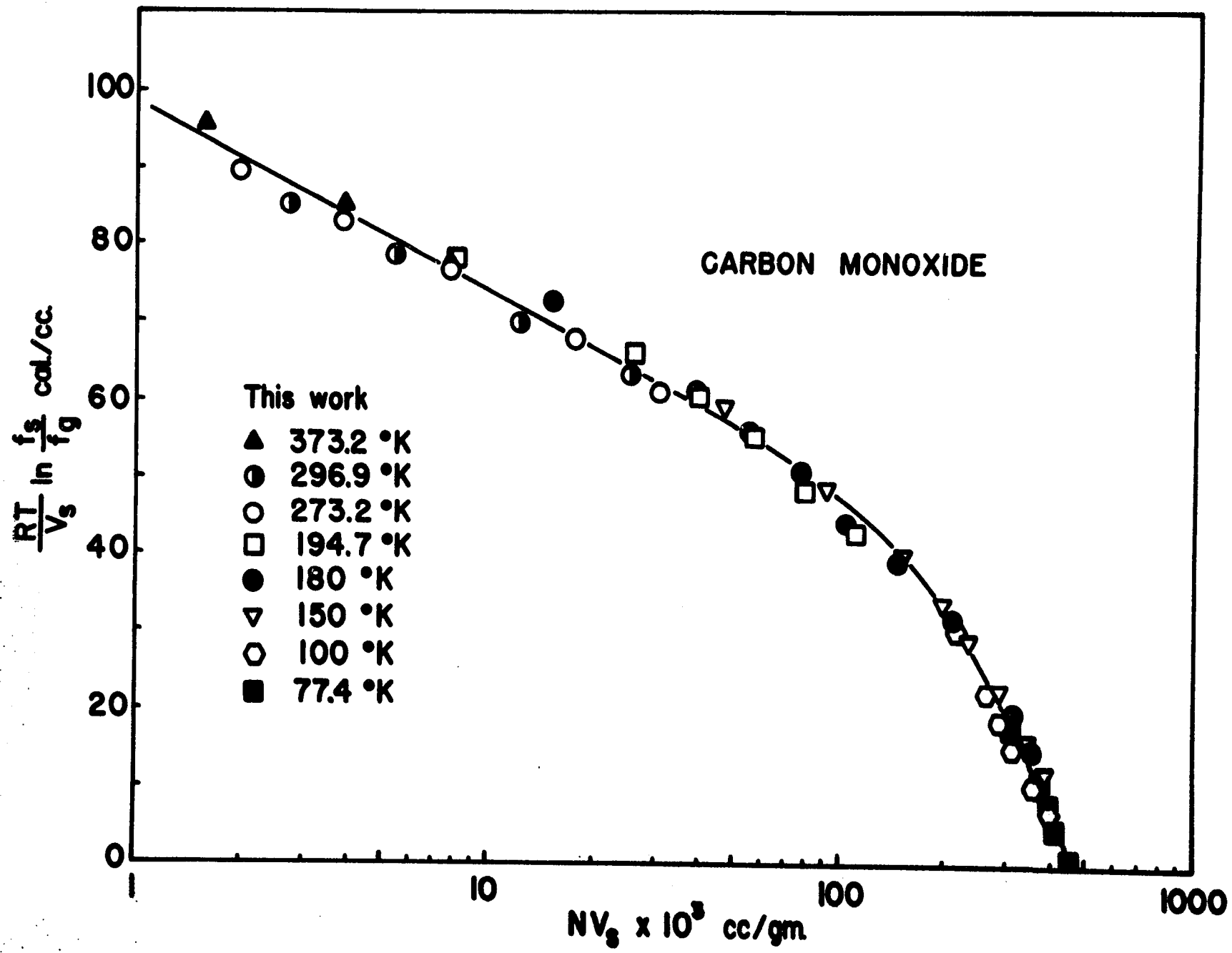
CARBON MONOXIDE
This work
373.2 °K
296.9 °K
273.2 °K
194.7 °K
180 °K
150 °K
100 °K
77.4 °K
$\frac{RT}{V_s} \ln \frac{f_s}{f_g}$ cal./cc.
$NV_s \times 10^3$ cc/gm.
0
20
40
60
80
100
1
10
100
1000

FIG A2-2

POTENTIAL DIAGRAM

DATA: THIS WORK

SYSTEM: ARGON - PITTSBURGH BPL CARBON

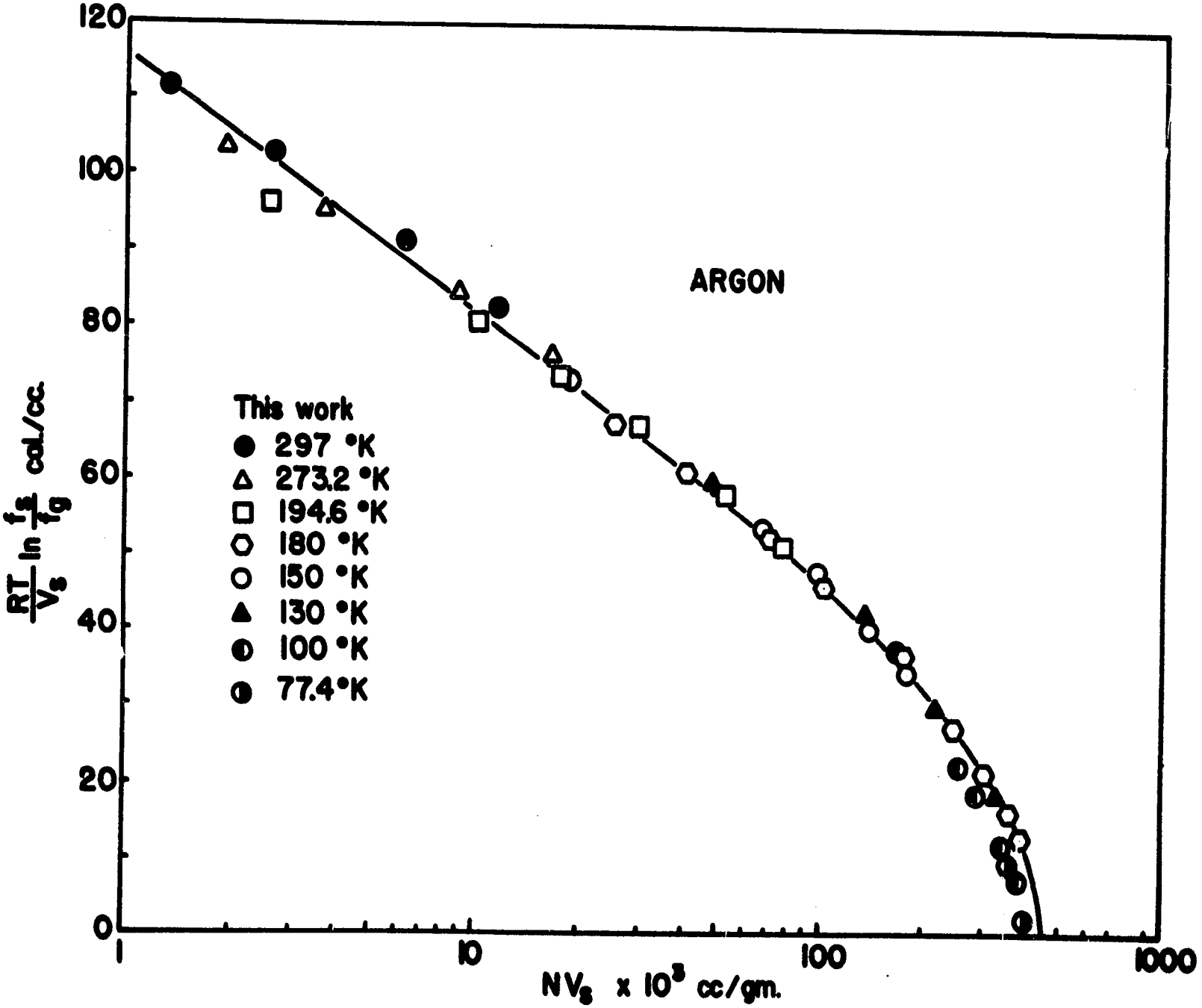
ARGON
This work
297 °K
273.2 °K
194.6 °K
180 °K
150 °K
130 °K
100 °K
77.4°K
$\frac{RT}{V_s} \ln \frac{f_s}{f_g}$ cal/cc.
$NV_s \times 10^3$ cc/gm.
0
20
40
60
80
100
120
1
10
100
1000

FIG A2-3

POTENTIAL DIAGRAM

DATA: ANTROPOFF (31)

SYSTEM: ARGON - AKT II CARBON

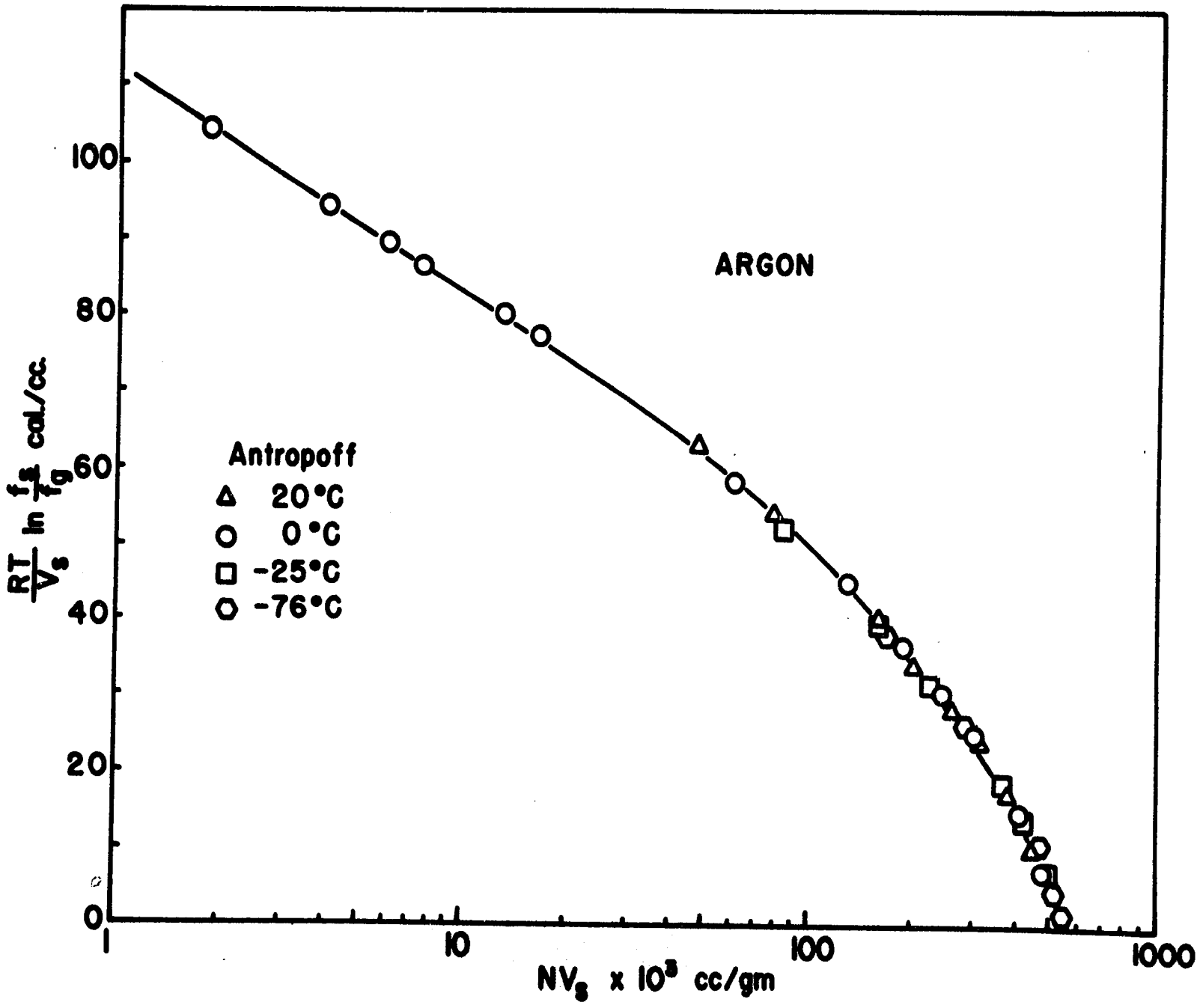
ARGON
Antropoff
△ 20°C
○ 0°C
□ -25°C
○ -76°C
$\frac{RT}{V_s} \ln \frac{f_s}{f_g}$ cal/cc.
$NV_s \times 10^3$ cc/gm
0
20
40
60
80
100
1
10
100
1000

FIG A2-4

POTENTIAL DIAGRAMS

DATA: 1) Ray and Box (58)

2) Szepesy (37,38)

SYSTEM: 1) Methane - Columbia L Carbon

2) Methane - Nuxit AL Carbon

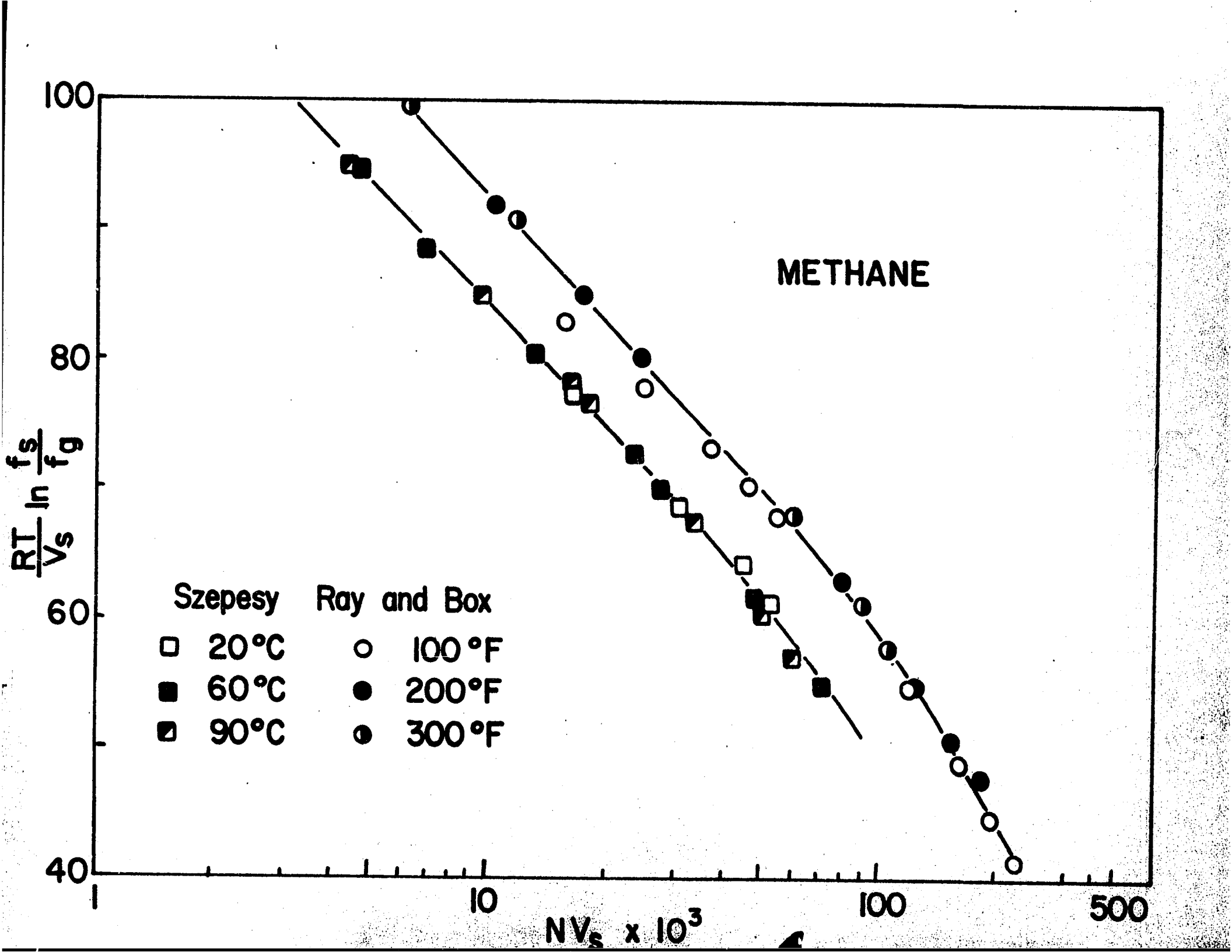
METHANE
Szepesy
20°C
60°C
90°C
Ray and Box
100°F
200°F
300°F
100
80
60
40
1
10
100
500
$\frac{RT}{V_s} \ln \frac{f_s}{f_g}$
$NV_s \times 10^3$

FIG A2-5

POTENTIAL DIAGRAMS

DATA: 1) Ray and Box (58)

2) Szepesy (37,38)

SYSTEM: 1) Ethane - Columbia L Carbon

2) Ethane - Nuxit AL Carbon

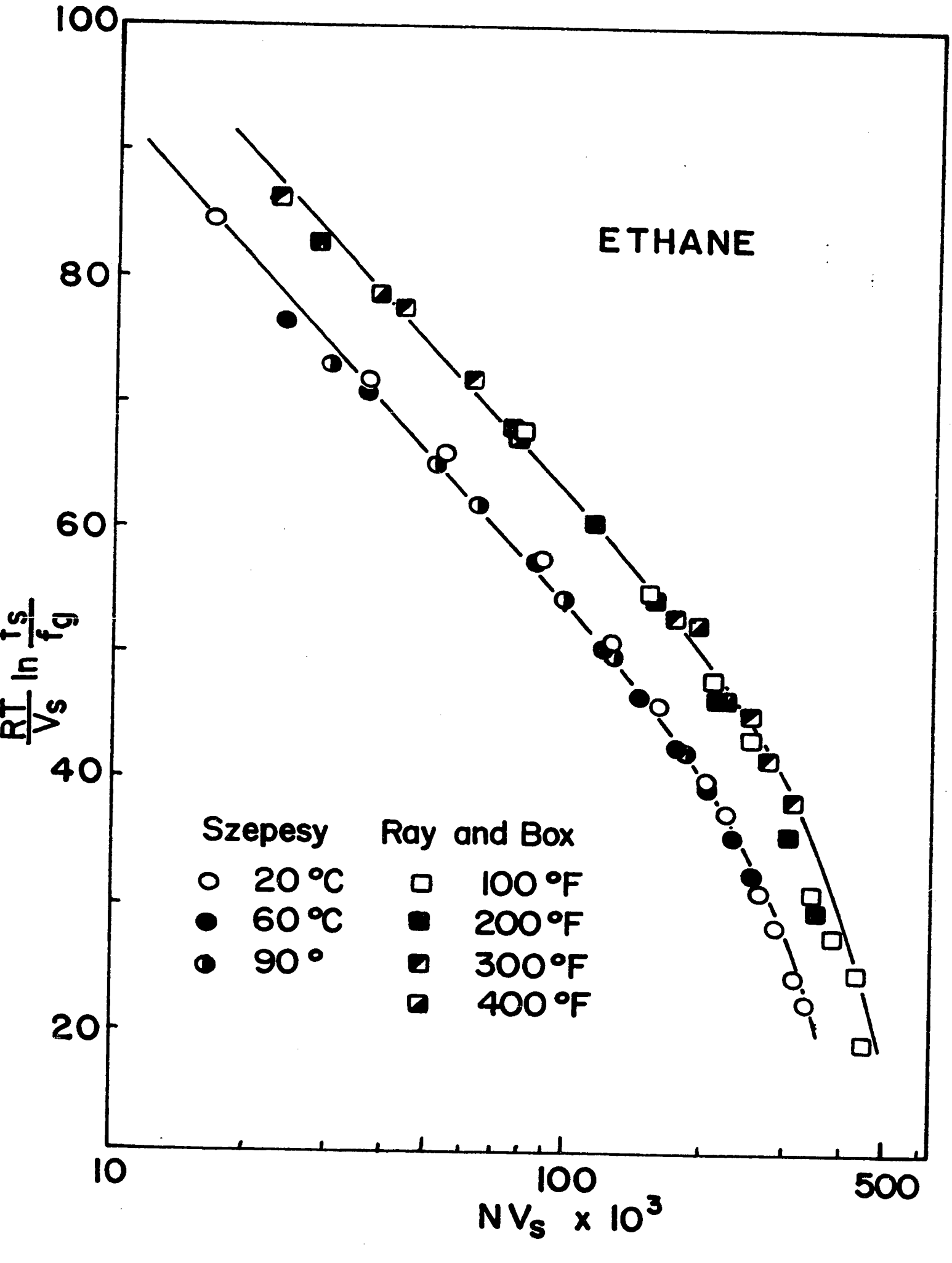
ETHANE
Szepesy
20 °C
60 °C
90 °
Ray and Box
100 °F
200 °F
300 °F
400 °F
100
80
60
40
20
10
100
500
$\frac{RT}{V_s} \ln \frac{f_s}{f_g}$
$NV_s \times 10^3$

FIG A2-6

POTENTIAL DIAGRAMS

DATA:

1) Ray and Box (58)

2) Szepesy (37,38)

3) Lewis (61)

SYSTEM:

1) Ethylene - Columbia L Carbon

2) Ethylene - Nuxit AL Carbon

3) Ethylene - Silica Gel (Davidson)

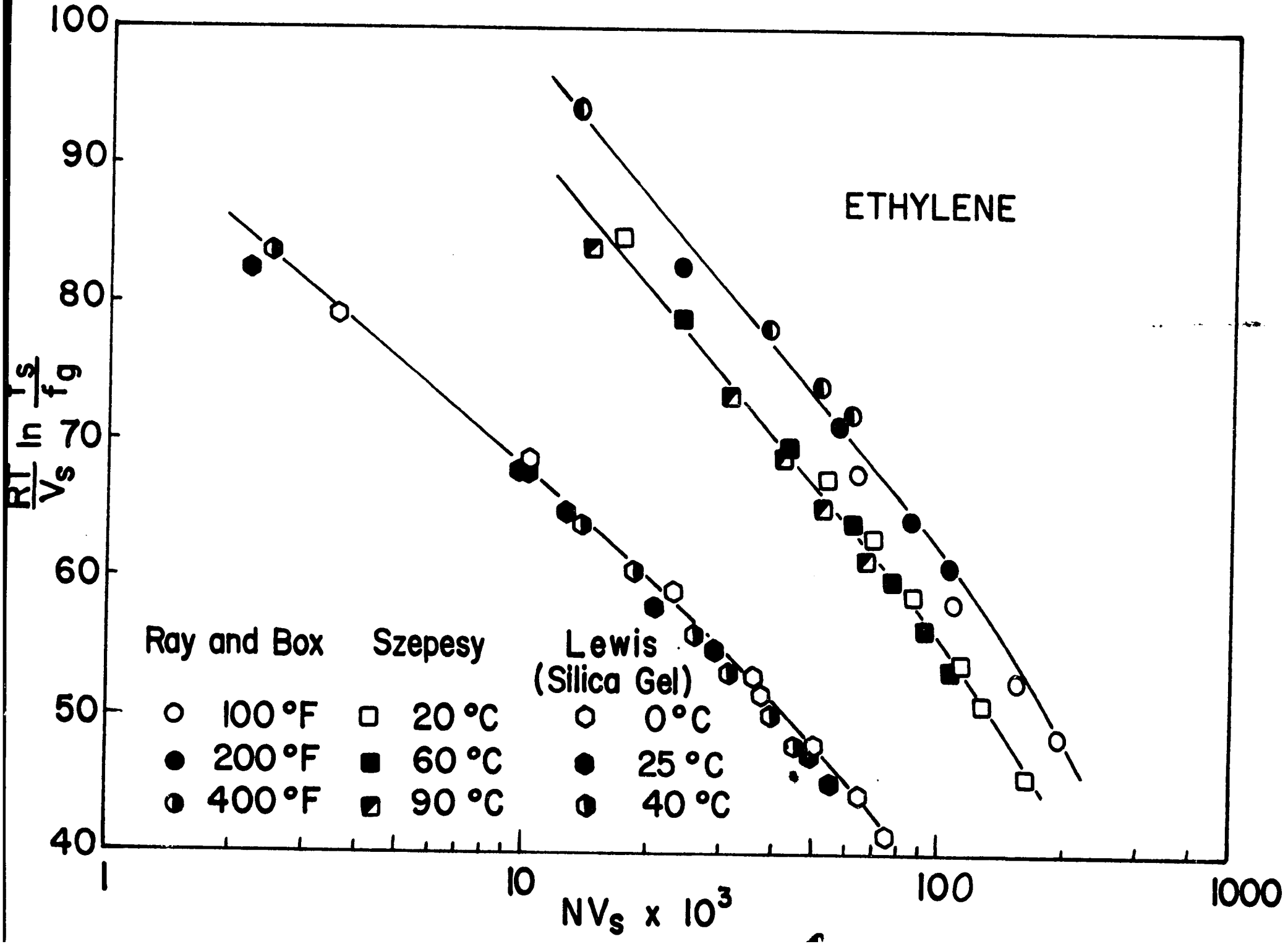
ETHYLENE
$\frac{RT}{V_s} \ln \frac{f_s}{f_g}$
$NV_s \times 10^3$
100
90
80
70
60
50
40
1
10
100
1000
Ray and Box
Szepesy
Lewis
(Silica Gel)
100 °F
200 °F
400 °F
20 °C
60 °C
90 °C
0 °C
25 °C
40 °C

FIG A2-7

POTENTIAL DIAGRAMS

DATA: 1) Ray and Box (58)

2) Szepesy (37,38)

SYSTEM: 1) CO_2 - Columbia L Carbon

2) CO_2 - Nuxit AL Carbon

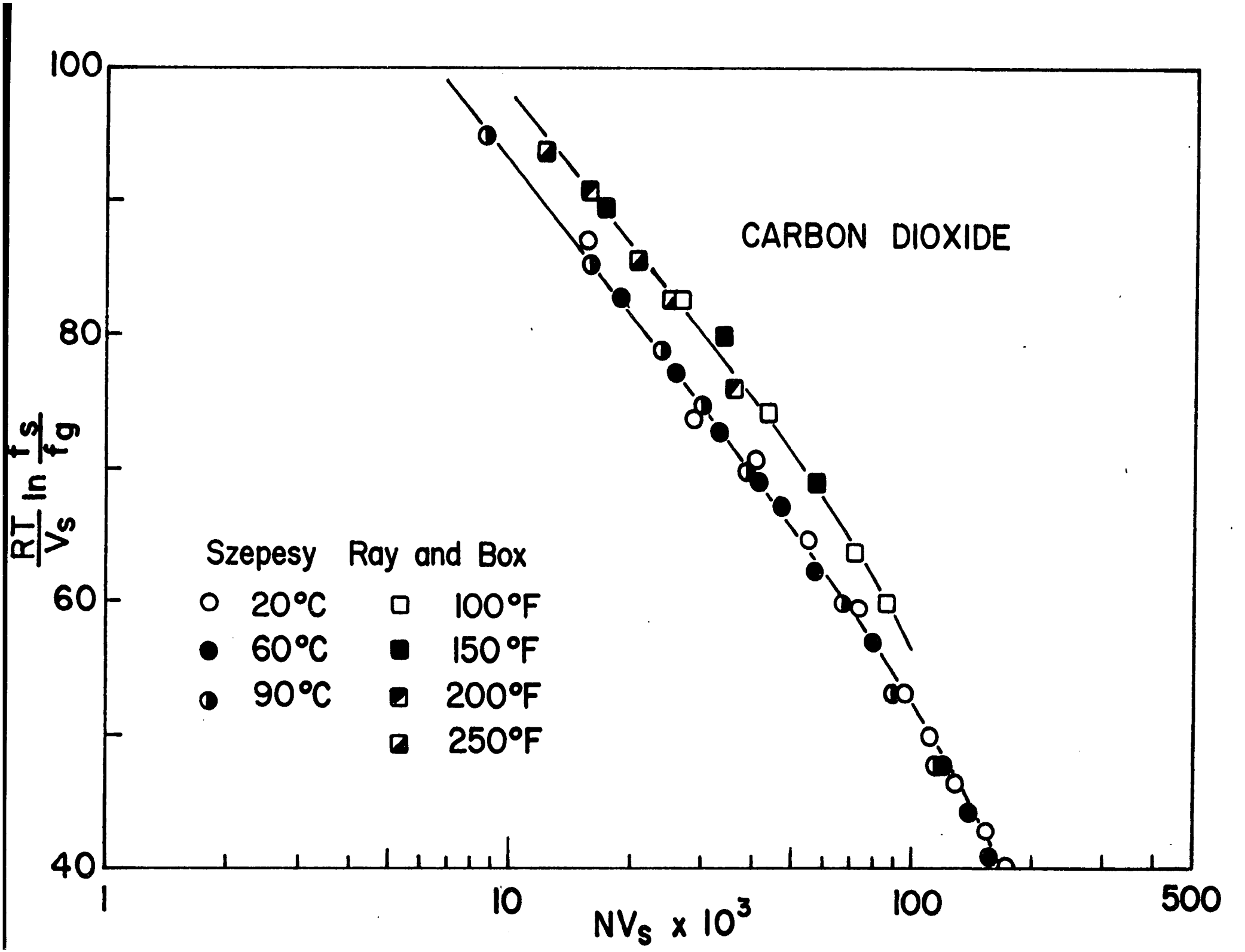
CARBON DIOXIDE
Szepesy Ray and Box
20°C 100°F
60°C 150°F
90°C 200°F
250°F
100
80
60
40
1
10
100
500
$\frac{RT}{V_s} \ln \frac{f_s}{f_g}$
$NV_s \times 10^3$

FIG A2-8

POTENTIAL DIAGRAM

DATA: ANTROPOFF (31)

SYSTEM: NITROGEN - AKT III CARBON

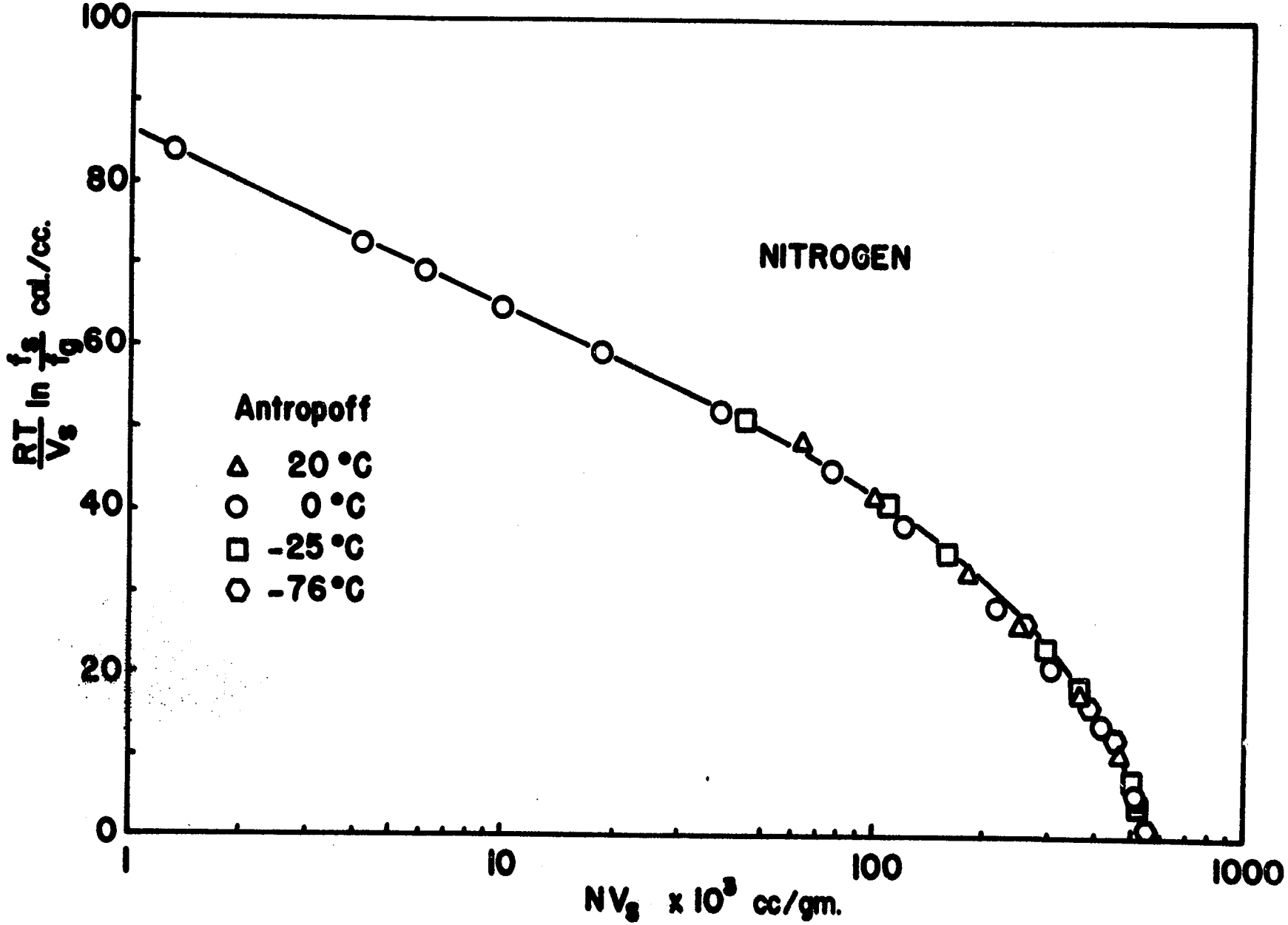
NITROGEN
Antropoff
20 °C
0 °C
-25 °C
-76 °C
$\frac{RT}{V_s} \ln \frac{f_s}{f_o}$ cal./cc.
$NV_s \times 10^3$ cc/gm.
0
20
40
60
80
100
1
10
100
1000

Appendix 3

TABLE A3-1

PROPERTIES OF SOLID ADSORBENT

PITTSBURGH ACTIVATED CARBON

Type BPL 6 x 16 mesh No. 12411

Pittsburgh Coke and Chemical Co.,
Pittsburgh, Pa

	THIS WORK	MANUFACTURER'S DATA
BET Surface m^2/g	828.0	1050.0
Pellet volume cc/g	1.22	1.25
Solid volume cc/g	0.55	0.48
Total Pore volume cc/g	0.67	0.80
Macro pore volume cc/g	0.30	-
Bulk density g/cc	-	0.48
lb/F_T^3	-	30.0

TABLE A3-2

DETERMINATION OF B.E.T. AREA

BET Equation $\frac{P}{V(P_o-P)} = \frac{1}{V_m C} \cdot \frac{C-1}{V_m C} \cdot \frac{P}{P_o}$

Sample Weight 0.436 gm Pittsburgh BPL Carbon

P_{mm}	V cc STP	(P_o-P)	$\frac{P}{V(P_o-P)}$	P/P_o
$P_o = 760$				
1.3	33.2	758.7	5.16×10^{-5}	.0017
6.8	74.42	753.2	12.13×10^{-5}	.0089
63.8	98.14	680.2	94.74×10^{-5}	.0839
174.0	107.88	586.0	275.7×10^{-5}	.229
390.8	114.70	369.2	922.8×10^{-5}	.514
715.0	126.27	45.0	.1258	.941
74.3	131.58	17.0	.332	.978
35.6	91.0	664.4	.00059	.0468
78.6	100.5	621.4	.00126	.103
233.5	111.6	466.5	.00449	.307
343.8	115.2	356.2	.00836	.452

$I = \frac{1}{V_m C} = .00001$ $M = \frac{C-1}{V_m C} = \frac{.00433}{.3.6} = .01201$

$V_m = \frac{1}{I+m} = \frac{1}{.01202} = 83.1$ $V = 190$ cc STP/gm

$\leq = 0.269\ (16.2)\ 190 = 828$ sq. metres/gm

TABLE A3-3

POROSITY DETERMINATIONS - MACROPORE VOLUME

Courtesy Department of Mines - Fuels Division

Pressure psi	Hg Penetration - cc		
	Pittsburgh BPL Carbor 0.413 gm	5A Molecular Sieve 0.456 gm	4A Molecular Sieve 0.433 gm
20	.010	.012	.003
30	.010	.012	.003
35	.010	.012	.003
42	.011	.013	.003
52	.013	.013	.004
60	.014	.013	.004
70	.015	.013	.004
85	.017	.014	.005
105	.020	.014	.006
140	.028	.014	.007
210	.041	.016	.010
300	.054		.057
400	.064		
500	.071	.082	.093
700	.081	.097	.100
1,000	.089	.106	.104
2,000	.195	.119	.110
3,000	.106	.127	.114
4,000	.109	.132	.117
5,000	.110	.136	.119
6,000	.113	.138	.121
7,000	.115	.140	.122
8,000	.117	.1405	.123
10,000	.121	.142	.124
12,000	.123		.126
14,000	.124		.127
15,000	.1245	.144	

TABLE A3-4

ADSORBENT SUPPLIERS

W.R. Grace and Co., "MICROTRAPS"
Davidson Chemical Division,
Baltimore 3, MD.

Minerals and Chemicals Corp. of America,
Menlo Park, N.J.

Filtrol Corporation,
3250 E. Washington Blvd.,
Los Angeles 23, Cal.

Pittsburgh Coke and Chemical Co.,
Pittsburgh, PA.

Union Carbide Can. Ltd.,
Metals and Carbon Division,
123 Eglinton Avenue 2,
Toronto, Ontario

F.M.C. International,
New York.

Floridin Company,
Tallahassee, Florida

Tamms Industries Inc.,
228 N. LaSalle Street,
Chicago 1, Ill.

United Norit Sales Corp.,
Amsterdam

Barnebey-Cheney,
Columbus 19, Ohio

Linde Gases Division,
Union Carbide Canada Ltd.,
Toronto, Ontario

TABLE A3-5

ADSORBATE GASES

All gases used as received without further purification

Gas	Supplier	Min. Purity %	Typical Analysis
A	Linde	99.996	Moisture 6 ppm
			O_2 < 1 ppm
			H_2 < 1 ppm
			Carbon Cmpds. < 3.3 ppm
			N_2 < 2.6 ppm
CO - (CP)	Matheson	99.5	
CH_4 - (CP)	Matheson	99.0	
D_2	General Dynamics	99.5	
H_2	Linde	99.7	Moisture 16 ppm
			O_2 < 1 ppm
			A < 2 ppm
			N_2 < 23 ppm
			CO_2 < 3 ppm
			Purity 99.995
N_2 (High Purity)	Linde	99.995	Moisture 9 ppm
			O_2 < 3.2 ppm
			H_2 < 1 ppm
			Carbon Cmpds. 2 ppm

TABLE A3-6

LIST OF EQUIPMENT ITEMS AND SUPPLIERS

ITEM	SUPPLIER
1. Bench-scale valves and fittings mat'l 316 s.s. operating press 5000 psi	Autoclave Engineers
i) valves 2-way TV-1200	
ii) valves 3-way	
iii) T's and X's	
iv) micro-reactor (5 cc)	
2. Test gauges - (bleed valves fitted) 1/4% F.S. accuracy	U.S. Gauge
RANGE i) 0-30 iv) 0-600 ii) 0-60 v) 0-2000 iii) 0-200	
Oil Filled System	
3. Mechanical vacuum pump Duo-seal	Fisher Scientific Co.
i) single stage 1400	
ii) two stage	
4. McLeod gauge Tilt type - Edwards	Edwards High Vac
5. LKB "Auto vac" pressure gauge 1 - 100 mm Hg	Edwards High Vac
7. Temperature Controller	Fisher Scientific Co.
i) Yellowstone RB 63 Thermistemp	
ii) Fisher thermistor 71 Matching probe	

TABLE A3-6 (cont'd)

ITEM		SUPPLIER
8. Potentiometer - Tinsley-type 3 range - minimum div. = 5μv		Tinsley Instruments
10. Thermistors		
i) Veco A-33 matched	2000Ω	Rocke International
ii) Low temp. J-49		Keystone Carbon
iii) Veco Lox-21A5		Rocke International
11. Santocel FRC silica aerogel		Monsanto
12. Custom glass blowing		P. Hernandez, Ottawa

Appendix 4

TABLE A4-1

CALIBRATION OF COPPER - CONSTANTAN THERMOCOUPLE

Courtesy National Research Council, Ottawa

1. For use with Thermal Conductivity Cell

Temperature °C	E.M.F. Absolute Millivolts
0	0.000
10	0.389
20	0.787
30	1.194
40	1.610
50	2.034
60	2.466
70	2.907
80	3.355
90	3.811
100	4.275

Uncertainty ± 0.02°C

2. For use with Cryostat

0	0.000
-30	1.115
-60	2.141
-90	3.071
-120	3.090
-150	4.621
-180	5.230

Uncertainty ± 0.1°C

TABLE A4-2

CALIBRATION OF PRESSURE GAUGES

Courtesy Fuels Div., Department of Mines and Technical Surveys, Ottawa

GAUGES - U.S. Gauge - 6" - 1/4%

TESTER - 1) Budenberg 0-1,000 psi
2) American Instruments 1,000-10,000 psi

1) 0-200

True Pressure	Gauge Up	Gauge Down
0	0.6	0.6
5	5.6	5.6
10	10.6	10.6
20	20.7	20.7
40	40.7	40.7
60	60.7	60.7
75	75.7	75.7
100	100.7	100.7
125	125.7	125.7
150	150.7	150.7
175	175.8	175.8
200	201.0	

2) 0-600

	Gauge Down
0	0
5	5
40	40
100	100
200	200
300	299
400	398
500	498
550	547

TABLE A4-2 (cont'd)

3) 0-2000

True Pressure	Gauge Up	Gauge Down
0	0	
10	10	
50	50	
100	100	100
200	201	201
400	402	403
600	603	604
800	800	801
1000	1000	1000
1200	1198	1200
1400	1395	1400
1600	1595	1601
1800	1798	1800
2000	1998	

TABLE A4-3

CALIBRATION: 200 ml GAS MEASURING BULB AND MANIFOLD

$T_{amb.}$ 23.5°C

P	V	V/P
mm Hg	cc STP	
438.0	118.6	0.2708
369.1	99.9	0.2707
311.8	84.2	0.2701
263.0	71.1	0.2705
221.5	60.0	0.2709
186.8	50.5	0.2706

V/P AV. = 0.2706

V/P AV. adjusted for ambient temperature changes in increments of 0.5°C

TABLE A4-4

CALIBRATION OF THERMAL CONDUCTIVITY CELL

HYDROGEN - NITROGEN

Volume Fraction N_2	Voltage Fraction	Vol Fract. / Volt. Fract.
.0825	.1244	1.5078
.0473	.0771	1.6300
.1273	.1936	1.5208
.1610	.2464	1.5304
.0126	.0199	1.5857
.4684	.3365	1.3920
.6133	.4774	1.2847
.7935	.6831	1.1616
.9620	.9338	1.0302

Typical Bridge Values

N_2 - 396.0 mv

H_2 + 3.75 mv

o-pH_2 Shift

77.4°K 1.36 mv

100.0°K 0.7 mv

150.0°K -

TABLE A4-5

CALIBRATION OF THERMAL CONDUCTIVITY CELL

HYDROGEN - CARBON MONOXIDE

Volume Fraction CO	Voltage Fraction	Vol Fract. / Volt. Fract.
.3957	.2698	1.4666
.1439	.0906	1.5883
.3970	.2728	1.4553
.4228	.2889	1.4635
	.2928	1.444
.6422	.4986	1.2880
.8855	.8062	1.0984

TABLE A4-6

CALIBRATION OF THERMAL CONDUCTIVITY CELL

NITROGEN - CARBON MONOXIDE

Volume Fraction CO	Voltage Fraction	Vol Fract. / Volt. Fract.
.0686	.0619	1.1082
.2489	.2293	1.0855
.4830	.4560	1.0592
.5062	.4758	1.0638
.7441	.7222	1.0303
.8871	.8818	1.0060